

PRACTICAL CONVERSION OF ZERO-POINT ENERGY

FEASIBILITY STUDY

OF ZERO-POINT ENERGY EXTRACTION

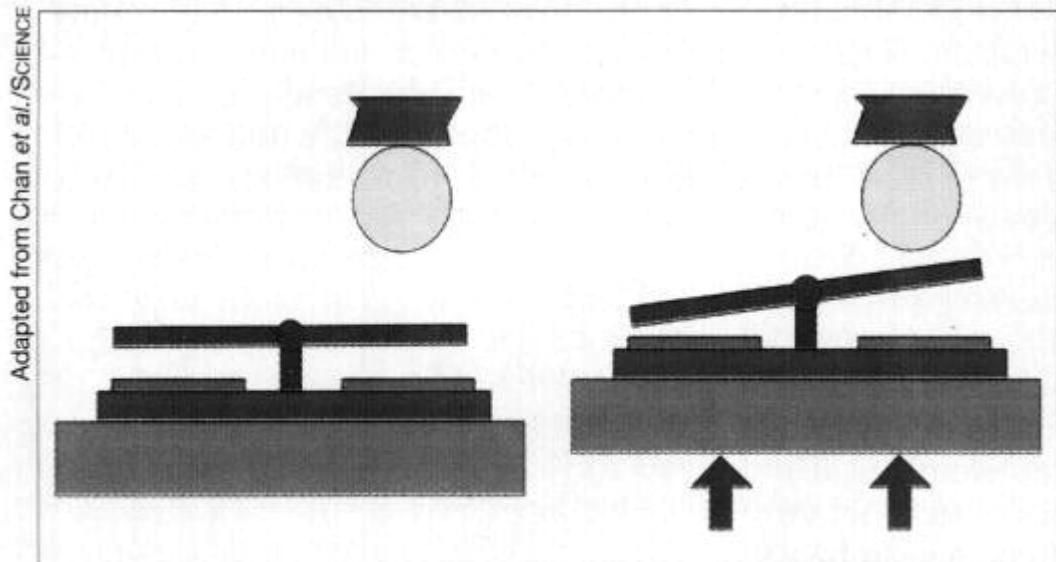
FROM THE QUANTUM VACUUM FOR THE PERFORMANCE OF USEFUL WORK

Now with "Vacuum Engineer's Toolkit" - Table 3 - p. 74

Revised Edition, 2020

By

Thomas F. Valone, Ph.D., P.E.



A chip with a see-saw plate suspended parallel to its surface (left) is pushed up (right) toward a ball. Quantum fluctuations in empty space produce a force that tilts the plate.

Drawing courtesy of *Science News*

Integrity Research Institute

PRACTICAL CONVERSION OF ZERO-POINT ENERGY

Feasibility Study of Zero-Point Energy Extraction from the Quantum Vacuum for the
Performance of Useful Work

Thomas F. Valone, PhD, PE

ISBN 0-9641070-8-2 updated to ISBN 978-0-9641070-8-3

Copyright © 2003 Thomas F. Valone

Second Edition, 2004

Third Edition, 2005 - - Fourth Edition, 2010 - - Fifth Edition, 2020

Integrity Research Institute, 5020 Sunnyside Ave., Suite 209, Beltsville MD 20705,

Phone 301-220-0440, 888-802-5243, 800-295-7674

A nonprofit 501(c)3 organization www.IntegrityResearchInstitute.org

This study is also summarized in a **70-minute lecture & slide presentation online** from the Institute for New Energy and the TeslaTech conferences: "Zero Point Energy Extraction from the Quantum Vacuum." The Valone ZPE lecture is available for free download from YouTube: <https://www.youtube.com/watch?v=RDvlgHV2US0>

The first edition of this study was a dissertation presented to the faculty of the School of General Engineering at Kennedy-Western University in partial fulfillment for the degree of Doctor of Philosophy in General Engineering on September 30, 2003.

Also see *Zero-Point Energy: The Fuel of the Future* – a popular paperback book by Dr. Valone

IRI PR-04-001

Final Report
for the period
1 Jun 2003 to
30 Dec 2003

Feasibility Study of Zero-Point Energy Extraction from the Quantum Vacuum for the Performance of Useful Work

December 2003

Author:
T. F. Valone, Ph.D.

Integrity Research Institute
1220 L St. NW, Suite 100-232
Washington, DC 20005

Approved for Public Release

Distribution is unlimited. The Board of Directors of Integrity Research Institute has reviewed this report, and it is releasable to distributors and to the general public, including foreign nationals.



**Integrity
Research
Institute**

Research and Education Division
1220 L Street NW, Suite 100-232
Washington DC 20005

TABLE OF CONTENTS

TABLE OF CONTENTS.....	3
PREFACE to Revised Edition	5
CHAPTER 1 - Introduction.....	6
Zero-Point Energy Issues	6
Fluctuation-Dissipation Theorem	11
Statement of the Problem	12
Purpose of the Study	13
Importance of the Study	13
Rationale of the Study	15
Definition of Terms	15
Overview of the Study	16
CHAPTER 2 - Review of Related Literature	17
Historical Perspectives	17
Casimir Predicts a Measurable ZPE Effect.....	18
Ground State of Hydrogen is Sustained by ZPE.....	19
Lamb Shift Caused by ZPE	19
Experimental ZPE.....	20
ZPE Patent Review	20
ZPE and Sonoluminescence	21
Gravity and Inertia Related to ZPE	22
Heat from ZPE.....	22
Summary	23
CHAPTER 3 - Methodology.....	24
Approach	24
What is a Feasibility Study?.....	24
Data Gathering Method	25
Database Selected for Analysis.....	25
Analysis of Data.....	25
Validity of Data	25
Uniqueness and Limitations of the Method.....	25
Summary	26
CHAPTER 4 - Analysis.....	27
Introduction to Vacuum Engineering.....	27
Electromagnetic Zero-Point Energy Converter	27
Microsphere Energy Collectors.....	31

Nanosphere Energy Scatterers	35
Picosphere Energy Resonators	37
Quantum Femtosphere Amplifiers	40
Deuteron Femtosphere.....	42
Electron Femtosphere	43
Casimir Force Electricity Generator.....	44
Cavity QED Controls Vacuum Fluctuations	47
Spatial Squeezing of the Vacuum.....	48
Focusing Vacuum Fluctuations.....	49
Stress Enhances Casimir Deflection	49
Casimir Force Geometry Design	50
Vibrating Cavity Photon Emission.....	53
Fluid Dynamics of the Quantum Vacuum	54
Quantum Coherence Accesses Single Heat Bath	56
Thermodynamic Brownian Motors	58
Transient Fluctuation Theorem.....	61
Power Conversion of Thermal Fluctuations	62
Rectifying Thermal Noise with Ratchets	63
Ferrofluid Thermal Rectifier Torque Engine.....	64
Rectifying Thermal Electric Noise.....	65
Quantum Brownian Nonthermal Rectifiers without Ratchets	65
Zero Point Energy Corresponds to Dark Energy	67
Vacuum Field Amplification	67
CHAPTER 5 - Summary, Conclusions and Recommendations	68
Summary	68
Electromagnetic Conversion.....	68
Mechanical Casimir Force Conversion	70
Fluid Dynamics	70
Thermodynamic Conversion.....	70
Conclusions	72
Recommendations.....	73
Table 3 - Vacuum Engineer's Toolkit.....	74
FIGURE CREDITS	76
REFERENCES	79
Proposed Use of Zero Bias Diode Arrays ... Energy Converters ... SPESIF 2009 paper.....	92

PREFACE to Revised Edition

Today this country faces a destabilizing dependency on irreplaceable fossil fuels which are also rapidly dwindling. As shortages of oil and natural gas occur with more frequency, the "New Energy Crisis" is now heralded in the news media.¹ However, an alternate source of energy that can replace fossil fuels has not been reliably demonstrated. **A real need exists for a portable source of power that can compete with fossil fuel and its energy density.** A further need exists on land, in the air, and in space, for a fuelless source of power which, by definition, does not require re-fueling. The future freedom, and quite possibly the future survival, of mankind depend on the utilization of such a source of energy, if it exists.

However, ubiquitous zero-point energy is known to exist. Yet, none of the world's physicists or engineers are participating in any national or international energy development project, such as advocated by the Apollo Alliance, that would extend beyond nuclear power. It is painfully obvious that zero-point energy does not appear to most scientists as the robust source of energy worth developing. Therefore, an aim of this study is to provide a clear understanding of the basic principles of the only known candidate for a limitless, fuelless source of power: zero-point energy. Another purpose is to look at the feasibility of various energy conversion methods that are realistically available to modern engineering, including emerging nanotechnology, for the possible use of zero-point energy.

To accomplish these proposed aims, a review of the literature is provided, which focuses on the major, scientific discoveries about the properties of zero-point energy and the quantum vacuum. Central to this approach is the discerning interpretation of primarily physics publications in the light of mechanical, nuclear, thermal, electronic and electrical engineering techniques. Applying an engineering analysis to the zero-point energy literature places more emphasis the practical potential for its energy conversion, especially in view of recent advances in nanotechnology.

With primary reference to the works of H. B. G. Casimir, Frank Mead, Fabrizio Pinto, and Peter Milonni, key principles for the proposed extraction of energy for useful work are identified and analyzed. **These principles fall into the thermodynamic, fluidic, mechanical, and electromagnetic areas of primary, forcelike quantities that apply to all energy systems.** A search of zero-point energy literature reveals that these principles also apply to the quantum level. Chapter 4 begins the Analysis section with the Frank Mead patent as the **Electromagnetic Zero-Point Energy Converter** from pages 27 – 44. The rest of the examples are much more brief, such as the Pinto patent **Casimir Force Electricity Generator** analysis from pages 44 – 50. Though the Mead analysis contains valuable comparisons of four different sphere sizes, it is the most technical physics in the study and may be skipped over for the first reading through, without loss of continuity.

The most feasible modalities for the practical conversion of zero-point energy into useful work, such as the fluctuation-driven transport of an electron ratchet, the quantum Brownian nonthermal rectifiers, and the Photo-Carnot engine are also explored in more detail. One-liner, **boldface key sentences** appear throughout the study for emphasis of the most important discoveries in the field. Specific suggestions for further research in this area conclude this feasibility study with a detailed section devoted to summary, conclusions and recommendations. For a less technical overview, my ZPE lecture DVD is highly recommended as well as the forthcoming book, *Zero-Point Energy: the Fuel of the Future*. A Definition of Terms appears on pages 15-16, Vacuum Engineer's Toolkit on page 74. It is also important to mention the latest emphasis on conversion of "negative energy" of the ZPF which is focusing on the entire quantum vacuum rather than just the vacuum fluctuations of the zero point field.

CHAPTER 1 - Introduction

Zero-Point Energy Issues

Zero-point energy (ZPE) is a universal natural phenomenon of great significance which has evolved from the historical development of ideas about the vacuum. In the 17th century, it was thought that a totally empty volume of space could be created by simply removing all gases. This was the first generally accepted concept of the vacuum. Late in the 19th century, however, it became apparent that the evacuated region still contained thermal radiation. To the natural philosophers of the day, it seemed that all of the radiation might be eliminated by cooling.

Zero Point Energy

(Emerging science, 1948...)

What?

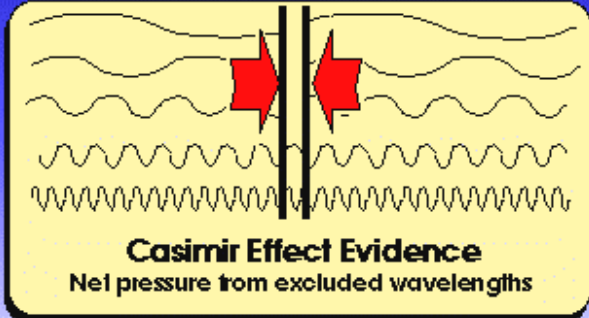
- Random Electromagnetic waves remain after all energy is removed
- Enormous energy density: 10^{24} to 10^{58} Joules/m³
- Theorized to indirectly cause gravity and inertia

Why?

- As an energy source?
- As a reactive medium?

Evidence?

- Casimir Effect
- Plank blackbody spectrum
- quantum effects



Casimir Effect Evidence

Net pressure from excluded wavelengths

NASA: www.grc.nasa.gov

CD-94-52307

Figure 1

Thus evolved the second concept of achieving a real vacuum: cool it down to zero temperature after evacuation. Absolute zero temperature (-273C) was far removed from the technical possibilities of that century, so it seemed as if the problem was solved. In the 20th century, both theory and experiment have shown that there is a non-thermal radiation in the vacuum that persists even if the temperature could be lowered to absolute zero. This classical concept alone explains the name of "zero-point" radiation².

In 1891, the world's greatest electrical futurist, **Nikola Tesla**, **predicted the existence of zero-point energy** by stating, "*Throughout space there is energy. Is this energy static or kinetic? If static our hopes are in vain; if kinetic – and we know it is, for certain – then it is a mere question of time when men will succeed in attaching their machinery to the very wheelwork of Nature. Many generations may pass, but in time our machinery will be driven by a power obtainable at any point in the Universe.*"³

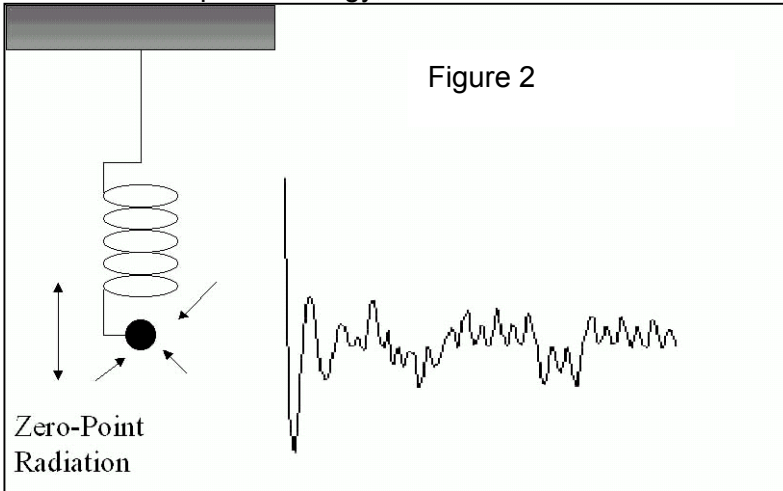
"From the papers studied the author has grown increasingly convinced as to the relevance of the ZPE in modern physics. The subject is presently being tackled with appreciable enthusiasm and it appears that there is little disagreement that the vacuum could ultimately be harnessed as an energy source. Indeed, the ability of science to provide ever more complex and subtle methods of harnessing unseen energies has a formidable reputation. Who would have ever predicted atomic energy a century ago?"⁴

A good experiment proving the existence of ZPE is accomplished by cooling helium to within microdegrees of absolute zero temperature. It will still remain a liquid. Only ZPE can account for the source of energy that is preventing helium from freezing.⁵

Besides the classical explanation of zero-point energy referred to above, there are rigorous derivations from quantum physics that prove its existence. "It is possible to get a fair estimate of the zero point energy using the uncertainty principle alone."⁶ As stated in Equation (1), Planck's constant h (6.63×10^{-34} joule-sec) offers physicists the fundamental size of the quantum. It is also the primary ingredient for the uncertainty principle. One form is found in the minimum uncertainty of position x and momentum p expressed as

$$\Delta x \Delta p \geq h/4\pi \quad (1)$$

In quantum mechanics, Planck's constant also is present in the description of particle motion. "The harmonic oscillator reveals the effects of zero-point radiation on matter. The oscillator consists of an electron attached to an ideal, frictionless spring. When the electron is set in motion, it oscillates about its point of equilibrium, emitting electromagnetic radiation at the frequency of oscillation. The radiation dissipates energy, and so in the absence of zero-point radiation and at a temperature of absolute zero the electron eventually comes to rest. Actually, zero-point radiation continually imparts random impulses to the electron, so that it never comes to a complete stop (as seen in Figure 2). Zero-point radiation gives the oscillator an average energy equal to the frequency of oscillation multiplied by one-half of Planck's constant."⁷



However, a question regarding the zero-point field (ZPF) of the vacuum can be asked, such as, "What is oscillating and how big is it?" To answer this, a background investigation needs to be done. The derivation which follows uses well-known physics parameters. It serves to present a conceptual framework for the quantum vacuum and establish a basis for the extraordinary nature of ZPE.

In quantum electrodynamics (QED), the fundamental size of the quantum is also reflected in the parton size. "In 1969 Feynman proposed the parton model of the nucleon, which is reminiscent of a model of the electron which was extant in the late 19th and early 20th centuries: The nucleon was assumed to consist of extremely small particles—the partons—which fill the entire space within a nucleon. All the constituents of a nucleon are identical, as are their electric charges. This is the simplest parton model."⁸

In quantum electrodynamics (QED), the fundamental size of the quantum is also reflected in the parton size. "In 1969 Feynman proposed the parton model of the nucleon, which is reminiscent of a model of the electron which was extant in the late 19th and early 20th centuries: The nucleon was assumed to consist of extremely small particles—the partons—which fill the entire space within a nucleon. All the constituents of a nucleon are identical, as are their electric charges. This is the simplest parton model."⁸

The derivation of the parton mass gives us a theoretical idea of how small the structure of the quantum vacuum may be and, utilizing $E = mc^2$, how large ZPE density may be. For convenience, we substitute $\hbar = "h_{\text{bar}}" = h/2\pi$ for which the average ZPE = $\frac{1}{2} hf = \frac{1}{2} \hbar \omega$, since the angular frequency $\omega = 2\pi f$.

The Abraham-Lorentz radiation reaction equation contains the relevant quantity, since the radiation damping constant Γ for a particle's self-reaction is intimately connected to the fluctuations of the vacuum.⁹ The damping constant is

$$\Gamma = \frac{2}{3} \frac{e^2}{m_0 c^3} \quad (2)$$

where m_0 is the particle mass.¹⁰ It is also known in stochastic electrodynamics (SED) that the radiation damping constant can be found from the ZPE-determined inertial mass associated with the parton oscillator.¹¹ It is written as

$$\Gamma = \pi m_0 c^2 / \hbar \omega_c^2 \quad (3)$$

Here ω_c is the zero-point cut-off frequency which is regarded to be on the order of the Planck cut-off frequency (see eq. 8), given by

$$\omega_c = \sqrt{\frac{\pi c^5}{\hbar G}} \quad (4)$$

Equating (2) and (3), substituting Equation (4) and rearranging for m_0 gives

$$m_0 = e \sqrt{\frac{2}{3G}} \quad (5)$$

Therefore, the parton mass is calculated to be

$$m_0 \approx 0.16 \text{ kg} \quad (6)$$

For comparison, the proton rest mass is approximately 10^{-27} kg, with a mass density of 10^{14} g/cc. Though "it might be suggested that quarks play the role of partons" the quark rest mass is known to be much smaller than loosely bound protons or electrons.¹² Therefore, Equation (6) suggests that partons are fundamentally different.

The answer to the question of how big is the oscillatory particle in the ZPF quantum vacuum comes from QED. "The length at which quantum fluctuations are believed to dominate the geometry of space-time" is the Planck length:¹³

$$\text{Planck length} = \sqrt{\frac{\hbar G}{c^3}} \approx 10^{-35} \text{ m} \quad (7)$$

The Planck length is therefore useful as a measure of the approximate size of a parton, as well as "a spatial periodicity characteristic of the Planck cutoff frequency."¹⁴ Since resonant wavelength is classically determined by length or particle diameter, we can use the Planck length as the wavelength λ in the standard equation relating wavelength and frequency,

$$c = f \lambda = \omega_c \lambda / 2\pi \quad (8)$$

and solving for ω_c to find the Planck cutoff frequency $\omega_c \approx 10^{43}$ Hz.¹⁵ This value sets an upper limit on design parameters for ZPE conversion, as reviewed in the later chapters. Taking Equation (6) divided by Equation (7), the extraordinary ZPF mass density estimate of 10^{101} g/cc seems astonishing, though, like positrons (anti-electrons), the ZPF consists mostly of particles in negative energy states. This derived density also compares favorably with other estimates in the literature: Robert Forward

calculates 10^{94} g/cc if ZPE was limited to particles of slightly larger size, with a ZPF energy density of 10^{108} J/cc.¹⁶ (NASA has a much smaller but still “enormous” estimate revealed in Figure 1.)

Another area of concern to the origin of the theoretical derivation of ZPE is a rudimentary understanding of what meaning Planck attributed to “the average value of an elementary radiator.”¹⁷ “The absorption of radiation was assumed to proceed according to classical theory, whereas emission of radiation occurred discontinuously in discrete quanta of energy.”¹⁸ Planck’s second theory, published in 1912, was the first prediction of zero-point energy.¹⁹ Following Boltzmann, Planck looked at a distribution of harmonic oscillators as a composite model of the quantum vacuum. From thermodynamics, the partial differential of entropy with respect to potential energy is $\partial S/\partial U = 1/T$. Max Planck used this to obtain the average energy of the radiators as

$$U = \frac{1}{2}hf + hf / (e^{hf/kT} - 1) \quad (9)$$

where here the ZPE term $\frac{1}{2}hf$ is added to the radiation law term of his first theory.

Using this equation, “which marked the birth of the concept of zero-point energy,” it is clear that as absolute temperature $T \rightarrow 0$ then $U \rightarrow \frac{1}{2}hf$, which is the average ZPE.²⁰

Interestingly, the ground state energy of a simple harmonic oscillator (SHO) model can also be used to find the average value for zero-point energy. *This is a valuable exercise to show the fundamental basis for zero-point energy parton oscillators.* The harmonic oscillator is used as the model for a particle with mass m in a central field (the “spring” in Figure 2). The uncertainty principle provides the only requisite for a derivation of the minimum energy of the simple harmonic oscillator, utilizing the equation for kinetic and potential energy,

$$E = p^2/2m + \frac{1}{2} m \omega^2 x^2 . \quad (10)$$

Solving the uncertainty relation from Equation (1) for p , one can substitute it into Equation (10). Using a calculus approach, one can take the derivative with respect to x and set the result equal to zero. A solution emerges for the value of x that is at the minimum energy E for the SHO. This x value can then be placed into the minimum energy SHO equation where the potential energy is set equal to the kinetic energy. The ZPE solution yields $\frac{1}{2}hf$ for the minimum energy E .²¹

This simple derivation reveals the profoundly fundamental effect of zero-point radiation on matter, even when the model is only a SHO. The oscillator consists of a particle attached to an ideal, frictionless spring. When the parton is in motion, it accelerates as it oscillates about its point of equilibrium, emitting radiation at the frequency of oscillations. The radiation dissipates energy and so in the absence of zero-point radiation and at a temperature of absolute zero the particle would eventually come to rest. In actuality, zero-point radiation continually imparts random impulses to the particle so that it never comes to rest. **This is Zitterbewegung motion.** The consequence of this Zitterbewegung is the averaged energy of Equation (15) imparted to the particle, which has an associated long-range, van der Waals, radiation field which can even be identified with Newtonian gravity. Information on this discovery is reviewed in Chapter 2.

In QED, the employment of perturbation techniques amounts to treating the interaction between the electron and photon (between the electron-positron field and the electromagnetic field) as a small perturbation to the collection of the ‘free’ fields. In the higher order calculations of the resulting perturbative expansion of the S-matrix (Scattering matrix), divergent or infinite integrals are encountered, which involve intermediate states of arbitrarily high energies. In standard QED, these divergencies are circumvented by redefining or ‘renormalizing’ the charge and the mass of the electron. By the renormalization procedure, all reference to the divergencies are absorbed into a set of infinite bare quantities. Although this procedure has made possible some of the most precise comparisons between theory and experiment (such as the $g - 2$ determinations) its logical consistency and mathematical justification remain a subject for controversies.²² Therefore, it is valuable to briefly review how the renormalization process is related to the ZPE vacuum concept in QED.

The vacuum is defined as the ground state or the lowest energy state of the fields. This means that the QED vacuum is the state where there are no photons and no electrons or positrons. However, as we shall see in the next section, since the fields are represented by quantum mechanical operators, they do not vanish in the vacuum state but rather fluctuate. The representation of the fields by operators also leads to a vacuum energy (sometimes referred to as vacuum zero-point energy).

When interactions between the electromagnetic and the electron-positron field in the vacuum are taken into account, which amounts to consider higher order contributions to the S-matrix, the fluctuations in the energy of the fields lead to the formation of so-called virtual electron-positron pairs (since the field operators are capable of changing the number of field quanta (particles) in a system). It is the evaluation of contributions like these to the S-matrix that lead to the divergencies mentioned above and prompt the need for renormalization in standard QED.

The vacuum state contains no stable particles. The vacuum in QED is believed to be the scene of wild activity with zero-point energy and particles/anti-particles pairs constantly popping out of the vacuum only to annihilate again immediately afterwards. This affects charged particles with oppositely charged virtual particles and is referred to as “vacuum polarization.” Since the 1930's, for example, theorists have proposed that virtual particles cloak the electron, in effect reducing the charge and electromagnetic force observed at a distance.

“Vacuum polarization is, however, a relativistic effect involving electron-positron pairs, as the hole-theoretic interpretation assumes: an electrostatic field causes a redistribution of charge in the Dirac sea and thus polarizes the vacuum. A single charged particle, in particular, will polarize the vacuum near it, so that its observed charge is actually smaller than its ‘bare charge.’ A proton, for instance, will attract electrons and repel positrons of the Dirac sea, resulting in a partial screening of its bare charge and a modification of the Coulomb potential in the hydrogen atom.”²³ Even “an atom, for instance, can be considered to be ‘dressed’ by emission and reabsorption of ‘virtual photons’ from the vacuum.”²⁴ This constant virtual particle flux of the ZPE is especially noticeable near the boundaries of bigger particles, because the intense electric field gradient causes a more prodigious “decay of the vacuum.”²⁵

In a notable experiment designed to penetrate the virtual particle cloud surrounding the electron (Figure 3), Koltick used a particle accelerator at energies of 58 GeV (gigaelectronvolts) without creating other particles.²⁶ From his data, a new value of the fine structure constant was obtained ($e^2/hc = 1/128.5$), while a smaller value of 1/137 is traditionally observed for a fully screened electron. This necessarily means that the value for a naked electron charge is actually larger than textbooks quote for a screened electron.

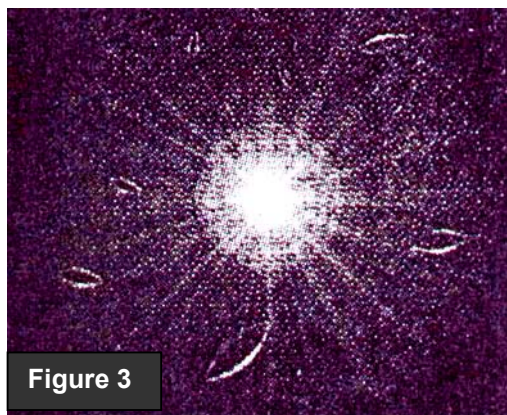


Figure 3

Often regarded as merely an artifact of a sophisticated mathematical theory, some experimental verification of these features of the vacuum has already been obtained, such as with the Casimir pressure effect (see Figure 6). An important reason for investigating the Casimir effect is its manifestation before interactions between the electromagnetic field and the electron/positron fields are taken into consideration. In the

language of QED, this means that the Casimir effect appears already in the zeroth order of the perturbative expansion. In this sense the Casimir effect is the most evident feature of the vacuum. On the experimental side, the Casimir effect has been tested very accurately.²⁷

Some argue that there are two ways of looking at the Casimir effect:

1) The boundary plates modify an already existing QED vacuum. That is, the introduction of the boundaries (e.g. two electrically neutral, parallel plates) modify something (a medium of vacuum zero-point energy/vacuum fluctuations) which already existed prior to the introduction of the boundaries.

2) The effect is due to interactions between the microscopic constituents in the boundary plates. That is, the boundaries introduce a source which give rise to the effect. The atomic or molecular constituents in the boundary plates act as fluctuating sources that generate the interactions between the constituents. The macroscopic attractive force between the two plates arises as an integrated effect of the mutual interactions between the many microscopic constituents in these boundary plates.²⁸

The second view is based on atoms within the boundary plates with fluctuating dipole moments that normally give rise to van der Waals forces. Therefore, the first view, I believe, is the more modern version, acknowledging the transformative effect of the introduction of the “Dirac sea” on modern QED and its present view of the vacuum.²⁹

Fluctuation-Dissipation Theorem

To conclude this introductory ZPE issues section, it is essential to review the *fluctuation-dissipation theorem*, which is prominently featured in QED, forming the basis for the treatment of an oscillating particle in equilibrium with the vacuum. It was originally presented in a seminal paper by Callen et al. based on systems theory, offering applications to various systems including Brownian motion and also electric field fluctuations in a vacuum.³⁰ In this theorem, the vacuum is treated as a bath coupled to a dissipative force.

“Generally speaking, if a system is coupled to a ‘bath’ that can take energy from the system in an effectively irreversible way, then the bath must also cause fluctuations. The fluctuations and the dissipation go hand in hand; we cannot have one without the other...*the coupling of a dipole oscillator to the electromagnetic field has a dissipative component, in the form of radiation reaction, and a fluctuation component, in the form of zero-point (vacuum) field*; given the existence of radiation reaction, the vacuum field must also exist in order to preserve the canonical commutation rule and all it entails.”³¹

The fluctuation-dissipation theorem is a generalized Nyquist relation.³² It establishes a relation between the “impedance” in a general linear dissipative system and the fluctuations of appropriate generalized “forces.”

The theorem itself is expressed as a single equation, essentially the same as the original formula by **Johnson** from Bell Telephone Laboratory who, using $k_B T$ with equipartition, discovered the thermal agitation “noise” of electricity,³³

$$\langle V^2 \rangle = \frac{2}{\pi} \int_0^\infty R(\omega) E(\omega, T) d\omega \quad (11)$$

Here $\langle V^2 \rangle$ is the root mean square (RMS) value of the spontaneously fluctuating force, $R(\omega)$ is the generalized impedance of the system and $E(\omega, T)$ is the mean energy at temperature T of an oscillator of natural frequency ω ,

$$E(\omega, T) = \frac{1}{2} \hbar \omega + \hbar \omega / \left(e^{\hbar \omega / k_B T} - 1 \right) \quad (12)$$

which is the same Planck law as Equation (9). The use of the theorem’s Equation (11) applies exclusively to systems that have an irreversible linear dissipative portion, such as an impedance, capable of absorbing energy when subjected to a time-periodic perturbation. This is an essential factor to understanding the theorem’s applicability.

“The system may be said to be linear if the power dissipation is quadratic in the magnitude of the perturbation.”³⁴ If the condition of irreversibility is satisfied, such as with resistive heating, then the theorem predicts that there must exist a spontaneously fluctuating force coupled to it in equilibrium.

This constitutes an insight into the function of the quantum vacuum in a rigorous and profound manner. "The existence of a radiation impedance for the electromagnetic radiation from an oscillating charge is shown to imply a fluctuating electric field in the vacuum, and application of the general theorem yields the Planck radiation law."³⁵

Applying the theorem to ZPE, Callen et al. use radiation reaction as the dissipative force for electric dipole radiation of an oscillating charge in the vacuum. Based on Equation (2), we can express this in terms of the radiation damping constant and the change in acceleration (2nd derivative of velocity),

$$F_d = \frac{2}{3}(e^2/c^3) \partial^2 v / \partial t^2 = \Gamma m \partial^2 v / \partial t^2 \quad (13)$$

which is also the same equation derived by Feynman with a subtraction of retarded and advanced fields, followed by a reduction of the particle radius $\rightarrow 0$ for the radiation resistance force F_d .³⁶ Then, the familiar equation of motion for the accelerated charge with an applied force F and a natural frequency ω_0 is

$$F = m \partial v / \partial t + m \omega_0^2 x + F_d \quad (14)$$

For an oscillating dipole and dissipative Equation (13), Callen et al. derive the real part of the impedance from the "ratio of the in-phase component of F to v ," which can also be expressed in terms of the radiation damping constant³⁷

$$R(\omega) = \frac{2}{3} (\omega^2 e^2 / c^3) = \Gamma m \omega^2 \quad (15)$$

which is placed, along with Equation (12), into Equation (11). This causes $\langle V^2 \rangle$ to yield the same value as the energy density for isotropic radiation. Interestingly, V must then be "a randomly fluctuating force eE on the charge" with the conclusion regarding the ZPF, "hence a randomly fluctuating electric field E ."³⁸

This intrinsically demonstrates the vital relationship between the vacuum fluctuation force and an irreversible, dissipative process. The two form a complimentary relationship, analogous to Equation (1), having great fundamental significance.

Statement of the Problem

The engineering challenge of converting or extracting zero-point energy for useful work is, at the turn of this century, plagued by ignorance, prejudice and disbelief. The physics community does not in general acknowledge the emerging opportunities from fundamental discoveries of zero-point energy. Instead, there are many expositions from prominent sources explaining why the use of ZPE is forbidden.

A scientific editorial opinion states, "Exactly how much 'zero-point energy' resides in the vacuum is unknown. Some cosmologists have speculated that at the beginning of the universe, when conditions everywhere were more like those inside a black hole, vacuum energy was high and may have even triggered the big bang. Today the energy level should be lower. But to a few optimists, a rich supply still awaits if only we knew how to tap into it. These maverick proponents have postulated that the zero-point energy could explain 'cold fusion,' inertia, and other phenomena and might someday serve as part of a 'negative mass' system for propelling spacecraft. In an interview taped for PBS's *Scientific American Frontiers*, which aired in November (1997), Harold E. Puthoff, the director of the Institute for Advanced Studies, observed: 'For the chauvinists in the field like ourselves, we think the 21st century could be the zero-point-energy age.' That conceit is not shared by the majority of physicist; some even regard such optimism as pseudoscience that could leech funds from legitimate research. The conventional view is that the energy in the vacuum is miniscule."³⁹

Dr. Robert Forward, who passed away in 2002, said, "**Before I wrote the paper**⁴⁰ **everyone said that it was impossible to extract energy from the vacuum.** After I wrote the paper, everyone had to acknowledge that you could extract energy from the vacuum, but began to quibble about the

details. The spiral design won't work very efficiently... The amount of energy extracted is extremely small... You are really getting the energy from the surface energy of the aluminum, not the vacuum... Even if it worked perfectly, it would be no better per pound than a regular battery... Energy extraction from the vacuum is a conservative process, you have to put as much energy into making the leaves of aluminum as you will ever get out of the battery... etc... etc... Yes, it is very likely that the vacuum field is a conservative one, like gravity. But, no one has proved it yet. In fact, there is an experiment mentioned in my Mass Modification [ref. 15] paper (an antiproton in a vacuum chamber) which can check on that. The amount of energy you can get out of my aluminum foil battery is limited to the total surface energy of all the foils. For foils that one can think of making that are thick enough to reflect ultraviolet light, so the Casimir attraction effect works, say 20 nm (70 atoms) thick, then the maximum amount of energy you get out per pound of aluminum is considerably less than that of a battery. To get up to chemical energies, you will have to accrete individual atoms using the van der Waals force, which is the Casimir force for single atoms instead of conducting plates. My advice is to accept the fact that the vacuum field is probably conservative, and invent the vacuum equivalent of the hydroturbine generator in a dam.”⁴¹

Professor John Barrow from Cambridge University insists that, **“In the last few years a public controversy has arisen as to whether it is possible to extract and utilise the zero-point vacuum energy as a source of energy.** A small group of physicists, led by American physicist Harold Puthoff have claimed that we can tap into the infinite sea of zero-point fluctuations. They have so far failed to convince others that the zero-point energy is available to us in any sense. This is a modern version of the old quest for a perpetual motion machine: a source of potentially unlimited clean energy, at no cost... The consensus is that things are far less spectacular. It is hard to see how we could usefully extract zero-point energy. It defines the minimum energy that an atom could possess. If we were able to extract some of it the atom would need to end up in an even lower energy state, which is simply not available.”⁴²

With convincing skeptical arguments like these from the experts, how can the extraction of ZPE for the performance of useful work ever be considered feasible? **What engineering protocol can be theoretically developed for the extraction of ZPE if it can be reasonably considered to be feasible?** These are the central problems that are addressed by my thesis.

Purpose of the Study

This study is designed to propose a defensible feasibility argument for the extraction of ZPE from the quantum vacuum. Part of this comprehensive feasibility study also includes an engineering analysis of areas of research that are proving to be fruitful in the theoretical and experimental approaches to zero-point energy extraction. A further purpose is to look at energy extraction systems, in their various modalities, based on accepted physics and engineering principles, which may provide theoretically fruitful areas of discovery. Lastly, a few alternate designs which are reasonable prototypes for the extraction of zero-point energy, are also proposed.

Importance of the Study

It is unduly apparent that a study of this ubiquitous energy is overdue. The question has been asked, “Can new technology reduce our need for oil from the Middle East?”⁴³ More and more sectors of our society are demanding breakthroughs in energy generation, because of the rapid depletion of oil reserves and the environmental impact from the combustion of fossil fuels. “In 1956, the geologist M. King Hubbert predicted that U.S. oil production would peak in the early 1970s. Almost everyone, inside and outside the oil industry, rejected Hubbert’s analysis. The controversy raged until 1970, when the U.S. production of crude oil started to fall. Hubbert was right. Around 1995, several analysts began applying Hubbert’s method to world oil production, and most of them estimate that the peak year for world oil will be between 2004 and 2008. These analyses were reported in some of the most widely circulated sources: *Nature*, *Science* and *Scientific American*. None of our political leaders seem to be paying attention. If the predictions are correct, there will be enormous effects on the world economy.”⁴⁴ **Figure 4 is taken from the Deffeyes book showing the Hubbert method predicting world peak oil production and decline.**

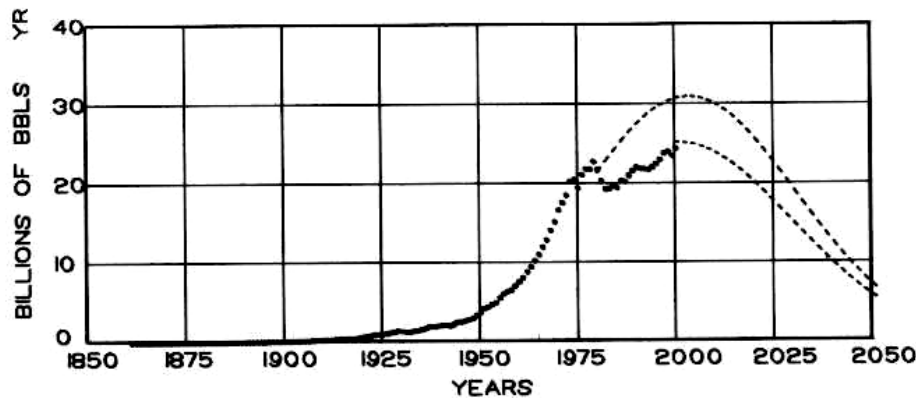


Figure 4

Hubbert's Peak: it predicted the world's oil production decline

It is now widely accepted, especially in Europe where I participated in the World Renewable Energy Policy and Strategy Forum, Solar Energy

Expo 2002 and the Innovative Energy Technology Conference, (all in Berlin, Germany), that the world oil production peak will probably only stretch to 2010, and that **global warming is now occurring faster than expected**. Furthermore, it will take decades to reverse the damage already set in motion, without even considering the future impact of "thermal forcing" which the future greenhouse gases will cause from generators and automobiles already irreversibly set in motion. The Kyoto Protocol, with its 7% decrease to 1990 levels of emissions, is a small step in the right direction but it does not address the magnitude of the problem, nor attempt to reverse it. "Stabilizing atmospheric CO₂ concentrations at safe levels will require a 60 – 80 per cent cut in carbon emissions from current levels, according to the best estimates of scientists."⁴⁵ Therefore, renewable energy sources like solar and wind power have seen a dramatic increase in sales every single year for the past ten years as more and more people see the future shock looming on the horizon. Solar photovoltaic panels, however, still have to reach the wholesale level in their cost of electricity that wind turbines have already achieved.

Another emerging problem that seems to have been unanticipated by the environmental groups is that too much proliferation of one type of machinery, such as windmills, can be objectionable as well. Recently, the Alliance to Protect Nantucket Sound filed suit against the U.S. Army Corps of Engineers to stop construction of a 197-foot tower being built to collect wind data for the development of a wind farm 5 miles off the coast of Massachusetts. Apparently, the wealthy residents are concerned that the view of Nantucket Sound will be spoiled by the large machines in the bay.⁴⁶ Therefore, **it is likely that only a compact, distributed, free energy generator will be acceptable to the public in the future**. Considering payback-on-investment, if it possessed a twenty-five year lifespan or more, while requiring minimum maintenance, then it will probably please most of the people, most of the time. The development of a ZPE generator theoretically would actually satisfy these criteria.

Dr. Steven Greer of the Disclosure Project has stated, "**classified above top-secret projects possess fully operational anti-gravity propulsion devices and new energy generation systems**, that, if declassified and put to peaceful uses, would empower a new human civilization without want, poverty or environmental damage."⁴⁷ However, since the declassification of black project, compartmentalized exotic energy technologies is not readily forthcoming, civilian physics research is being forced to reinvent fuelless energy sources such as zero-point energy extraction.

Regarding the existing conundrum of interplanetary travel, with our present lack of appropriate propulsion technology and cosmic ray bombardment protection, Arthur C. Clarke has predicted, that in 3001 the "inertialess drive" will most likely be put to use like a controllable gravity field, thanks to the landmark paper by Haisch et al.⁴⁸ "...if HR&P's theory can be proved, it opens up the prospect—however remote—of antigravity 'space drives,' and the even more fantastic possibility of controlling inertia."⁴⁹

Rationale of the Study

The hypothesis of the study is centered on the accepted physical basis for zero-point energy, its unsurpassed energy density, and the known physical manifestations of zero-point energy, proven by experimental observation. Conversion of energy is a well-known science which can, in theory, be applied to zero-point energy.

The scope of the study encompasses the known areas of physical discipline: mechanical, thermal, fluidic, and electromagnetic. Within these disciplines, the scope also extends from the macroscopic beyond the microscopic to the atomic. This systems science approach, which is fully discussed and analyzed in Chapter 4, includes categories such as:

1. Electromagnetic conversion of zero-point energy radiation
2. Fluidic entrainment of zero-point energy flow through a gradient
3. Mechanical conversion of zero-point energy force or pressure
4. Thermodynamic conversion of zero-point energy.

Definition of Terms

Following are terms that are used throughout the study:

1. **Bremsstrahlung**: Radiation caused by the deceleration of an electron. Its energy is converted into light. For heavier particles the retardations are never so great as to make the radiation important.⁵⁰
2. **Dirac Sea**: The physical vacuum in which particles are trapped in negative energy states until enough energy is present locally to release them.
3. **Energy**: The capacity for doing work. Equal to power exerted over time (e.g. kilowatt-hours). It can exist in linear or rotational form and is quantized in the ultimate part. It may be conserved or not conserved, depending upon the system considered. Mostly all terrestrial manifestations can be traced to solar origin, except for zero-point energy.
4. **Lamb Shift**: A shift (increase) in the energy levels of an atom, regarded as a Stark effect, due to the presence of the zero-point field. Its explanation marked the beginning of modern quantum electrodynamics.
5. **Parton**: The fundamental theoretical limit of particle size thought to exist in the vacuum, related to the Planck length (10^{-35} meter) and the Planck mass (22 micrograms), where quantum effects dominate spacetime. Much smaller than subatomic particles, it is sometimes referred to as the charged point particles within the vacuum that participate in the ZPE Zitterbewegung.
6. **Planck's Constant**: The fundamental basis of quantum mechanics which provides the measure of a quantum ($h = 6.6 \times 10^{-34}$ joule-second), it is also the ratio of the energy to the frequency of a photon.
7. **Quantum Electrodynamics**: The quantum theory of light as electromagnetic radiation, in wave and particle form, as it interacts with matter. Abbreviated "QED."
8. **Quantum Vacuum**: A characterization of empty space by which physical particles are unmanifested or stored in negative energy states. Also called the "physical vacuum."
9. **Uncertainty Principle**: The rule or law that limits the precision of a pair of physical measurements in complimentary fashion, e.g. the position and momentum, or the energy and time, forming the basis for zero-point energy.
10. **Virtual Particles**: Physically real particles emerging from the quantum vacuum for a short time determined by the uncertainty principle. This can be a photon or other particle in an intermediate state which, in quantum mechanics (Heisenberg notation) appears in matrix elements connecting

initial and final states. Energy is not conserved in the transition to or from the intermediate state. Also known as a virtual quantum.

11. Zero-point energy: The non-thermal, ubiquitous kinetic energy (averaging $\frac{1}{2}hf$) that is manifested even at zero degrees Kelvin, abbreviated as "ZPE." Also called vacuum fluctuations, zero-point vibration, residual energy, quantum oscillations, the vacuum electromagnetic field, virtual particle flux, and recently, dark energy.
12. Zitterbewegung: An oscillatory motion of an electron, exhibited mainly when it penetrates a voltage potential, with frequency greater than 10^{21} Hertz. It can be associated with pair production (electron-positron) when the energy of the potential exceeds $2mc^2$ (m = electron mass). Also generalized to represent the rapid oscillations associated with zero-point energy.

Overview of the Study

In all of the areas of investigation, so far no known extractions of zero-point energy for useful work have been achieved, though it can be argued that incidental ZPE extraction has manifested itself macroscopically. By exploring the main physical principles underlying the science of zero-point energy, certain modalities for energy conversion achieve prominence while others are regarded as less practical. Applying physics and engineering analysis, a scientific research feasibility study of ZPE extraction, referenced by rigorous physics theory and experiment is generated.

With a comprehensive survey of conversion modalities, new alternate, efficient methods for ZPE extraction are presented and analyzed. Comparing the specific characteristics of zero-point energy with the known methods of energy conversion, the common denominators should offer the most promising feasibility for conversion of zero-point energy into useful work. The advances in nanotechnology are also examined, especially where ZPE effects are already identified as interfering with mechanical and electronic behavior of nanodevices.

CHAPTER 2 - Review of Related Literature

Historical Perspectives

Reviewing the literature for zero-point energy necessarily starts with the historical developments of its discovery. In 1912, **Max Planck** published the first journal article to describe the discontinuous emission of radiation, based on the discrete quanta of energy.⁵¹ In this paper, Planck's now-famous "blackbody" radiation equation contains the residual energy factor, one half of hf , as an additional term ($\frac{1}{2}hf$), dependent on the frequency f , which is always greater than zero (where h = Planck's constant). It is therefore widely agreed that "Planck's equation marked the birth of the concept of zero-point energy."⁵² This mysterious factor was understood to signify the average oscillator energy available to each field mode even when the temperature reaches absolute zero. In the meantime, Einstein had published his "fluctuation formula" which describes the energy fluctuations of thermal radiation.⁵³ Today, "the particle term in the Einstein fluctuation formula may be regarded as a consequence of zero-point field energy."⁵⁴

During the early years of its discovery, Einstein^{55,56} and **Dirac**^{57,58} saw the value of zero-point energy and promoted its fundamental importance. The 1913 paper by Einstein computed the specific heat of molecular hydrogen, including zero-point energy, which agreed very well with experiment. Debye also made calculations including zero-point energy (ZPE) and showed its effect on Roentgen ray (X-ray) diffraction.⁵⁹

Throughout the next few decades, zero-point energy became intrinsically important to quantum mechanics with the birth of the uncertainty principle. "In 1927, **Heisenberg**, on the basis of the Einstein-de Broglie relations, showed that it is impossible to have a simultaneous knowledge of the [position] coordinate x and its conjugate momentum p to an arbitrary degree of accuracy, their uncertainties being given by the relation $\Delta x \Delta p \geq h / 4\pi$."⁶⁰ This expression of Equation (1) is not the standard form that Heisenberg used for the uncertainty principle, however. He invented a character \hbar called "h-bar," which equals $h/2\pi$ (also introduced in Chapter 1). If this shortcut notation is used for the uncertainty principle, it takes the form $\Delta x \Delta p \geq \hbar / 2$ or $\Delta E \Delta t \geq \hbar / 2$, which is a more familiar equation to physicists and found in most quantum mechanics texts.

By 1935, the application of harmonic oscillator models with various boundary conditions became a primary approach to quantum particle physics and atomic physics.⁶¹ Quantum mechanics also evolved into "wave mechanics" and "matrix mechanics" which are not central to this study. However, with the evolution of matrix mechanics came an intriguing application of matrix "operators" and "commutation relations" of x and p that today are well known in quantum mechanics. With these new tools, the "quantization of the harmonic oscillator" is all that is required to reveal the existence of the zero-point ground state energy.⁶²

"This residual energy is known as the zero-point energy, and is a direct consequence of the uncertainty principle. Basically, it is impossible to completely stop the motion of the oscillator, since if the motion were zero, the uncertainty in position Δx would be zero, resulting in an infinitely large uncertainty in momentum (since $\Delta p = \hbar / 2\Delta x$). The zero-point energy represents a sharing of the uncertainty in position and the uncertainty in momentum. The energy associated with the uncertainty in momentum gives the zero-point energy."⁶³

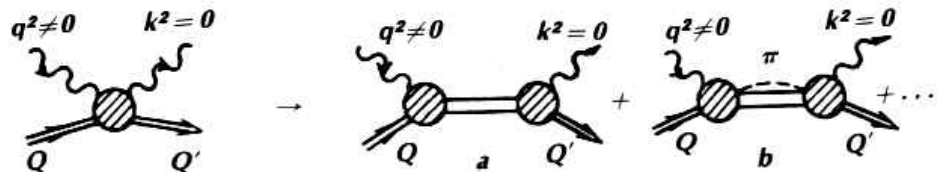
Another important ingredient in the development of the understanding of zero-point energy came from the Compton effect. "Compelling confirmation of the concept of the photon as a concentrated bundle of energy was provided in 1923 by **A. H. Compton** who earned a Nobel prize for this work in 1927."⁶⁴ **Compton scattering**, as it is now known, can only be understood using the energy-frequency relation $E = hf$ that was proposed previously by **Einstein** to explain the photoelectric effect in terms of Planck's constant, h .⁶⁵

Ruminations about the zero-point vacuum field (ZPF), in conjunction with Einstein's famous equation $E = mc^2$ and the limitations of the uncertainty principle, suggested that photons may also be created and destroyed "out of nothing." Such photons have been called "virtual" and are prohibited by classical laws of physics. **"But in quantum mechanics the uncertainty principle allows energy conservation to be violated for a short time interval $\Delta t = \hbar / 2\Delta E$.** As long as the energy is conserved after this time, we can regard the virtual particle exchange as a small fluctuation of energy that is entirely consistent with quantum mechanics."⁶⁶ Such virtual particle exchanges later became an integral part of an advanced theory called quantum electrodynamics (QED) where "Feynmann diagrams," developed by Nobel-prize winner **Richard Feynmann** to describe particle collisions, often show the virtual photon exchange between the paths of two nearby particles.⁶⁷ Figure 5 shows a sample of the Compton scattering of a virtual photon as it contributes to the radiated energy effect of bremsstrahlung (see Definition of Terms on page 15).⁶⁸

Casimir Predicts a Measurable ZPE Effect

In 1948, it was predicted that virtual particle appearances should exert a force that is measurable.⁶⁹ **Casimir** not only predicted the presence of such a force but also explained why van der Waals forces dropped off unexpectedly at long range separation between atoms. The Casimir effect was first verified experimentally using a variety of conductive plates by **Sparnaay**.⁷⁰

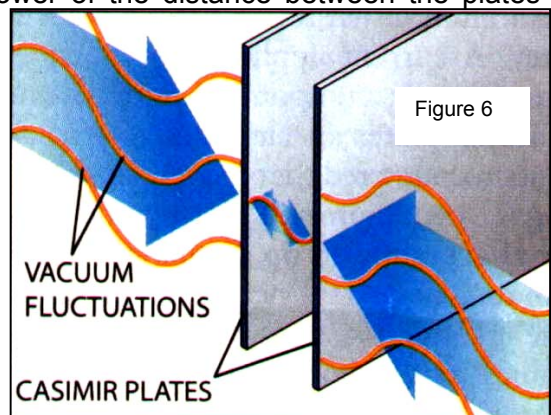
Figure 5 – A virtual photon hits a particle causing deflection (Compton scattering) which QED also analyzes as (a) and (b)



There was still an interest for an improved test of the Casimir force using conductive plates as modeled in Casimir's paper to better accuracy than Sparnaay. In 1997, Dr. **Lamoreaux**, from Los Alamos Labs, performed the experiment with less than one micrometer (micron) spacing between gold-plated parallel plates attached to a torsion pendulum.⁷¹ In retrospect, he found it to one of the most intellectually satisfying experiments that he ever performed since the results matched the theory so closely (within 5%). This event also elevated zero-point energy fluctuations to a higher level of public interest. **Even the *New York Times* covered the event.**⁷²

The Casimir Effect has been posited as a force produced solely by activity in the empty vacuum (see Figure 6). The Casimir force is also very powerful at small distances. Besides being independent of temperature, it is inversely proportional to the fourth power of the distance between the plates at larger distances and inversely proportional to the third power of the distance between the plates at short distances.⁷³ (Its frequency dependence is a third power.)

Lamoreaux's results come as no surprise to anyone familiar with quantum electrodynamics, but they serve as a material confirmation of a bazaar theoretical prediction: that QED predicts the all-pervading vacuum continuously spawns particles and waves that spontaneously pop in and out of existence. Their time of existence is strictly limited by the uncertainty principle but they create some havoc while they bounce around during their brief lifespan. The churning quantum foam is believed to extend throughout the universe even filling the empty space within the atoms in human bodies. Physicists theorize that on an infinitesimally small scale, far, far smaller than the diameter of atomic nucleus, quantum fluctuations produce a foam of



erupting and collapsing, virtual particles, visualized as a topographic distortion of the fabric of space time (Figure 7).

Ground State of Hydrogen is Sustained by ZPE

Looking at the electron in a set ground-state orbit, it consists of a bound state with a central Coulomb potential that has been treated successfully in physics with the harmonic oscillator model. However, the anomalous repulsive force balancing the attractive Coulomb potential remained a mystery

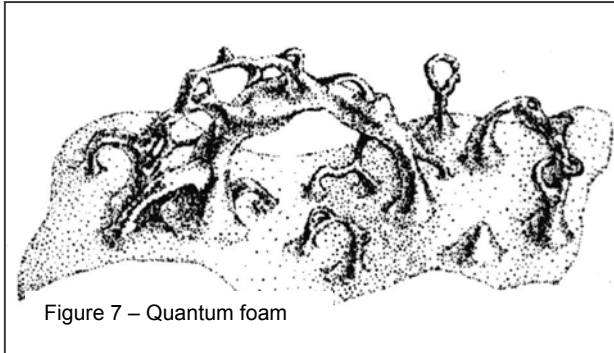


Figure 7 – Quantum foam

until Puthoff published a ZPE-based description of the hydrogen ground state.⁷⁴ This derivation caused a stir among physicists because of the extent of influence that was now afforded to vacuum fluctuations. It appears from Puthoff's work that the ZPE shield of virtual particles surrounding the electron may be the repulsive force. Taking a simplistic argument for the rate at which the atom absorbs energy from the vacuum field and equating it to the radiated loss of energy from accelerated charges, the Bohr quantization condition for the

ground state of a one-electron atom like hydrogen is obtained. "We now know that the vacuum field is in fact formally necessary for the stability of atoms in quantum theory."⁷⁵

Lamb Shift Caused by ZPE

Another historically valid test in the verification of ZPE has been what has been called the "Lamb shift." Measured by Dr. Willis Lamb in the 1940's, it actually showed the effect of zero point fluctuations on certain electron levels of the hydrogen atom, causing a fine splitting of the levels on the order of 1000 MHz.⁷⁶ Physicist Margaret Hawton describes the Lamb shift as "a kind of one atom Casimir Effect" and predicts that the vacuum fluctuations of ZPE need only occur in the vicinity of atoms or atomic particles.⁷⁷ This seems to agree with the discussion about Koltick in Chapter 1, illustrated in Figure 3.

Today, "the majority of physicists attribute spontaneous emission and the Lamb shift entirely to vacuum fluctuations."⁷⁸ This may lead scientists to believe that it can no longer be called "spontaneous emission" but instead should properly be labeled forced or "stimulated emission" much like laser light, even though there is a random quality to it. However, it has been found that radiation reaction (the reaction of the electron to its own field) together with the vacuum fluctuations contribute equally to the phenomena of spontaneous emission.⁷⁹

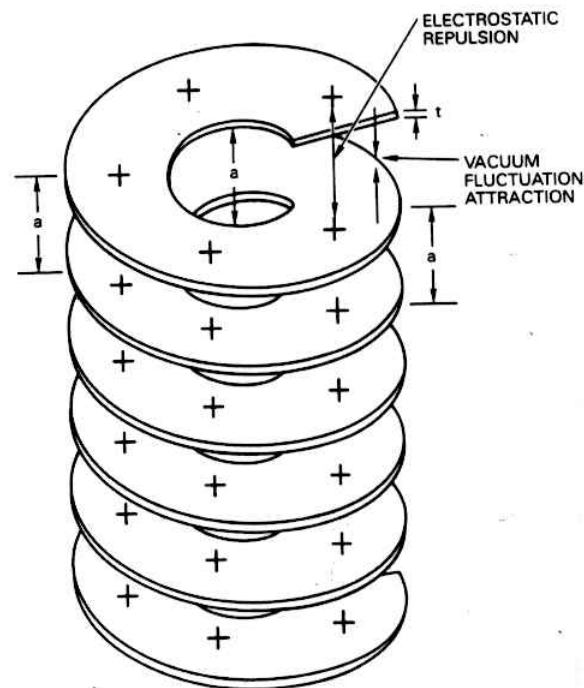


Figure 8 Spiral design for a vacuum-fluctuation battery.

Experimental ZPE

The first journal publication to propose a Casimir machine for "the extracting of electrical energy from the vacuum by cohesion of charge foliated conductors" is summarized here.⁸⁰ Dr. Forward describes this "parking ramp" style corkscrew or spring as a ZPE battery that will tap electrical energy from the vacuum and allow charge to be stored. The spring tends to be compressed from the Casimir force but the like charge from the electrons stored will cause a repulsion force to balance the spring separation distance. It tends to compress upon dissipation and usage but expand physically with charge storage. He suggests using micro-fabricated sandwiches of ultrafine metal dielectric layers. Forward also points out that ZPE seems to have a definite potential as an energy source.

Another interesting experiment is the "Casimir Effect at Macroscopic Distances" which proposes observing the Casimir force at a distance of a few centimeters using confocal optical resonators within the sensitivity of laboratory instruments.⁸¹ This experiment makes the microscopic Casimir effect observable and greatly enhanced.

In general, many of the experimental journal articles refer to vacuum effects on a cavity that is created with two or more surfaces. Cavity QED is a science unto itself. "Small cavities suppress atomic transitions; slightly larger ones, however, can enhance them. When the size of the cavity surrounding an excited atom is increased to the point where it matches the wavelength of the photon that the atom would naturally emit, vacuum-field fluctuations at that wavelength flood the cavity and become stronger than they would be in free space."⁸² It is also possible to perform the opposite feat. "Pressing zero-point energy out of a spatial region can be used to temporarily increase the Casimir force."⁸³ The materials used for the cavity walls are also important. It is well-known that the attractive Casimir force is obtained from highly reflective surfaces. However, "...a repulsive Casimir force may be obtained by considering a cavity built with a dielectric and a magnetic plate. The product r of the two reflection amplitudes is indeed negative in this case, so that the force is repulsive."⁸⁴ **For parallel plates in general, a "magnetic field inhibits the Casimir effect."**⁸⁵

An example of an idealized system with two parallel semiconducting plates separated by an variable gap that utilizes several concepts referred to above is Dr. Pinto's "optically controlled vacuum energy transducer."⁸⁶ By optically pumping the cavity with a microlaser as the gap spacing is varied, "the total work done by the Casimir force along a closed path that includes appropriate transformations does not vanish...In the event of no other alternative explanations, one should conclude that major technological advances in the area of endless, by-product free-energy production could be achieved."⁸⁷ More analysis on this revolutionary invention will be presented in Chapter 4.

ZPE Patent Review

For any researcher reviewing the literature for an invention design such as energy transducers, it is well-known in the art that it is vital to perform a patent search. In 1987, Werner and Sven from Germany patented a "Device or method for generating a varying Casimir-analogous force and liberating usable energy" with patent #DE3541084. It subjects two plates in close proximity to a fluctuation which they believe will liberate energy from the zero-point field.

In 1996, Jarck Uwe from France patented a "Zero-point energy power plant" with PCT patent #WO9628882. It suggests that a coil and magnet will be moved by ZPE which then will flow through a hollow body generating induction through an energy whirlpool. It is not clear how such a macroscopic apparatus could resonate or respond to ZPE effectively.

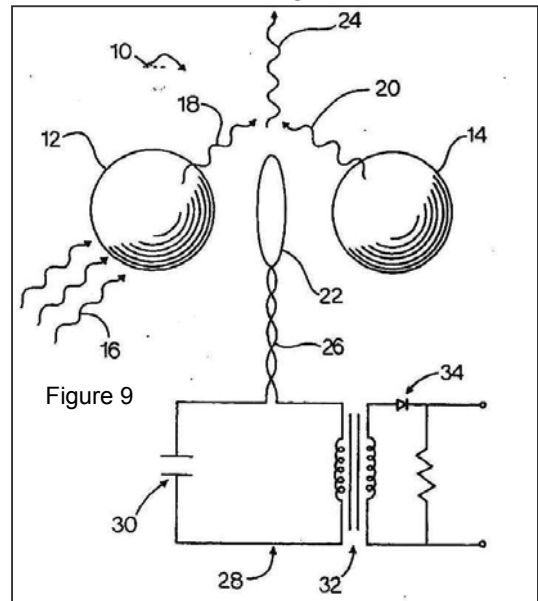
On Dec. 31, 1996 the conversion of ZPE was patented for the first time in the United States with US patent #5,590,031. The inventor, Dr. Frank Mead, Director of the Air Force Research Laboratory, designed receivers to be spherical collectors of zero point radiation (see Figure 9). One of the interesting considerations was to design it for the range of extremely high frequency that ZPE offers, which by some estimates, corresponds to the Planck frequency of 10^{43} Hz. We do not have any apparatus to amplify or even oscillate at that frequency currently. For example, gigahertz radar is only 10^{10} Hz or so. Visible light is about 10^{14} Hertz and gamma rays reach into the 20th power, where the

wavelength is smaller than the size of an atom. However, that's still a long way off from the 40th power. The essential innovation of the Mead patent is the "beat frequency" generation circuitry, which creates a lower frequency output signal from the ZPE input.

Another patent that utilizes a noticeable ZPE effect is the AT&T "Negative Transconductance Device" by inventor, Federico Capasso (US #4,704,622). It is a resonant tunneling device with a one-dimensional quantum well or wire. The important energy consideration involves the additional zero-point energy which is available to the electrons in the extra dimensional quantized band, allowing them to tunnel through the barrier. **This solid state, multi-layer, field effect transistor demonstrates that without ZPE, no tunneling would be possible. It is supported by the virtual photon tunnel effect.**⁸⁸

Grigg's Hydrosonic Pump is another patent (U.S. #5,188,090), whose water glows blue when in cavitation mode, that consistently has been measuring an over-unity performance of excess heat energy output. It appears to be a dynamic Casimir effect that contributes to sonoluminescence.⁸⁹

Joseph Yater patented his "Reversible Thermoelectric Converter with Power Conversion of Energy Fluctuations" (#4,004,210) in 1977 and also spent years defending it in the literature. In 1974, he published "Power conversion of energy fluctuations."⁹⁰ In 1979, he published an article on the "Relation of the second law of thermodynamics to the power conversion of energy fluctuations"⁹¹ and also a rebuttal to comments on his first article.⁹² It is important that he worked so hard to support such a radical idea, since it appears that energy is being brought from a lower temperature reservoir to a higher one, which normally violates the 2nd law. The basic concept is a simple rectification of thermal noise, which also can be found in the Charles Brown patent (#3,890,161) of 1975, "Diode array for rectifying thermal electrical noise."



Many companies are now very interested in such processes for powering nanomachines. While researching this ZPE thesis, I attended the AAAS workshop by IBM on nanotechnology in 2000, where it was learned that R. D. Astumian proposed in 1997 to rectify thermal noise (as if this was a new idea).⁹³ **This apparently has provoked IBM to begin a "nanorectifier" development program.**

Details of some of these and other inventions are analyzed in Chapter 4.

ZPE and Sonoluminescence

Does sonoluminescence (SL) tap ZPE? This question is based upon the experimental results of ultrasound cavitation in various fluids which emit light and extreme heat from bubbles 100 microns in diameter which implode violently creating temperatures of 5,500 degrees Celsius. Scientists at UCLA have recently measured the length of time that sonoluminescence flashes persist. Barber discovered that they only exist for 50 picoseconds (ps) or shorter, which is too brief for the light to be produced by some atomic process. Atomic processes, in comparison, emit light for at least several tenths of a nanosecond (ns). "To the best of our resolution, which has only established upper bounds, the light flash is less than 50 ps in duration and it occurs within 0.5 ns of the minimum bubble radius. The SL flashwidth is thus 100 times shorter than the shortest (visible) lifetime of an excited state of a hydrogen atom."⁹⁴

Critical to the understanding of the nature of this light spectrum however, is what other mechanism than atomic transitions can explain SL. Dr. Claudia Eberlein in her pioneering paper "Sonoluminescence and QED" describes her conclusion that only the ZPE spectrum matches the light

emission spectrum of sonoluminescence, and could react as quickly as SL.⁹⁵ She thus concludes that SL must therefore be a ZPE phenomena. It is also acknowledged that “Schwinger proposed a physical mechanism for sonoluminescence in terms of photon production due to changes in the properties of the quantum-electrodynamic (QED) vacuum arising from a collapsing dielectric bubble.”⁹⁶

Gravity and Inertia Related to ZPE

Another dimension of ZPE is found in the work of Dr. Harold Puthoff, who has found that gravity is a zero-point-fluctuation force, in a prestigious Physical Review article that has been largely uncontested.⁹⁷ He points out that the late Russian physicist, Dr. Sakharov regarded gravitation as not a fundamental interaction at all, but an induced effect that's brought about by changes in the vacuum when matter is present. The interesting part about this is that the mass is shown to correspond to the kinetic energy of the zero-point-induced internal particle jittering, while the force of gravity is comprised of the long ZPE wavelengths. This is in the same category as the low frequency, long range forces that are now associated with Van der Waal's forces.

Referring to the inertia relationship to zero-point energy, Haisch et al. find that first of all, that inertia is directly related to the Lorentz Force which is used to describe Faraday's Law.⁹⁸ As a result of their work, **the Lorentz Force now has theoretically been shown to be directly responsible for an electromagnetic resistance arising from a distortion of the zero-point field in an accelerated frame.** They also explain how the magnetic component of the Lorentz force arises in ZPE, its matter interactions, and also a derivation of Newton's law, $F = ma$. From quantum electrodynamics, Newton's law appears to be related to the known distortion of the zero point spectrum in an accelerated reference frame.

Haisch et al. present an understanding as to why force and acceleration should be related, or even for that matter, what is mass.⁹⁹ Previously misunderstood, mass (gravitational or inertial) is apparently more electromagnetic than mechanical in nature. The resistance to acceleration defines the inertia of matter but interacts with the vacuum as an electromagnetic resistance. To summarize the inertia effect, it is connected to a distortion at high frequencies of the zero-point field. Whereas, the gravitational force has been shown to be a low frequency interaction with the zero point field.

Recently, Alexander Feigel has proposed that **the momentum of the virtual photons can depend upon the direction in which they are traveling, especially if they are in the presence of electric or magnetic fields.** His theory and experiment offers a possible explanation for the accelerated expansion of distant galaxies.¹⁰⁰

Heat from ZPE

In what may seem to appear as a major contradiction, it has been proposed that, in principle, basic thermodynamics allows for the extraction of heat energy from the zero-point field via the Casimir force. “However, the contradiction becomes resolved upon recognizing that two different types of thermodynamic operations are being discussed.”¹⁰¹ Normal thermodynamically reversible heat generation process is classically limited to temperatures above absolute zero ($T > 0$ K). “For heat to be generated at $T = 0$ K, an irreversible thermodynamic operation needs to occur, such as by taking the systems out of mechanical equilibrium.”¹⁰² Examples are given of theoretical systems with two opposite charges or two dipoles in a perfectly reflecting box being forced closer and farther apart. Adiabatic expansion and irreversible adiabatic free contraction curves are identified on a graph of force versus distance with reversible heating and cooling curves connecting both endpoints. Though a practical method of energy or heat extraction is not addressed in the article, the basis for designing one is given a physical foundation.

A summary of all three ZPE effects introduced above (heat, inertia, and gravity) can be found in the most recent Puthoff et al. publication entitled, **“Engineering the Zero-Point Field and Polarizable Vacuum for Interstellar Flight.”**¹⁰³ In it they state, “One version of this concept involves the projected possibility that empty space itself (the quantum vacuum, or space-time metric) might be manipulated so as to provide energy/thrust for future space vehicles. Although far-reaching, such a proposal is solidly

grounded in modern theory that describes the vacuum as a polarizable medium that sustains energetic quantum fluctuations."¹⁰⁴ A similar article proposes that "monopolar particles could also be accelerated by the ZPF, but in a much more effective manner than polarizable particles."¹⁰⁵ Furthermore, "...the mechanism should eventually provide a means to transfer energy...from the vacuum electromagnetic ZPF into a suitable experimental apparatus."¹⁰⁶ With such endorsements for the use of ZPE, the value of this present study seems to be validated and may be projected to be scientifically fruitful.

Summary

To summarize the scientific literature review, the experimental evidence for the existence of ZPE include the following:

- 1) Anomalous magnetic moment of the electron¹⁰⁷
- 2) Casimir effect¹⁰⁸
- 3) Diamagnetism¹⁰⁹
- 4) Einstein's fluctuation formula¹¹⁰
- 5) Gravity¹¹¹
- 6) Ground state of the hydrogen atom¹¹²
- 7) Inertia¹¹³
- 8) Lamb shift¹¹⁴
- 9) Liquid Helium to $T = 0\text{ K}$ ¹¹⁵
- 10) Planck's blackbody radiation equation¹¹⁶
- 11) Quantum noise¹¹⁷
- 12) Sonoluminescence¹¹⁸
- 13) Spontaneous emission¹¹⁹
- 14) Uncertainty principle¹²⁰
- 15) Van der Waals forces¹²¹

The apparent discrepancy in the understanding of the concepts behind ZPE comes from the fact that ZPE evolves from classical electrodynamics theory and from quantum mechanics. For example, Dr. Frank Mead (US Patent #5,590,031) calls it "zero point electromagnetic radiation energy" following the tradition of Timothy Boyer who simply added a randomizing parameter to classical ZPE theory thus inventing "stochastic electrodynamics" (SED).¹²² Lamoreaux, on the other hand, refers to it as "a flux of virtual particles", because the particles that react and create some of this energy are popping out of the vacuum and going back in.¹²³ The *New York Times* simply calls it "quantum foam." But the important part about it is from Dr. Robert Forward, **"the quantum mechanical zero point oscillations are real."**¹²⁴

CHAPTER 3 - Methodology

In this chapter, the methods used in this research feasibility study will be reviewed, including the approach, the data gathering method, the database selected for analysis, the analysis of the data, the validity of the data, the uniqueness (originality) and limitations of the method, along with a brief summary.

Approach

The principal argument for the feasibility study of zero-point energy extraction is that it provides a systematic way of evaluating the fundamental properties of this phenomena of nature. Secondly, research into the properties of ZPE offer an opportunity for innovative application of basic principles of energy conversion. These basic transduction methods fall into the disciplines of mechanical, fluidic, thermal, and electrical systems.¹²⁵ It is well-known that these engineering systems find application in all areas of energy generation in our society. Therefore, it is reasonable that this study utilize a systems approach to zero-point energy conversion while taking into consideration the latest quantum electrodynamic findings regarding ZPE.

There are several important lessons that can be conveyed by a feasibility study of ZPE extraction.

- 1) It permits a grounding of observations and concepts about ZPE in a scientific setting with an emphasis toward engineering practicability.
- 2) It furnishes information from a number of sources and over a wide range of disciplines, which is important for a maximum potential of success.
- 3) It can provide the dimension of history to the study of ZPE thereby enabling the investigator to examine continuity and any change in patterns over time.
- 4) It encourages and facilitates, in practice, experimental assessment, theoretical innovation and even fruitful generalizations.
- 5) It can offer the best possible avenues, which are available for further research and development, for the highest probability of success.

A feasibility study enables an investigation to take place into every detail of the phenomena being researched. The feasibility study is an effective vehicle for providing an overview of the breadth and depth of the subject at hand, while providing the reader an opportunity to probe for internal consistency.

What is a Feasibility Study?

A feasibility study is a complete examination of the practicability of a specific invention, project, phenomena, or process. It strives to provide the requisite details necessary to support its conclusion concerning the possibility or impossibility of accomplishing the goal of the research study. As such, it takes an unbiased viewpoint toward the subject matter and reflects a balanced presentation of the facts that are currently available in the scientific literature.

Feasibility studies are the hallmark of engineering progress, often saving investors millions of dollars, while providing a superior substitute for risk assessment. Therefore, such studies are required before any consideration is made of the investment potential of an invention, project, process, or phenomena by venture capitalists. Feasibility studies thus provide all of the possible engineering details that can be presented beforehand so that the construction stage can proceed smoothly and with a prerequisite degree of certitude as to the outcome.

Feasibility studies can also provide a wealth of information just with the literature survey that is an integral part of the research. Along with the survey, an expert engineering and physics assessment is usually provided regarding the findings reported in the literature and how they directly relate to the capability of the process, phenomena, project, or invention to be put into effect.

As such, a feasibility study offers the best possible original research of the potential for successful utilization, with a thick descriptive style so necessary for an accurate and honest judgment.¹²⁶

“A good feasibility study will contain clear supporting evidence for its recommendations. It’s best to supply a mix of numerical data with qualitative, experience-based documentation (where appropriate). The report should also indicate a broad outline of how to undertake any recommended development work. This will usually involve preparing an initial, high-level project plan that estimates the required project scope and resources and identifies major milestones. An outline plan makes everyone focus more clearly on the important implementation issues and generate some momentum for any subsequent work. This is especially true if feasibility teams suspect that the development itself will become their baby. A sound, thorough feasibility study will also ease any subsequent development tasks that gain approval. The feasibility study will have identified major areas of risk and outlined approaches to dealing with these risks. Recognising the nature of feasibility projects encourages the successful implementation of the best ideas in an organisation and provides project managers with some novel challenges.”¹²⁷

Data Gathering Method

The method used in this feasibility study is the same that is used in pure as well as applied research. Through a review of the scientific literature, certain approaches to the conversion of zero-point energy into useful work demonstrate more promise and engineering feasibility than others. Combining the evaluation with the known theories and experimental discoveries of zero-point energy and the author’s professional engineering knowledge of electromechanical fabrication, a detailed recommendation and assessment for the most promising and suitable development is then made. This procedure follows the standard method used in most feasibility studies.^{128,129,130}

Database Selected for Analysis

The database for this study consists of mostly peer-reviewed physics journals, engineering journals, science magazines, patent literature, textbooks, which are authored by physicists and engineers.

Analysis of Data

The analysis of the data is found in Chapter 4, where the findings are explored. The most promising possibilities, from an engineering standpoint, are the zero-point energy conversion concepts that are past the research stage or the proof-of-principle stage and into the developmental arena. Using the scientific method, a thorough examination of the data is presented, with physics and engineering criteria, to determine the feasibility of zero-point energy extraction.

Validity of Data

The data used in this study can be presumed to be valid beyond a reasonable doubt. Ninety years ago, when zero-point energy was first discovered, the validity of the data may have been questioned. However, after so much experimental agreement with theory has followed in the physics literature, it can be said that the data has stood the test of time. Furthermore, in the past decade, there has been a dramatic increase in the number of journal publications on the subject of zero-point energy, demonstrating the timeliness and essential value of this study. Excluding any anomalous findings that have not been replicated or verified by other scientists, it can be presumed that the data presented in this feasibility study represents the highest quality that the scientific community can offer.

Uniqueness and Limitations of the Method

The method applied in this study, though it appears to be universal in its approach, is being applied for the first time to determine the utility of zero-point energy extraction. Only through experimental verification can the method be validated. However, many intermediate steps required for utilization have already been validated by experiment, as mentioned in the above sections.

As with any study of this nature, certain limitations are inherent in the method. The feasibility study draws from a large database and involves a great number of variables, which is, in itself, a limitation. The nature of ZPE is also a limitation because it is so unusual and foreign to most scientists, while many standard testing methods used for other fields and forces fail to reveal its presence.

These variables and limitations have been minimized to every extent possible.

Summary

The method used in this feasibility study is the application of the basic principles of energy conversion in the mechanical, fluidic, thermal, and electromagnetic systems to zero-point energy research. It is a systems approach that has a fundamental basis in the scientific method. By reviewing journal articles and textbooks in the physics and engineering field of zero-point energy, certain data has been accumulated. The analysis of the data is conducted in a critical manner with an approximate rating system in order to evaluate the practical applications of both theory and experiment, and the likelihood of success for energy conversion. **It is believed that this is the first time such an approach has been used and applied to the field of zero-point energy conversion.** As such, new and exciting conclusions are bound to emerge.

CHAPTER 4 - Analysis

Introduction to Vacuum Engineering

The emerging discipline of vacuum engineering encompasses the present investigation into energy conversion modalities that offer optimum feasibility. It is believed by only a minority of physicists that the vacuum can be engineered to properly facilitate the transduction of energy to useful work. In this chapter, two intriguing energy converters (Electromagnetic and Casimir) are examined and analyzed according to the methodology outlined in Chapter 3. Then, several ZPE techniques for the vacuum engineer's toolkit are examined, such as focusing vacuum fluctuations, spatial squeezing, etc.

The scope of this feasibility study is detailed in Chapter 1 and will include zero-point energy conversion methodologies in the areas of electromagnetism, fluid mechanics, thermodynamics, mechanical physics, and some quantum theories.

Vacuum engineering considerations often exhibit a particular bias toward wave or particle. It is difficult or perhaps impossible to design a zero-point energy converter that will utilize both wave and particle aspects of the quantum vacuum, since the size of the transducer determines which will dominate.

Electromagnetic Zero-Point Energy Converter

Treating the quantum vacuum initially as an all-pervading electromagnetic wave with a high bandwidth is a classical physics approach. Among various examples, the most intriguing is a U.S. patent (#5,590,031) proposing microscopic antennae for collecting and amplifying zero-point electromagnetic energy. Introduced in Figure 9, it is **a US Air Force invention by Mead et al. that offers sufficient scientific rigor and intrigue to warrant further analysis**. The patent's spherical resonators are small scatterers of the zero-point vacuum flux and capitalize on the electromagnetic wave nature of the ZPF. Utilizing this design to start the inquiry at least into the microscopic and nanotechnology realm, it is helpful to review the key design parameters in the Mead patent,

- the energy density increases with frequency (col. 7, line 63),
- the spheres are preferably microscopic in size (col. 8, line 3),
- a volume of close proximity spheres enhances output (col. 8, line 20),
- resonant "RHO values" which correspond to propagation values are sought for which coefficients a_n or b_n is infinity (col. 6, line 40),
- spherical structures are of different size so that the secondary fields will be a lower frequency than the incident radiation (col. 3, line 7),
- the converter circuitry may also include a transformer for voltage optimization and possibly a rectifier to convert the energy into a direct current (col. 3, line 30),
- the system also includes an antenna which receives the beat frequency (col. 7, line 35).

It is noted in the patent that **"zero point radiation is homogeneous and isotropic as well as ubiquitous**. In addition, since zero point radiation is also invariant with respect to Lorentz transformation, the zero point radiation spectrum has the characteristic that the intensity of the radiation at any frequency is proportional to the cube of that frequency" (col. 1, line 30). This sets the stage for an optimum design of the highest frequency collector possible that the inventors believe will work anywhere in the universe.

Another area of interest upon review is the opinion of the inventors that, "At resonance, electromagnetically induced material deformations of the receiving structures produce secondary fields of electromagnetic energy therefrom which may have evanescent energy densities several times that of

the incident radiation" (col. 2, line 65). However, this does not seem to be a physically justifiable statement, nor is it defended anywhere else in the patent. Furthermore, the discussion diverges and instead proceeds toward the formation of "beat frequencies" which are produced through interference resulting in the sum and difference of two similar frequencies. It is noted that the subtraction of the frequencies from two receivers of slightly different size is of primary importance to the invention claimed (col. 3, line 7).

The engineering considerations in the patent include the statement that "packing a volume with such spheres in close proximity could enhance the output of energy" (col. 8, line 20). The enhancement referred to here is understood to mean the multiplied effect from having several interference sources for the beat frequency production and amplification. Upon researching this aspect of the invention, it is found however, that scattering by a collection of scatterers can actually reduce the output of energy, especially if the spheres are randomly distributed. In that case, an incoherent superposition of individual contributions will have destructive instead of constructive interference. A large regular array of scatterers, even if transparent, tends to absorb rather than scatter, such as a simple cubic array of scattering centers in a rock salt or quartz crystal.¹³¹

This crucial feature of the patent involving the receiver's output involves a method for analyzing electromagnetic or Mie scattering from dielectric spheres¹³² (col. 4, line 60). The patent relies upon a report detailing the calculations by Cox (which has been obtained from the inventor) of two infinite series equations for the electric and magnetic components of the spherical reflection of incident electromagnetic waves.¹³³ The report, summarized in the patent, utilizes spherical Bessel functions to solve two pairs of inhomogeneous equations for the components of radiation scattering from a dielectric sphere.

For a particular radius of the spheres, resonance will occur at a corresponding frequency. In the patent, with the sphere diameter set equal to 2 microns (2×10^{-6} m) one solution is found as an example (col. 7, line 10). The resonant frequency is calculated to be about 9×10^{15} radians per second (1.5×10^{14} Hz), which is the

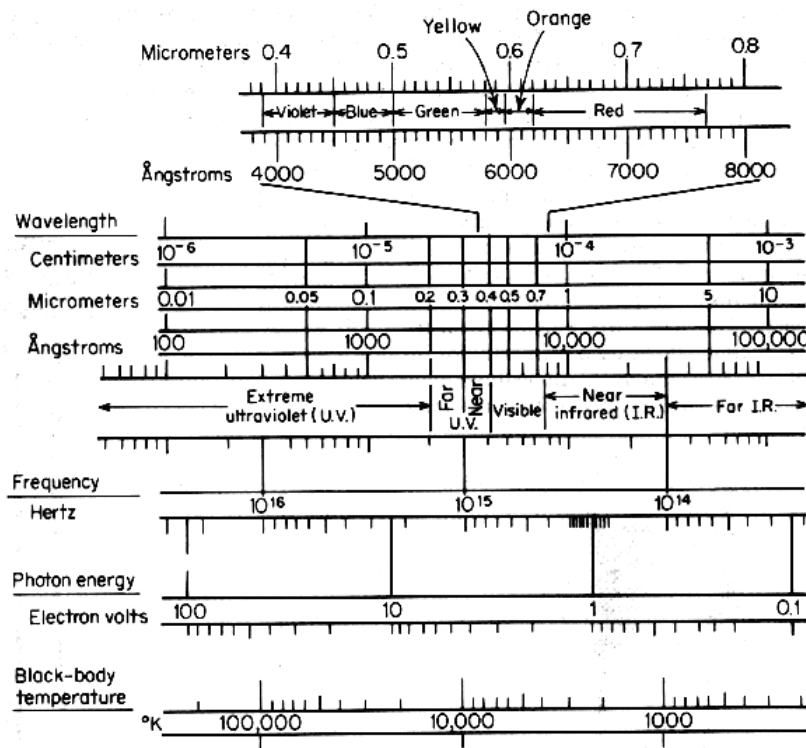


Figure 10 - Electromagnetic Energy Conversion Chart

be selected. Then, one should analyze the beat frequency produced by the interaction of the two

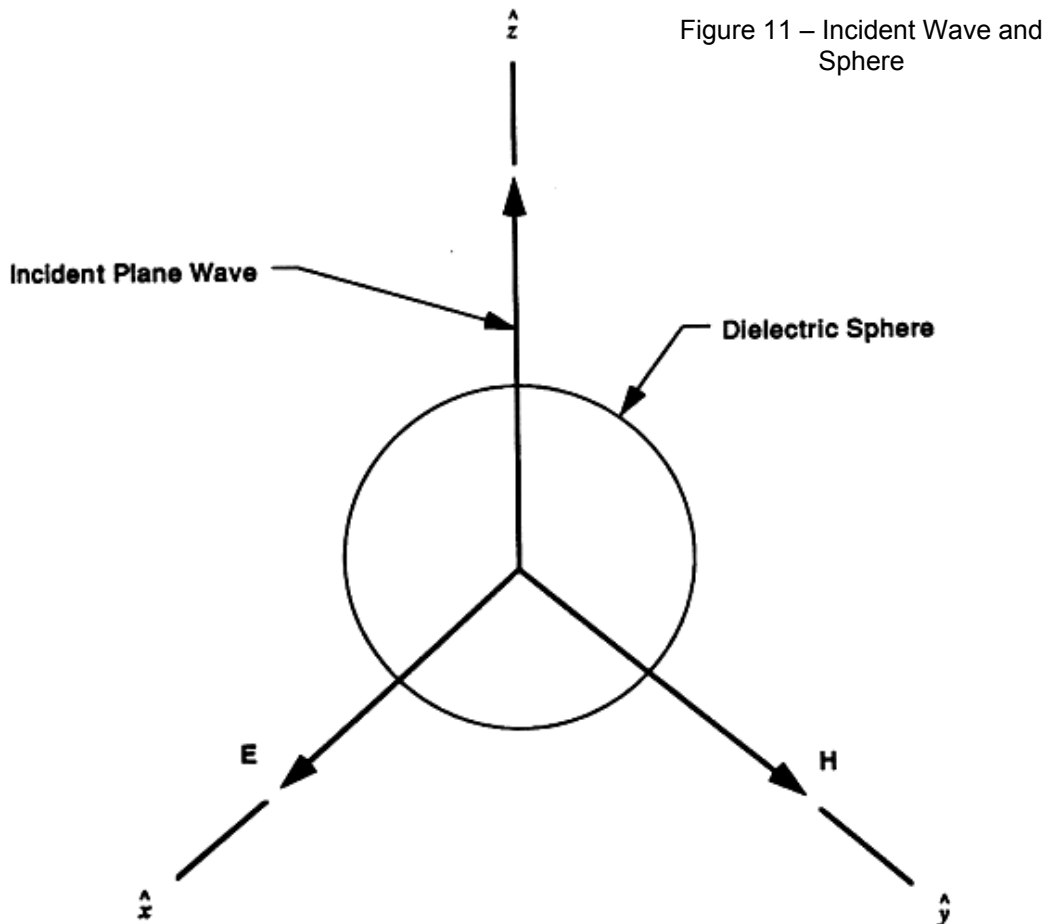
corresponding frequency calculated from the wavelength ($c = f \lambda$) that can be assumed to classically resonate with a sphere of that size, as also found in the light spectrum chart (Figure 10). This serves as one check for the feasibility of the patent's prediction, since it is within a power of ten of this answer for a microsphere. The spacing between spheres, seen in Figure 14, may resonate at a higher harmonic.

The Cox report, supplied to this author by Dr. Mead, ends with an offer of general guidance, which is not found in the patent, regarding research in this area: "Much work still remains in finding more resonances and in studying other areas of the theory. A source of EM radiation having a broad enough range of

frequencies to achieve resonances between two chosen spheres needs to

resonant waves, as well as the effect of separation distance of the two spheres on the beat frequency. Finally, a method of rectifying this beat frequency should be established using currently available equipment, if possible. It is also important to know how much energy is available at the resonant points. As a practical matter, manufacturing processes must be investigated that would allow structures to be fabricated with close enough tolerances to be of use."¹³⁴

It is not difficult to examine each of the above-mentioned recommendations offered by the report, in order to assess the feasibility of this ZPE invention. First of all, the analysis used by the inventors in the patent and the report depends upon one rather involved and somewhat obscure approach to scattering from an older textbook. "The main area of concern addressed in this report is the



interaction of electromagnetic radiation with a dielectric sphere; i.e., the diffracting of a plane wave by a sphere, more commonly known as Mie scattering.¹³⁵ It is assumed that the sphere is made of a homogeneous material and that the medium surrounding the sphere is a vacuum. The incident radiation is assumed to be a plane wave propagating in the z -direction. Electrical vibrations of the incident wave are assumed to occur in the x -direction, with magnetic vibrations in the y -direction (see Figure 11). As explained in Stratton,¹³⁶ "a forced oscillation of free and bound charges, synchronous with the applied field, arises when a periodic wave falls incident upon a body, regardless of the sphere's material. This creates a secondary field in and around the body. The vector sum of these primary and secondary fields gives the value of the overall field. In theory, a transient term must be added to account for the failure of the boundary conditions to hold during the onset of forced oscillations. However, in practice it is acceptable to consider only the steady-state, synchronous term because the transient oscillations are quickly damped by absorption and radiation losses."¹³⁷

While this introductory viewpoint is sophisticated, it is also rudimentary, classical physics. The calculations used by Stratton and Cox become cumbersome however, aimed toward the supposedly obscure resonance between two spheres, though only one sphere is analyzed.

The culmination of the work solves for “RHO” (ρ) which is defined as the propagation constant multiplied by the radius of the dielectric sphere and alternately defined as the radius times the frequency of interest divided by the speed of light c .¹³⁸ The report and patent furthermore emphasize “resonant peaks,” seen in Figure 12, which are claimed to be worthy of special design considerations. However, it is noted that these peaks of “FRHO” are less than a power of ten from baseline, which, considering standard engineering practice, will not warrant special design attention. Considering feasibility analysis, if each sphere successfully amplified free energy from the vacuum, the improvement in output from resonance beat frequency design can only be a secondary consideration for quality management to reduce waste and improve efficiency after prototype manufacture, not a primary focus patent and laboratory reports.¹³⁹

Secondly, neither the patent nor the report mentions the power density of the scattered energy even once. It is assumed that RHO is related to such a power consideration, which is of primary interest for an energy invention, but surprisingly, the concept of energy density is not discussed in either publication.

These two issues create the distinct impression

that this invention is presented in such a way that distracts attention from the essential issue of quantitative energy extraction.

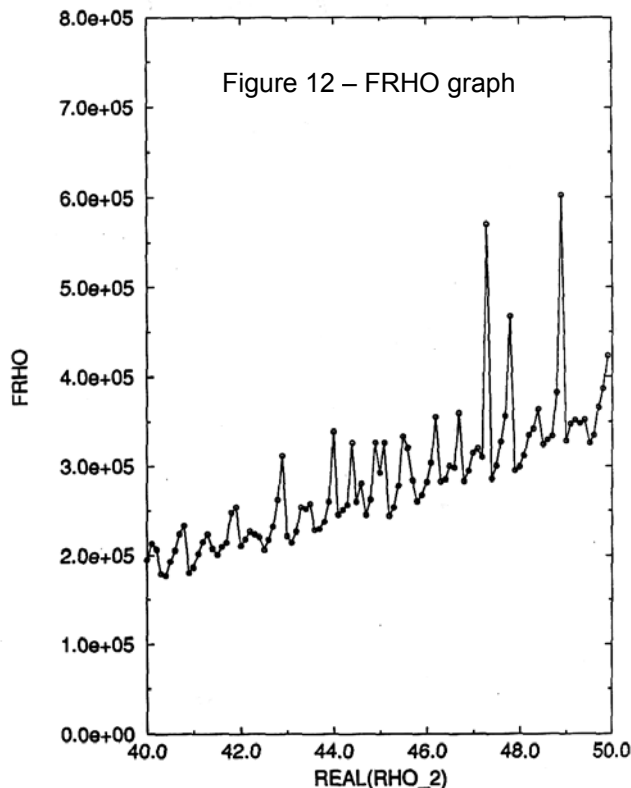
With that preliminary assessment, **the following physics analysis separates this theoretical ZPE invention into four spheres of interest:**

- **microsphere**: micron-sized (10^{-6} m) electrolithography,
- **nanosphere**: nanometer-sized (10^{-9} m) molecular nanotechnology,
- **picosphere**: picometer-sized (10^{-12} m) atomic technology,
- **femtosphere**: femtometer-sized (10^{-15} m) nuclear technology.

However, only the first two or three are amenable to electromagnetic analysis, with corresponding wavelengths of interest. The fourth category requires quantum analysis. The relative comparison of $\lambda > R$, $\lambda = R$, or $\lambda < R$ may only differ if a resonance occurs near $R = \lambda$. The diameter ($= 2R$) of the sphere is most often considered to resonate with the fundamental wavelength of interest but a factor of two may not be significant in every case. In quantum mechanics however, de Broglie's standing matter waves correspond to the Bohr quantization condition for angular momentum, and are equal to an integral multiple of the circumference ($= 2\pi R$) of an electron orbit of an atom.¹⁴⁰

Scattering and absorption of electromagnetic radiation by a conducting or dielectric sphere varies considerably in classical physics.¹⁴¹ Therefore, two additional distinctions, dielectric or conductor, should also be considered for microspheres and nanospheres. A general benefit of the ubiquitous zero-

FRHO vs. REAL(RHO_2)



point electromagnetic radiation in regards to scattering is that with all of the spheres, *no shadow or transition regions need to be considered*. Based on this nature of the ZPF, all parts of the surface of the sphere considered are in the illumined region, which simplifies the analysis.

Regarding the patent's reference to an increase of energy with frequency (col. 7, line 62), in reality, the spectral energy density of the ZPF depends on the third power of frequency:¹⁴²

$$\rho_o(\omega) = \frac{\hbar \omega^3}{2\pi^2 c^3} = 3 \times 10^{-40} f^3 \quad \text{eV/m}^3 \quad (16)$$

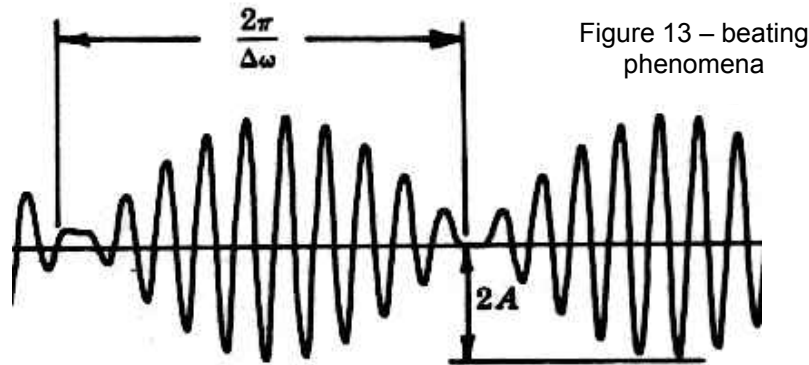
which is integrated further on to yield Equation (21) for a band of frequencies. It is noted that Equation (16) is directly related to the third order dependence of radiation reaction, according to the fluctuation-dissipation theorem.¹⁴³

It is agreed that the general design criteria of the patent is feasible: “the spheres must be small *in direct proportion* to the wavelength of the high frequencies of the incident electromagnetic radiation at which resonance is desirably obtained” (col. 7, line 66).

Before proceeding with individual categories of spherical sizes and wavelengths, it is useful to briefly review the “beating phenomena” as it is known in vibrational physics, whether in mechanical or electromagnetic systems. Starting with two harmonic motions of the same amplitude but of slightly different frequencies imposed upon a vibrating body, the amplitudes of the two vibrations can be expressed as $x_1 = A \cos \omega t$ and $x_2 = A \cos (\omega + \Delta\omega)t$. Adding these together and using a trigonometry identity, it is found that the composite amplitude $x = x_1 + x_2$ is mathematically expressed as:¹⁴⁴

$$x = \{2A \cos (\Delta\omega/2)t\} \cos (\omega + \Delta\omega/2)t. \quad (17)$$

It is noted that $\Delta\omega$ is normally a constant in most systems while ω may vary. Two observations for



application to the ZPE patent being examined are the following:

- the amplitude of the composite vibration is doubled ($2A$)
- the beat frequency of the vibration is $f_b = \Delta\omega/2\pi$ Hz .

The period (wavelength) of the beating phenomena is $T = 1/f_b$ (see Figure 13).

Also common in electronic and optical systems, where it is called “heterodyning,” the beating phenomena permits reception at lower frequencies where a local oscillator is used to interfere with the signal.

Microsphere Energy Collectors

The micron-sized sphere (microsphere) is already mentioned in the patent and in the Cox report. Looking at some of the risks involved, it is assumed to have a radius $R = 10^{-6}$ m but the second

adjacent sphere will unpredictably vary by at least 5%, due to manufacturing tolerances. A primary example in the patent, general engineering considerations would question the advantage of designing for a single beat frequency in this case, which tends to limit the bandwidth and energy output. Using Figure 10 as mentioned previously, we find that a wavelength of a micrometer (micron) resonates with a frequency of 10^{14} Hz, which is in the optical region. In this region, it would be prudent to utilize photovoltaic (PV) technology for the converter 222 in Figure 14, which is already developed for the conversion of optical radiation to electrical energy, which for silicon photovoltaic cells, peaks around 0.8 micron in optical wavelength.¹⁴⁵ With that in mind, Figure 10 implies that the sphere might be a tenth of a micron in size instead, with a wavelength in the UV region. Then, at the most, a 10% variation in size will create a maximum beat frequency of about 1×10^{14} Hz. However, the feasibility of inducing a prominent beat frequency with broadband ZPE electromagnetic wave scattering by uncoupled dielectric spheres has to be questioned in this case. Because the beating phenomena, which only doubles the amplitude, will not be significant in this regime, individual spheres constructed adjacent to a micron-sized PV converter, may be preferable, as seen in Figure 14 from the patent.

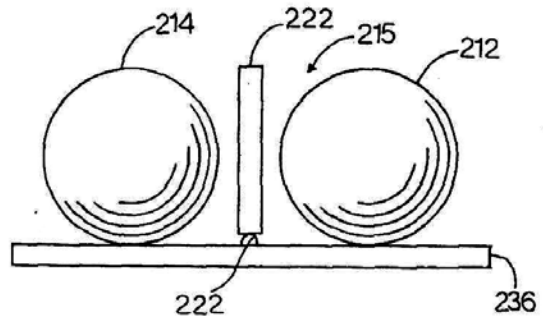


Figure 14 – Mead's semiconductor spheres

Scattering contributions by these microspheres can be analyzed from classical electrodynamic equations that apply. The range $\lambda > R$ is scattering of electromagnetic waves by systems whose individual dimensions are small compared with a wavelength, which "is a common and important occurrence."¹⁴⁶ Without polarization of the incident wave, since ZPE radiation is ubiquitous, it will not contribute to dipole or multipole formation on the sphere. Assumptions include a permeability $\mu = 1$ and a uniform dielectric constant ϵ which varies with frequency. Energy output is calculated by the total scattering cross section σ .¹⁴⁷ With units of area, σ is "an area normal to the incident beam which intercepts an amount of incident power equal to the scattered power."¹⁴⁸

The total scattering cross section of a dielectric sphere for $\lambda > R$ is,

$$\sigma = \frac{1}{3} 8\pi b^4 R^6 \frac{|\epsilon - 1|^2}{|\epsilon + 2|^2} \quad (18)$$

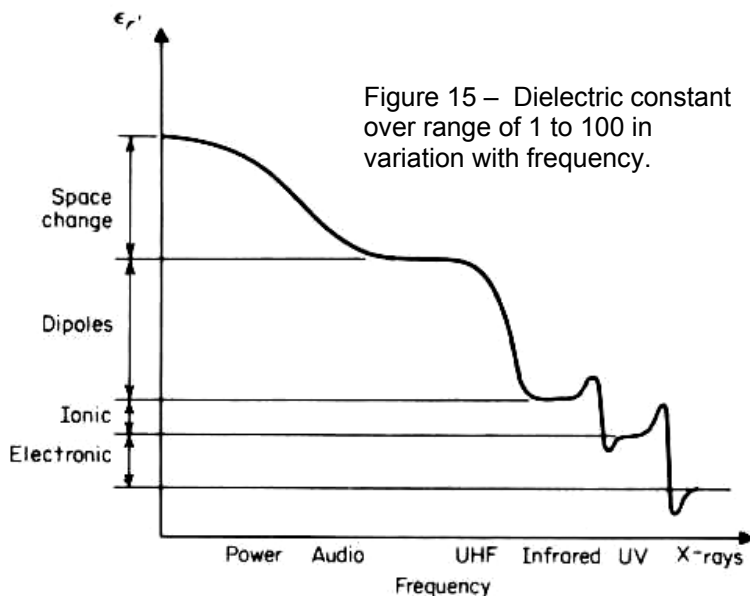


Figure 15 – Dielectric constant over range of 1 to 100 in variation with frequency.

where wave number $b = \omega / c = 2\pi / \lambda$. The dielectric constant ϵ is actually the "relative dielectric constant" which is a ratio of substance permittivity to the permittivity of free space ϵ_0 . In order to appreciate the range of values that Equation (18) may assume, it is noted that "At optical frequencies, only the electrons can respond significantly. The dielectric constants are in the range $\epsilon = 1.7 - 10$, with $\epsilon = 2 - 3$ for most solids. Water has $\epsilon = 1.77 - 1.80$ over the visible range, essentially independent of temperature from 0 to 100C."¹⁴⁹ With this information in mind, a graph of the behavior with frequency is also shown in Figure 15. A declining ϵ with frequency can only make Equation (18) even smaller as ϵ tends toward

the limit of 1 (where the permittivity equals ϵ_0).

As an example of the total cross section for scattering by a relatively good dielectric, $\epsilon = 3$ can be chosen. Then, with $f = 10^{14}$ Hz and $R = 0.1 \times 10^{-6}$ m (thus keeping $\lambda > R$), Equation (18) is found to yield $\sigma = 2.6 \times 10^{-17}$ m². Dividing σ by the actual cross sectional area of a microsphere (πR^2) for comparison, scattering by a dielectric sphere of optical frequency electromagnetic radiation yields a loss of about 8×10^{-6} in power.

In comparison, for $\lambda > R$, small conducting spheres have a total scattering cross section that is significantly larger, where

$$\sigma = \frac{1}{3} 10\pi b^4 R^6 . \quad (19)$$

There is an advantage of using conducting spheres in place of the dielectric spheres which is more significant than designing for the doubling effect from possible beat frequencies. The cross section σ for a one-tenth micron-sized conducting sphere ($R = 0.1 \times 10^{-6}$ m) with visible light incident ($f = 10^{14}$ Hz) yields about 2×10^{-16} m² for $\lambda > R$.¹⁵⁰ Dividing this as before by the actual cross sectional area yields only 6×10^{-5} loss of power or ten times better than the dielectric scattering cross section.

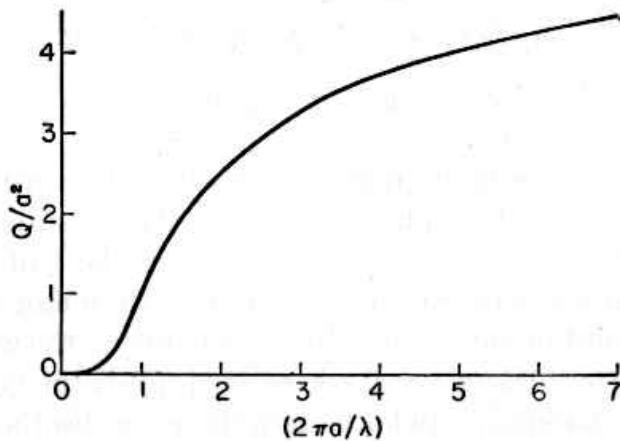


Figure 16 – Total scattering cross section Q for a plane wave scattering from a sphere $R = a$.

While both of these total cross section calculations still may seem very low, there seems to be an explanation for it. Since they were still within a power of ten from $\lambda = R$, Figure 16 shows there is an interference scattering effect for plane waves, within a few wavelengths of this region. Utilizing the spherical Bessel function expansion for a plane wave, similar to the inventor Mead, the solution with amplitudes and phases is found for the boundary condition that the wave function is zero at $R = a$ but the radial velocity of the wave is zero at $R = 0$. As seen in Figure 16 (the textbook uses Q for total cross section), the surprise is that in the region of $\lambda = 2\pi R$ and smaller (<1 on the abscissa), the total cross section becomes very small, tending to zero.

The graph, however, reflects the boundary conditions used, such as the radial velocity v_r of the ratio S (of scattered intensity to incident intensity) = 0, the total cross section calculation with the proper Bessel function tends toward the limit of $\frac{2\pi R^2}{\lambda}$ for $\lambda \ll R$, which is twice the actual cross sectional area. However, for very long wavelengths compared to the radius ($\lambda \gg R$) the total cross section for plane wave scattering by a sphere tends toward $\frac{4\pi R^2}{\lambda}$ which is four times the actual cross sectional area.¹⁵¹

Also confirmed from Figure 17, based on the same text with a Bessel function treatment of a plane wave incident (from the left) on a rigid sphere, the scattered intensity grows larger with smaller wavelength, instead of exhibiting a trend toward resonance when $\lambda \approx R$, tending to be “spherically symmetrical” in the limit where $bR \rightarrow 0$, $S \rightarrow 1$, and $\sigma \rightarrow 4\pi R^2$. These figures seem to contradict the inventor’s assertion of a ZPE electromagnetic resonance with a microsphere and any number of microspheres in close proximity. Furthermore, the penetration of electromagnetic waves throughout dielectric spheres is another complication which is treated in detail in the above-mentioned theoretical

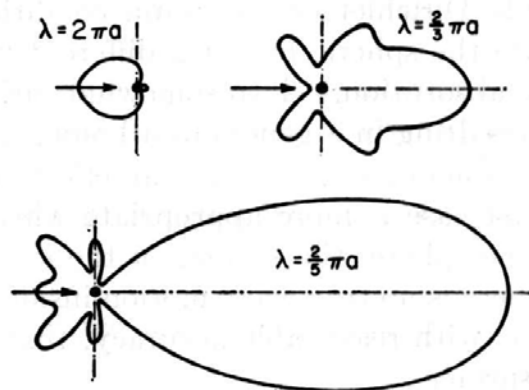


Figure 17 – Scattered intensity for a plane wave scattering from a sphere $R = a$.

physics text, including a complex index of refraction when required, to account for transmission,

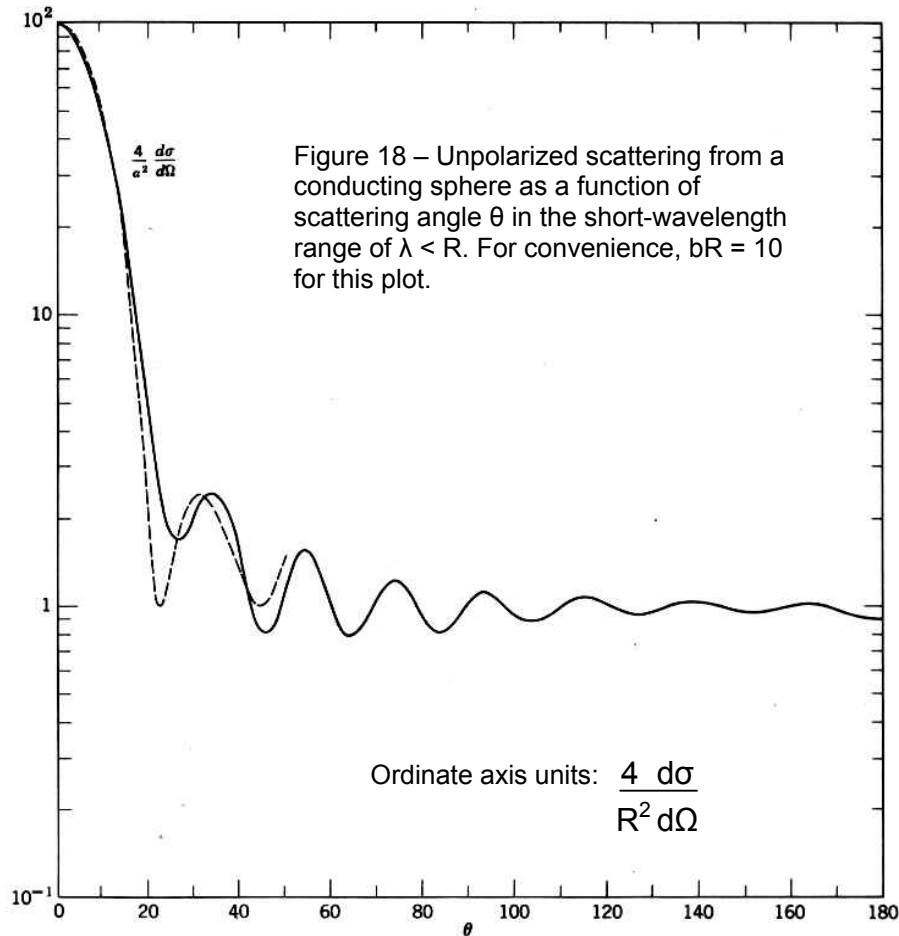
reflection, and absorption.¹⁵² **These two issues diminish the feasibility of the inventor's microsphere design significantly.**

In the region of $\lambda < R$, classical ray theory applies since the wavelength is short compared to the radius of curvature. Fresnel equations can also be utilized, *treating the surface as locally flat*.¹⁵³ This argument also leads to the standard description in physics of specular reflection.

To show the value of Bessel function analysis of plane wave scattering and the strong directional dependence, a graph of the differential cross section is plotted in Figure 18. Considering the previously mentioned advantage of using conducting spheres of the micron size, the analysis is also more straightforward. Under these circumstances, the tangential magnetic fields and normal electric fields of the electromagnetic wave will be approximately equal to the incident wave.¹⁵⁴ The differential backward scattering of the incident radiation, for $\lambda < R$ and $\theta < 10/bR$ is found to be,

$$\frac{d\sigma}{d\Omega} = R^2 (bR)^2 \left| \frac{J_1(bR \sin \theta)}{bR \sin \theta} \right|^2 \quad (20)$$

where J_1 is a Bessel function of the first kind of order one. The forward differential scattering for $\theta \gg 1/bR$ (higher θ angles) is simply $R^2/4$. A plot of Equation (20), for the smaller angles, is the dashed line in Figure 18, with the exact solution as the solid line. Destructive interference is noted where it dips below unity.¹⁵⁵



The peak in the graph of Figure 18 indicates a strong reflection back-scattering for a conductive sphere. This is a common phenomenon since silver, a very good conductor, is used often for coating glass to create mirrors. The conductive surface allows the electric field vector of the electromagnetic wave to oscillate freely upon contact, with very little resistance, thus creating the reflective wave.

Such electromagnetic radiation scattering is distinguished from Thomson scattering, Rayleigh scattering, Coulomb scattering, Compton and Rutherford scattering, which also use cross section formulae as well. Each of these, more common with particle scattering, will be discussed

in the following sections.

It should be emphasized that the same two σ limits discussed above, $2\pi R^2$ and $4\pi R^2$, for small wavelengths ($\lambda \ll R$) and large wavelengths ($\lambda \gg R$) respectively, are also derived in quantum

mechanics using the method of partial waves for scattering of wave packets by a perfectly rigid sphere and thus will also be applied in the further sections to follow.¹⁵⁶

For feasibility consideration of energy extraction, to collect and transduce the total scattered ZPE radiation from the vacuum flux, it would be necessary to place one sphere at the focus of an evacuated, reflecting 3-D ellipsoid cavity with the PV converter at the other, for example, instead of the spherical cavity the inventors refer to. However, in the interest of maximizing energy output per volume, it may be more convenient to engineer sheets of single spheres placed in alternate planes between planar PV converters, which may unfortunately limit the available ZPF frequencies.

An important calculation for each sphere of interest is to find whether significant scattered zero-point energy is available at these wavelengths. Therefore, the **spectral density of ZPE** Equation (16) is integrated as,¹⁵⁷

$$\int_{\omega_1}^{\omega_2} d\omega \rho_o(\omega) = \frac{\hbar}{8\pi^2 c^3} (\omega_2^4 - \omega_1^4) \quad (21)$$

For the wavelength range of 0.4 to 0.7 microns (micrometers) in the visible light band, using Equation (8), the radial frequencies can be generated for the integrated energy density equation. Substituting these for ω_2 and ω_1 we find an energy density of only 22 J/m³ or 22 microjoules/cc which equals approximately 0.24 eV/ μm^3 (electron volts per cubic micron).

To create a simple standard calculation for the frequency band of each sphere of interest, ω_2 is chosen to correspond to the radius R and ω_1 is chosen to be 1/10 of that frequency. For a microsphere, with $\lambda = R = 10^{-6}$ m, the spectral energy density from Equation (21) is $\rho(\omega) = \underline{0.62 \text{ J/m}^3}$ or 3.9 eV/ μm^3 for the decade range: $\Delta f = 3 \times 10^{13}$ to 3×10^{14} Hz. From Figure 10, this energy density is also comparable to the photon energy (2 eV) in the visible band.

Nanosphere Energy Scatterers

In the region of $\lambda > R$ for the scattering by these nano-sized spheres (nanosphere) the classical electrodynamic equations still apply. However, with a radius R of the sphere considered to be 10^{-9} m, the effect on the ZPF spectral energy density is quite dramatic. In Figure 22, it is noted that 1 nm is in the keV region. A resonant correspondence with the sphere diameter of 2×10^{-9} m equals a full wavelength antenna, the resonant frequency will be in the range of 1×10^{17} Hz. The spectral energy density of ZPE at this frequency is substantially more promising. Using Equation (21), we find that the ZPE spectral energy density is $6.2 \times 10^{11} \text{ J/m}^3$, which is a billion times more energy per cubic meter than was available from the ZPF for the micro-sized spheres. Converting to electronvolts per cubic nanometer, it is interesting that the ZPF offers about 390 eV/nm³ which is three orders of magnitude more energy than available to the micron-sized sphere. The advantage as well is that a billion of these spheres will fit into a cubic micrometer, if a collection was found to be coherently constructive with regards to scattering. **Vacuum polarization is probably more pronounced at the nanometer dimensions**, yielding more ZPE virtual particles which would be expected contribute more significantly to scattering off of nanospheres.

Evaluating Equation (19) at this resonant frequency and radius, it is found that for a conducting nanosphere, the scattering cross section $\sigma = 1 \times 10^{-15} \text{ m}^2$ for the region $\lambda > R$. Comparing with cross-sectional area πR^2 for the nanospheres, it is found to be 318 times its cross-sectional area πR^2 . (The ratio of σ to spherical surface area is also constant $\sigma / 4\pi R^2 = 83$). This demonstrates that the scattering cross section σ is geometrically correlated to the object's actual cross-sectional area.

For the consideration of $\lambda \approx 2R$, resonance is still not expected to affect the amplitude of scattered radiation appreciably.

For the consideration of $\lambda < R$ the scattering profile seen in Figure 18 would still apply because quantum mechanical effects become important only when $hf \approx mc^2$. This may be anticipated for the femtosphere.¹⁵⁸

The present state of the art for engineering capabilities in the microsphere and nanosphere regions is illustrated in Figure 19. Called “nanoboxes,” they are electrically conductive single crystals of silver, produced at the University of Washington, with slightly truncated edges and corners. “Each box was bounded by two sets of facets (eight triangular facets and six square ones), and any one of these facets could lie against a solid substrate. The inset shows the SEM image of an individual box sitting on a silicon substrate against one of its triangular facets, illustrating the high symmetry of this polyhedral hollow nanoparticle.”¹⁵⁹ Octahedra and tetrahedra, such as the inset have also been produced, which

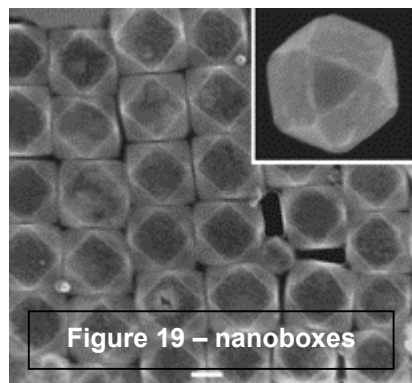
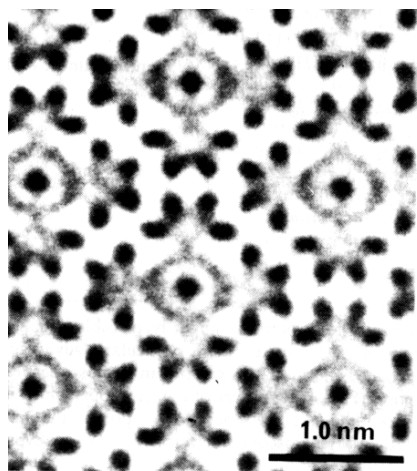


Figure 19 – nanoboxes

approach the patent-proposed ideal of a nanosphere. The white scale bar at the bottom of Figure 19 is 100 nm in length for comparison. For 17-min and 14-min growth times, the nanocubes had a mean edge length of 115 ± 9 and 95 ± 7 nm, respectively. For the sake of the feasibility discussion, regarding the microsphere’s difficulty of predictable beat frequencies, it is noted that the tolerances quoted here are between 7% and 8%. Thus, the benefit of a single beat frequency production of two adjacent silver nanopolyhedrons is judged to be not feasible at either microsphere or nanosphere sizes because of the large manufacturing errors. Nanocubes with sides as small as 50 nm have also been obtained, though some of them were not able to evolve into complete truncated cubes.

Regarding the scale of 1 nanometer in diameter, such as the nanosphere that is proposed, the error control may not require a higher tolerance range than quoted above. As seen in Figure 20, if individual molecular crystals were used for 1 nm range, they do not vary widely in size.¹⁶⁰ A sphere of carbon-60, for example, would be a real possibility, though it is not highly conductive. If metal nanopolygons are used, it is noted that “nonspherical gold and silver nanoparticles absorb and scatter light of different wavelengths, depending on nanoparticle size and shape.”¹⁶¹

Figure 20 – molecular picture



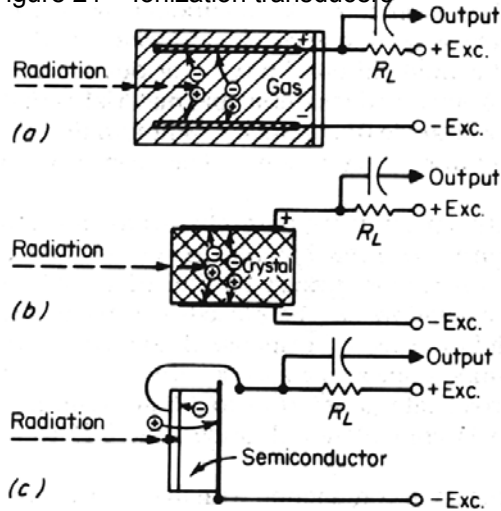
Interestingly, **gold and silver nanoparticles have been used as sensors**, since they have surface-enhanced Raman scattering and other optical effects peculiar to the ~10- to 100-nm range.¹⁶² Instead, using heavy metal atoms, such as Polonium with a diameter of 0.336 nm should be considered in this section because of superior spherical shape and reproducibility. Polonium may also be an interesting candidate because it is the only element known to crystallize in a primitive cubic unit cell under room temperature conditions.¹⁶³ Therefore, the interatomic spacing is also very well known. ZPE virtual particles, or equivalent ZPE electromagnetic radiation, would not be expected to play a large part in scattering off polonium atoms however. Instead, they already are known to contribute to the Lamb shift of the 2p electron levels, with about 1.06 GHz worth of energy. Furthermore, **virtual particle scattering “contributes the same energy to every state,” consisting of $e^2 A^2 / 2mc^2$** in the nonrelativistic theory with the Hamiltonian, where A is the vector potential.¹⁶⁴ Beat frequencies would be unlikely and very difficult to engineer with polonium atoms since the atoms would

normally share the same energy, being at the same temperature, etc.

Picosphere Energy Resonators

In the picosphere range, it is more likely that some of the key elements of this patent may be more effectively applied. One of the reasons for this is that up until this point, there has not been a necessity for lower frequency scattering. To review some of the transduction methods available, Figure 21 shows some of the standard devices for transducing ionization into electricity. Note that ionizing radiation can also consist of electromagnetic X-rays or gamma rays since there is sufficient energy at these frequencies to cause ionization. The method of ionizing transduction relies upon the production of ion pairs in a gas or solid by the incidence of radiation. The applied electric field in Figure 21 is an excitation voltage (Exc.) used to separate the ionized positive and negative charges to produce an electromotive force.¹⁶⁵ For the picosphere range, it is also expected that small individual atoms can be arranged to meet the specifications for the patent more effectively since nature has much better error tolerances than engineers can manufacture artificially.

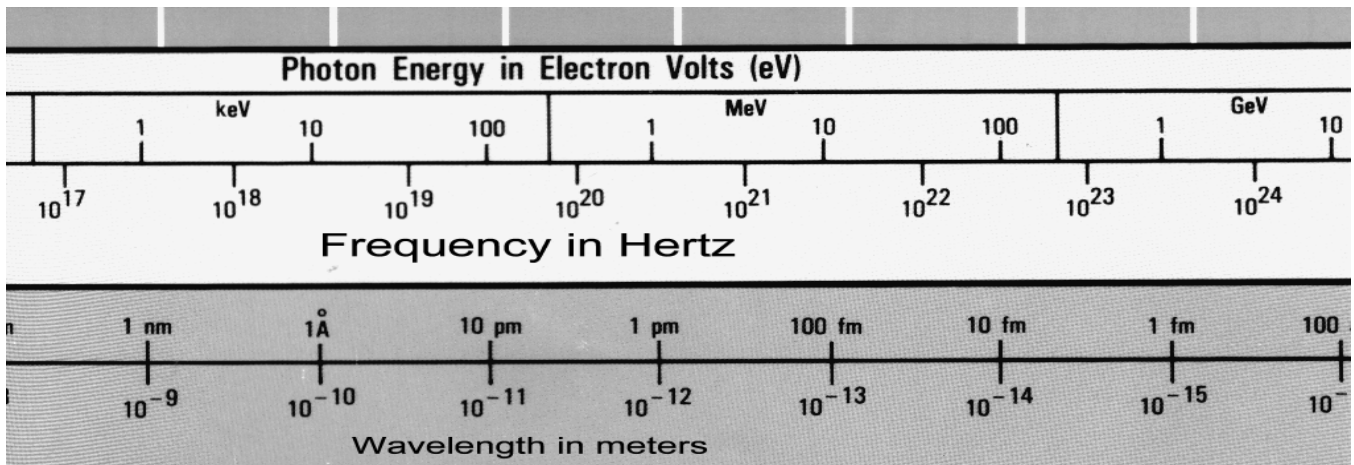
Figure 21 – Ionization transducers



frequency of 1.5×10^{20} Hz using Equation (8). Using Einstein's equation $E = hf$, the photon energy at that frequency can be found to be about 650 keV which is useful to compare with the spectral energy density. Using Equation (21), we calculate a spectral energy density of 6.2×10^{23} J/m³ or 390 keV/pm³.

In the range of $\lambda > R$ the scattering cross section $\sigma = 1 \times 10^{-21}$ m² is in the same proportion of 318 times sphere cross sectional area.

Figure 22 – Electromagnetic spectrum



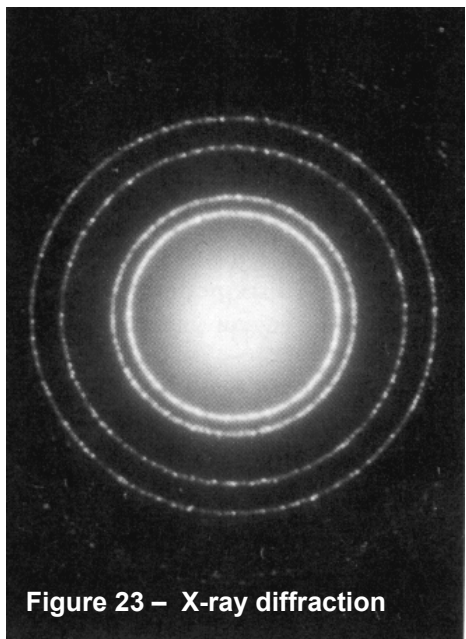


Figure 23 – X-ray diffraction

At the resonant wavelength of $\lambda \approx 2R$, the amplitude of scattering can be expected to be higher. It is also anticipated that here is where the concept of beat frequency may be applied more conveniently, with greater precision than in either larger category. However, since all atomic radii vary between 50 pm (e.g., Helium) and 660 pm (e.g., Cesium), the picosphere with a proposed radius of 1 pm has to be declared to be impractical and therefore, not feasible.

In the range of $\lambda < R$ the scattering seen in Figures 16 and 17 would still apply. The diffraction pattern is also very predictable. The intensity distribution of X-ray diffraction could be correlated to the theoretical scattering off a sphere from Equation (21). An example is seen in Figure 23 where the wavelength of the X-rays is 71 pm and the target is an aluminum atom, which has an atomic radius of 182 pm.¹⁶⁷

If a smaller target on the order of a picosphere were used, it is expected that the scattering pattern would be the same for $\lambda < R$.

In this region, the need for a heterodyned frequency might emerge if, for example, the ionization transducers of Figure 21 were not configured for high efficiency capturing of the ZPE scattered radiation. However, the production of a beat frequency that also resonates with the geometry of an array of atoms may be problematic, for two reasons. The array would preferably need to be a 2-D sheet only one atom thick, such as thin metal foil used for diffraction studies, to prevent destructive interference of the ZPF scattering. Secondly, the real barrier to creating a useful ZPE beat frequency atomic array is producing picospheres that vary reliably in one part in one thousand with a maximum error tolerance of one part in ten thousand. An avenue of speculative physics would require the engineer to estimate the diameter of a suitable metal atom in the ground state and pursue a manufacturing procedure to excite alternate adjacent atoms to a very long metastable state, which is known to expand its size, much like Ryberg atoms.¹⁶⁸ Hypothetically, this ideal situation would achieve a small difference in diameter of adjacent atoms sufficient to produce beat frequencies of resonant scattered ZPE.

Utilizing the Fermi-Thomas model of the atom, most atomic radii can be approximated by

$$a \approx 1.4 a_0 / Z^{1/3} \quad (22)$$

where Z = atomic number and $a_0 = \hbar^2 / me^2$, the hydrogenic Bohr radius.¹⁶⁹ Taking an excellent example of two atoms with similar size, platinum (Pt) and gold (Au) would be good candidates since they are next to each other on the periodic table and relatively inert, Noble metals. It is presumed that the diameter may resonate with a full wavelength, with 183 pm and 179 pm as the radii for Pt and Au respectively.¹⁷⁰ In that case, 8.20×10^{17} Hz is the corresponding Pt frequency and 8.37×10^{17} Hz is the corresponding Au frequency, both in the soft X-ray band. Subtracting the two frequencies, the beat frequency would theoretically be a difference of 1.83×10^{16} Hz, moving it down into the UV band. If the conversion of UV incident electromagnetic energy is more efficient than transducing soft X-rays, then this method would offer a chance to collect ZPE, so long as the arrangement of multiple pairs of Pt and Au atoms could constructively interfere at their beat frequency. However, the wavelength of 1.83×10^{16} Hz is about 16 nm, which forces the placement of individual atomic pairs to be fairly distant from each other, compared to their size. With *only a 2% difference* in diameter, the beat frequency difference yields a power of ten difference for lower frequency detection, as the Mead-Cox resonant microsphere analysis of Figure 11. The improvement in amplitude from resonance would reasonably be only a power of two, unless a resonant cavity was used as well.

Another example, representing the smallest atomic pair that is available for this experiment, is hydrogen (H) and deuterium (D), an isotope of hydrogen with one proton and one neutron in the nucleus. The Bohr radius a_0 for hydrogen is 53 pm and the atomic radius of deuterium is about the same. In fact, the H_α emission lines (Balmer series) for deuterium and hydrogen are 656.10 nm and

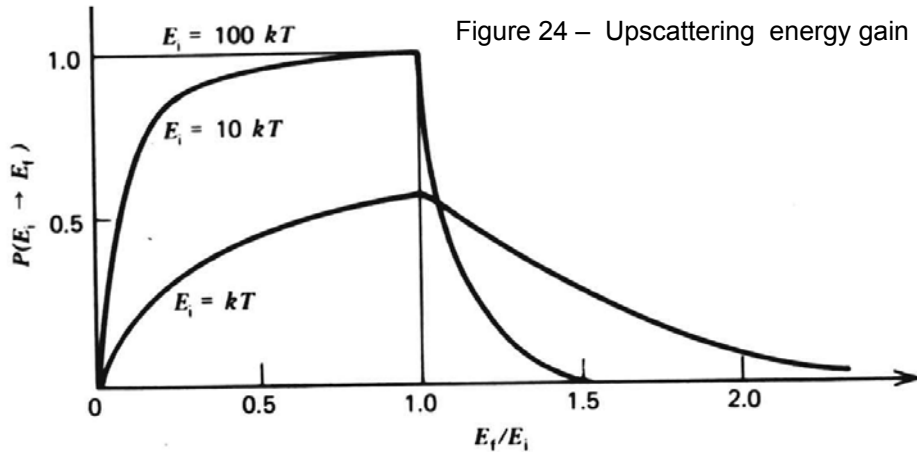


Figure 24 – Upscattering energy gain

656.28 nm respectively, a difference of only 0.03%.¹⁷¹ Such a similar size will force the beating frequency to be more than a power of ten difference, which apparently is viewed as an advantage by the patent holders. For such gaseous atoms, the phenomenon of “upscattering” might be achieved with this gas at a finite temperature T with a Maxwell-Boltzmann

velocity distribution if the incident ZPE virtual particles fell into a regime of low energy up to about 10 kT.¹⁷² This implies that it is possible for the incident particle to *gain* energy in a scattering collision. In the situation where the hydrogen or deuterium nuclei might be at rest, the scattering probability $P(E_i \rightarrow E_f)$ inversely depends upon the incident particle energy E_i . However, for elastic scattering in a hydrogen (proton) gas, the scattering probability depends on the final particle energy E_f and is *not zero* even for $E_f > E_i$. In Figure 24, a graph is shown of the scattering probability for scattering of a proton gas with various incident particle energies. With resonance considerations seen in Figure 25 added to the design as well, such a regime might be a test, with a minimum of risk, for the Mead spherical collector concept in an atomic, picosphere region. However, with or without a successfully amplified beat frequency, the upscattering of virtual particles from a proton gas may still have inherent flaws for two reasons: 1) most such proton gas experiments have been conducted only with low energy incident neutrons; 2) “the dissipative effect of radiation reaction precludes spontaneous absorption of energy from the vacuum field” which normally applies only to an atom in the ground state.¹⁷³ Yet, the gain of one to two times the incident $E_i = k_B T$ may be valuable to the energy equation as the gas transfers energy to the incident particles, even if the probability drops to 50%, since theoretically an abundant number of virtual particles are available. At room temperature ($T = 300K$) for example, $1 k_B T = 0.026$ eV

which is about 10^{13} Hz or an infrared terahertz frequency.

Figure 25 – Broadening of the resonance peak with increasing temperature

In Figure 25, an example of a capture resonance is shown at temperature T_1 , where the average cross section dramatically increases for a certain resonant incident energy E_0 . Another aspect of temperature increase is also graphically demonstrated. This is called “Doppler broadening” caused by the Doppler shift in frequency as a thermally excited atom moves away from or toward the incident particle with greater temperature-dependent speed.¹⁷⁴ Therefore, an increase in temperature causes the increased cross section of a resonant peak to be lost. Lower temperatures are important for preserving the advantage of resonance.

Thus examining the options for the resonant sphere, the two atomic pairs of deuterium and hydrogen are the best beating examples in the picosphere region, still demonstrating major unknowns in the “beat frequency” design concept of the Mead patent. At the present state of nanotechnology development however, the picospheres cannot be manufactured, except by atomic force “pick and place” devices.

Quantum Femtosphere Amplifiers

With the examination of the femtosphere ($R = 10^{-15} \text{ m} = 1 \text{ fm}$) there are a number of phenomena that synchronize so well with this dimension that the patent being examined seems to be more compatible with the nuclear particle than any other size sphere. The first obvious advantage is the spectral energy density of Equation (21) which is found to be $6.2 \times 10^{35} \text{ J/m}^3$ or 390 MeV/fm^3 . This is also interesting in that the quantum mechanical realm applies where hf is about the same as mc^2 . Testing for this condition, both energies are calculated with a wavelength of $2 \times 10^{-15} \text{ m}$ and a corresponding frequency (see Figure 22) of $1.5 \times 10^{23} \text{ Hz}$. The Einstein formula for photon energy of the femtosphere is

$$E = hf = 9.9 \times 10^{-11} \text{ J} = 619 \text{ MeV} . \quad (23)$$

To determine the mass of the femtosphere, it is known that the radius of either the proton or neutron is about $8 \times 10^{-16} \text{ m}$.^{175,176} This is remarkably close (within 20%) to the conceptual femtosphere radius R of 1 fm . Therefore, it is reasonable to use the average mass of either nuclear particle ($1.7 \times 10^{-27} \text{ kg}$) in the Einstein equation for mass-energy, to find the energy equivalent of the femtosphere’s mass:

$$E = mc^2 = 1.5 \times 10^{-10} \text{ J} = 938 \text{ MeV} . \quad (24)$$

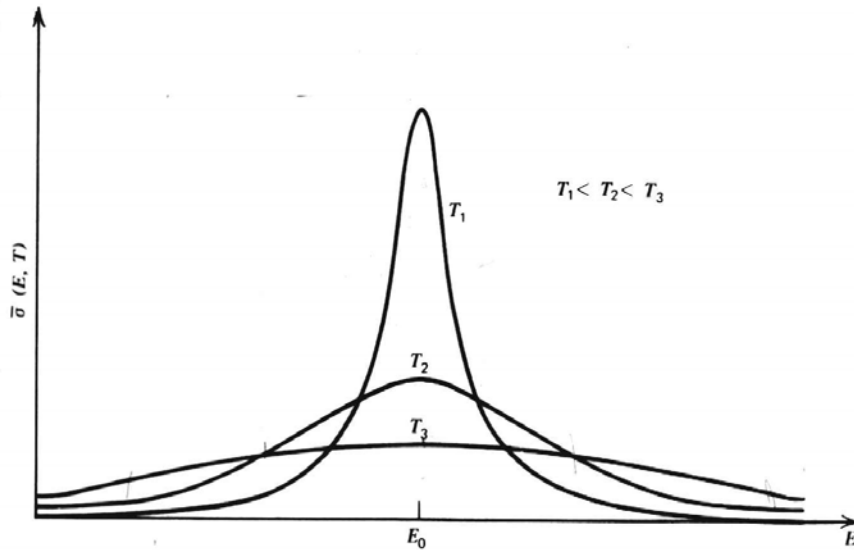
Comparing Equations (23) and (24), they are the same order of magnitude, so it is determined that **quantum mechanical rules apply in this region**. The classical equations for energy and scattering cross section are still applicable. However, they may be regarded as classical approximations, in view of the correspondence principle, to quantum mechanical phenomena. “The important quantum effects

are (1) discreteness of the possible energy transfers, and (2) limitations due to the wave nature of the particles and the uncertainty principle.”¹⁷⁷

In this femtosphere range, Rutherford scattering is applicable. The total nuclear Rutherford scattering cross section is

$$\sigma = \pi R^2 \frac{(2zZe^2)^2}{(\hbar v)^2} , \quad (25)$$

where z is the number of charges (particles) in the



incident at a velocity v and Z is the number of charges (particles) in the target. For example, at high velocities, even for incident virtual photon radiation, the total cross section can be far smaller than the classical value of πR^2 , which is its geometrical area.¹⁷⁸ The parenthetical terms in Equation (25) can result in a reduction of 10^{-24} times the geometrical area πR^2 of the target for an incident photon at the speed of light.

For this size of target, due to vacuum polarization, it is important to mention that more incident virtual particles from the vacuum, as discussed in Chapter 1 (with an artist rendering in Figure 3), will also be present for a charged femtosphere. Therefore, the de Broglie wavelength of the incident particle will also be important, treating the ZPF virtual particles on the same level as electromagnetic waves:

$$\lambda = h/p = h/mv \quad (26)$$

The de Broglie requirement of quantum mechanics, postulated in 1924,¹⁷⁹ thus affects the possibilities for energy generation for the Mead patented design. "For a nucleus of finite size...the de Broglie wavelength of the incident particle does enter...The situation is quite analogous to the diffraction of waves by a spherical object."¹⁸⁰

Vacuum polarization will also enhance the natural electromagnetic radiation from the vacuum for the femtosphere. Since double slit experiments with particles like electrons and neutrons demonstrate the wave phenomenon of diffraction, femtosphere particles can also be regarded as "wave packets."¹⁸¹

This type of scattering utilizes the continuously distributed energy eigenvalues of quantum mechanics which consider the boundary conditions at great distances from the collision. The scattering is treated here only as elastic scattering, so there is no absorption by the target. This is different from photoelectric scattering or Rayleigh scattering, which are inelastic.

For the region of $\lambda > R$ this can be represented by the low energy limit where $2\pi R \ll \lambda$ (the circumference is much less than the wavelength). For the femtosphere, the total cross section is approximately $\sigma \approx 10^{-30} \text{ m}^2$ in this low frequency, long wavelength region.

For the region of $\lambda \approx 2R$ or $2\pi R$, there is a uniquely quantum mechanical phenomenon of resonant scattering called "**resonance fluorescence**" that applies "to the absorption of radiation by an atom, molecule, or nucleus in a transition from its ground state to an excited state with the subsequent re-emission of the radiation in other directions in the process of de-excitation."¹⁸² The reaction of the target when the frequency of the incident equals the binding energy of the target, the scattering becomes very great, exhibiting a formal resonance peak seen in Figure 26.

Note that a single femtosphere, such as a free neutron or proton would not possess the requisite binding energy for this type of oscillator resonance. In addition, this process reveals an

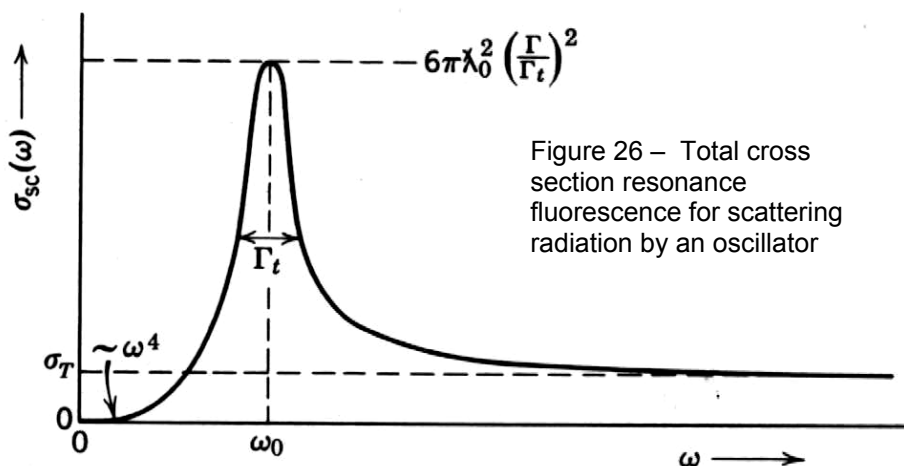


Figure 26 – Total cross section resonance fluorescence for scattering radiation by an oscillator

inelastic form of scattering but the dramatically increased cross section apparent in the resonant peak of Figure 26 more than makes up for any energy lost in absorption and re-emission. Resonance fluorescence brings a number of phenomena into play that are seen in Figure 26, such as Thomson scattering, which is scattering of radiation by a free

charge. It can be X-rays by electrons or gamma rays by a proton for example.¹⁸³ Thomson scattering occurs along a baseline of higher frequencies in Figure 26 above ω_0 ,

where the cross section is

$$\sigma_T = \frac{8\pi\pi^4}{3m^2c^4} \quad (27)$$

The Thomson cross section of Equation (27), evaluated for a target electron, yields $6.6 \times 10^{-25} \text{ cm}^2$ for σ_T where $e^2/mc^2 = 2.8 \text{ fm}$, the classical electron radius.

By comparison, the Rayleigh scattering (which causes the atmosphere to take on a blue color) cross section has a dependence on the fourth power of the incident frequency. Thus, the highest visible frequency (blue color) has a much larger scattering cross section and consequently, a stronger interaction with air molecules, including a wide scattering angle. Both phenomena illustrate the dominance of cross section scattering terms with cubic and quartic exponents.

Deuteron Femtosphere

One example of an intriguing femtosphere oscillator is the deuteron (a proton bound to a neutron in close contact), which also demonstrates resonant fluorescence. It would satisfy the requirement of “binding energy” for the target and is also treated as an oscillator. However, it should be mentioned that it is unlikely that the deuteron would exhibit beat phenomena, since the wave functions overlap **making the deuteron behave as one nucleus** (ionized deuterium), with a single resonant frequency and a radius of about 2 fm.¹⁸⁴

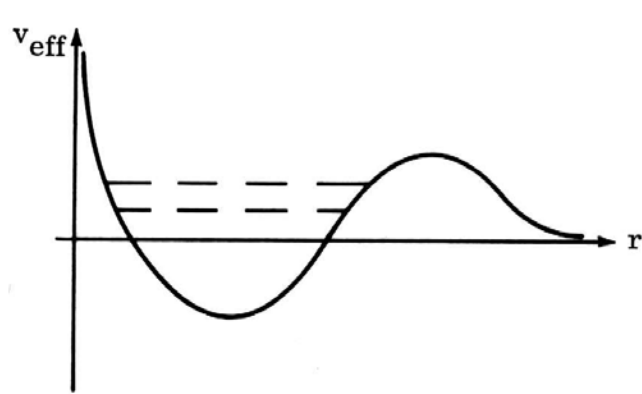
Recalling that the beat frequency design of the Mead patent is simply a means to downshift the radiated frequency, it is also possible to use the standard electrical engineering approach instead. Frequency converters, for example, utilize a “local oscillator” which mixes with the incoming signal to produce a subtracted intermediate frequency one or two orders of magnitude lower, for the same purpose. Once the resonant frequency of the deuteron is determined to be beyond the useful energy transduction range, an engineering recommendation therefore, would be to find a lower local oscillator in the same range, so that a substantially reduced intermediate frequency can be produced.

The deuteron has one bound state ($l = 0$) of a proton and neutron with binding energy of $E_b = 2.23 \text{ MeV}$. The more preferred state (75%) is where the spin $\frac{1}{2}$ of the proton and neutron are parallel (triplet state). The cross section for the deuteron is

$$\sigma = \frac{2\pi\hbar^2/m}{E - E_b} \quad (28)$$

Equation (28) is about $70 \times 10^{-24} \text{ cm}^2$ for the singlet (antiparallel) state and about $20 \times 10^{-24} \text{ cm}^2$ for the triplet state, which computes to 550 times and 157 times the geometrical cross sectional area, respectively.

With resonance fluorescence, the condition is in a sense an almost bound state that isn't below zero energy to be a true bound state (see the dashed line levels in Figure 27). If the potential $V(r)$ is an attractive well, then the effective potential is,



$$V_{\text{eff}} = V(r) + \hbar^2 l(l+1) / 2mr^2 \quad (29)$$

where the integer angular momentum quantum number, $l \geq 1$. “Resonances are the ‘bound states’ of the well at the positive energy, indicated by the dotted lines...What happens in scattering at a

resonant energy is that the incident particle has a large probability of becoming temporarily trapped in such a quasi-bound state of the well; this possibility increases the scattering cross section.”¹⁸⁵ In Figure 27, the depth of the potential well for the deuteron must be $V_0 = 36$ MeV for the deuteron.¹⁸⁶

With that introduction to resonance with the deuteron, it should be mentioned that it is also an advantageous oscillator since the binding energy of $E_b = 2.23$ MeV corresponds to an X-ray frequency of $f_b = 5.4 \times 10^{20}$ Hz, instead of the gamma ray frequency of 10^{23} Hz that should resonate with the diameter of a femtosphere. Thus, the deuteron binding energy satisfies the need for a lowering of the resonant frequency for

transduction purposes, voiced in the Mead patent. The cross section is complicated by the existence of a singlet and triplet state depending on the proton and neutron spin direction. “There are no bound excited states of the deuteron. Neutron-proton scattering experiments indicate that the force between n and p in the singlet state (antiparallel spins) is just sufficiently less strong than in the triplet state to make the deuteron unstable if the spins are antiparallel...there is a small, measurable quadrupole moment.”¹⁸⁷

For the region of even smaller sizes, beyond the femtosphere resonance, where $\lambda < R$, the cross section can be represented by the high energy limit where $R \gg \lambda$. Here the scattering by a perfectly rigid femtosphere can be approximated, as mentioned with the microsphere, with a total cross section of

$$\sigma \approx 2 \pi R^2 \quad (29)$$

which is twice the actual geometrical cross section area.¹⁸⁸ The reason for the apparently anomalous result of Equation (29) is that the asymptotic form of the wave function is composed of the incident and the scattered wave, which also experiences interference between the two partial waves. “However, so long as $2\pi R/\lambda$ is finite, diffraction around the sphere in the forward direction actually takes place, and the total measured cross section...is approximately $2\pi R^2$.”¹⁸⁹

Electron Femtosphere

The electron may actually be the preferred femtosphere for many reasons. Its classical radius r_0 is calculated to be 2.8×10^{-15} m or 2.8 fm and is suitable for a Mead patent test. As seen in Figure 3, the electron, like the proton, offers a steep electrical gradient at its boundary that creates a decay or polarization of the vacuum locally. It is expected that electron charge clusters like Cooper pairs or bigger boson charge bundles can offer a substantially enhanced vacuum activity in their vicinity. The patents of Ken Shoulders (US #5,018,180) and Hal Puthoff (US #5,208,844) on charge cluster devices discuss the potentials of such an approach but they seem to lack sufficient engineering skills to control their volatility. Therefore, an ion trap or “force field” confinement process is required. In fact, Hans Dehmelt at the University of Washington used such a trap to compress 1000 electrons into a 300 micron spherical plasma drop in order to study them.¹⁹⁰ When dealing with high speed electron cluster production, it is also reasonable to suggest the use of multiple toroid inductive couplers to convert the kinetic energy into electricity.

QED vacuum effects such as the coupling of the atomic electron to the vacuum electromagnetic field show that the electron is more intimately connected to the vacuum flux than most other particles. “The zero-point oscillations of the field contribute to the electron a certain amount of energy... $E_{\text{fl}} \sim e^2 \hbar / 4 m c a^2$,” with an upper bound of $\hbar f_{\text{max}} = 15$ MeV for a free electron.¹⁹¹ The coupling term for the atomic electron in the Hamiltonian is $(e^2 / 2 m c^2) \mathbf{A}^2$ where \mathbf{A} is the vector potential and the parenthetical modifier is familiar from Equation (27) as half of the classical electron radius. “Since this term does not involve atomic operators, it contributes the same energy to every state” in the atom.¹⁹² Besides the ground state contribution, called the Lamb shift, it is true that every other electron level is also shifted upwards from vacuum flux energy or virtual particles. For this reason alone, it should be emphasized that **extraction of energy from the vacuum is already occurring in every atom throughout the universe, since every atomic electron and every free electron is ZPE-powered.** However within the

atomic system, “the effects of the vacuum field and radiation reaction cancel, so that the ‘spontaneous absorption’ rate is”¹⁹³

$$A_{12} = R_{VF} - R_{RR} = \frac{1}{2} A_{21} - \frac{1}{2} A_{21} = 0 \quad (30)$$

where A_{12} is the Einstein A coefficient for the electron transition from the ground state to the first atomic energy level. The spontaneous emission rate sums the rate of energy absorption from the vacuum field R_{VF} and the radiation reaction rate R_{RR} to equal the Einstein A coefficient.

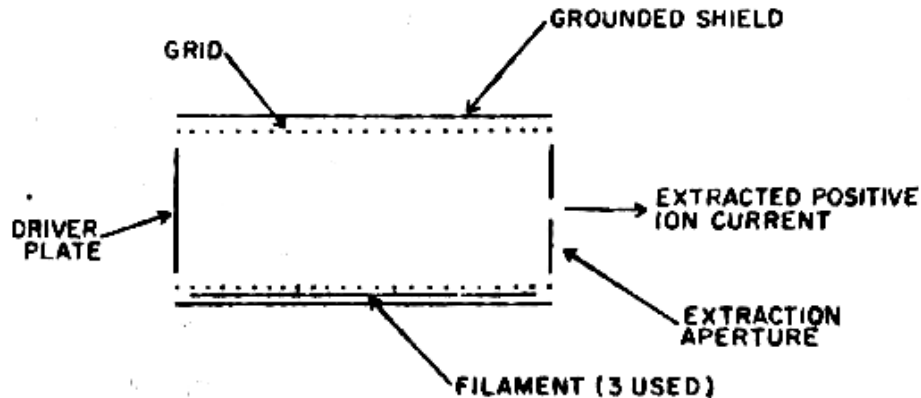


Figure 28 – Nonresonant ion trap with voltage applied to grid, driver plate, and extraction plate. Thoriated filaments supply electrons.

The energetic scattering of the vacuum flux on a free electron, clearly seen in Figure 3, may be optimally amplified in the gaseous state of a plasma, such as within the confines of an ion trap. This author collaborated in the construction of such a trap, which proved that electron and ion densities

can be increased with such a trap, as the electrons are retained in

one place for measurements and energy extraction.¹⁹⁴ Such an apparatus may also work well for charge clusters, after applying inductive toroidal braking to their kinetic energy. For an applied voltage of 300V and vacuum pressures of at least a microTorr, the concentration of ions ranged between 10^8 and 10^{10} ions per cc. As seen in Figure 29, the voltage profile or potential distribution inside the grid with the presence of negative space charge from the Thoriated filaments exhibits a large concentration of electrons. Assuming that charge clusters cannot be trapped by any other means without destroying them, the nonresonant ion trap should provide a reliable method for study and possible energy extraction if an additional collection and amplification method for the femtosphere is optimized and implemented.

Weisskopf notes that if the electron is assumed to be a sphere of radius a , then only waves with a wavelength $\lambda / 2\pi \geq a$ will act upon the electron, while the wavelengths $\lambda / 2\pi \gg a$ will not be that significant. The upper bound of hf_{\max} assumes an electron radius of $a = c/f_{\max}$ while the number of

vibration modes of the ZPF gives rise to a value of $a \approx r_0 (hc/e^2)^{1/2}$ so that “the fluctuation energy seemingly pushes the electron radius to even greater values...”¹⁹⁵

Casimir Force Electricity Generator

A fascinating example of utilizing mechanical forces from the Casimir effect and a change of the surface dielectric properties, to intimately control the abundance of virtual particles, is an optically-controlled vacuum energy transducer developed by a Jet Propulsion Lab scientist.¹⁹⁶ A moving cantilever or membrane is proposed to cyclically change the active volume of the chamber as it generates electricity with a thermodynamic engine cycle. The invention proposes to use the Casimir force to power the microcantilever beam produced with standard micromachining

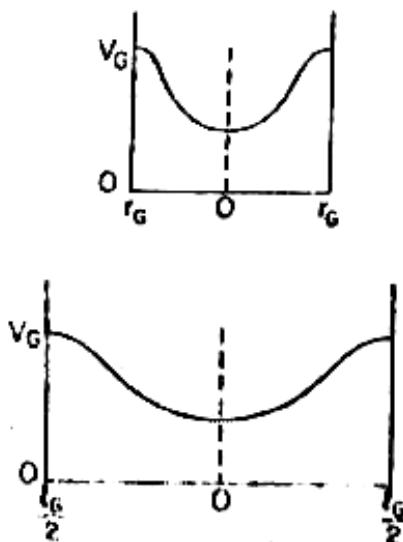


Figure 29 – Potential distribution in ion trap

technology. The silicon structure may also include a microbridge or micromembrane instead, all of which have a natural oscillation frequency on the order of a free-carrier lifetime in the same material. The discussion will refer the (micro)cantilever design but it is understood that a microbridge or flexible membrane could also be substituted. The invention is based on the cyclic manipulation of the dimensions of Casimir cavity created between the cantilever and the substrate as seen in Figure 30. The semiconducting membrane (SCM) is the cantilever which could be on the order of 50-100 microns in size with a few micron thickness in order to obtain a resonant frequency in the range of 10 kHz, for example.

Two monochromatic lasers (RS) are turned on thereby increasing the Casimir force by optically changing the dielectric properties of the cantilever. This frequency dependence of a dielectric constant, can be seen in Figure 15. It can vary with frequency by a few orders of magnitude inversely proportional to the frequency. The standard analysis of cavity modes usually identifies the resonant modes of the cavity, dependent on the boundary conditions.^{197,198} However, Pinto's

pro-active approach is to excite a particular frequency mode in the cavity. In doing so, an applied electrostatic charge (V_b) increases as the cantilever is pulled toward the adjacent substrate (SCP) by the Casimir force. Bending the charged cantilever on a nanoscale, the Casimir attractive force is theoretically balanced with opposing electrostatic forces, in the same way as Forward's "parking ramp" of Figure 8. As the potential difference to the cantilever assembly is applied with reference to a conducting surface (CP2) nearby, the distance to this surface is also kept much larger than the distance between the cantilever and the substrate (SCP). Upon microlaser illumination, which changes the dielectric properties of the surface and increases the Casimir force, there is also predicted an increase in electrostatic energy due to an increase in capacitance and voltage potential.

Therefore a finite electrical current can be

extracted and the circuit battery is charged by an energy amount equal to the net work done by the Casimir force. Pinto estimates the Casimir force field energy transfer to be approximately 100 to 1000 erg/cm².¹⁹⁹ Converting this to similar units used previously, this Casimir engine should produce in the range of 60 to 600 TeV/cm² (teraelectron volts per square centimeter) which is also equal to 0.01 to 0.1 mJ/cm² for every thermodynamic engine cycle diagrammed in Figure 31.

Analysis of the Casimir engine cycle demonstrates its departure from hydroelectric, gaseous, or

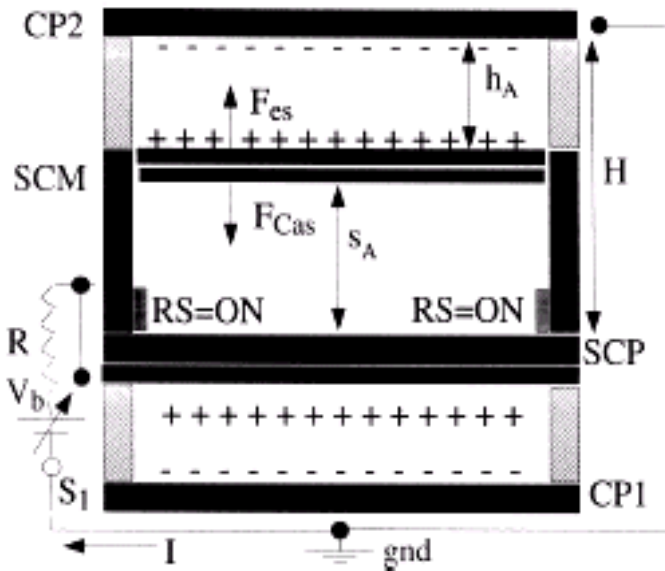


Figure 30 – Pinto's optically controlled vacuum engine

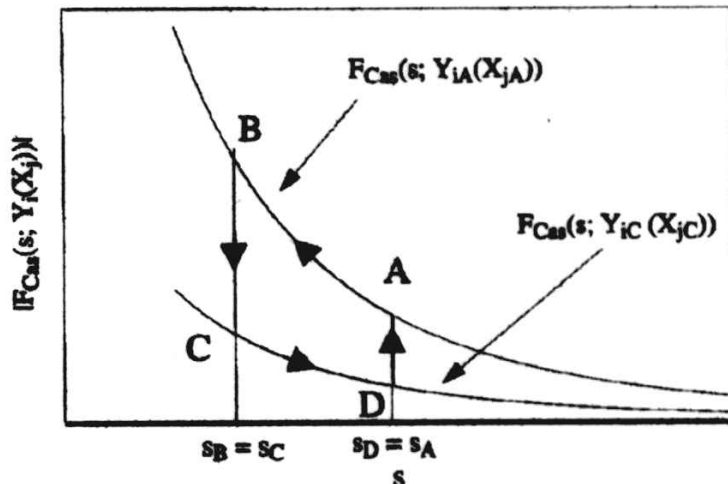


Figure 31 – Thermodynamic engine cycle of Pinto's vacuum energy transducer where F_{Cas} = Casimir force

gravitational systems. For example, the **Casimir pressure always acts opposite to the gas pressure** of classical thermodynamics and the energy transfer which causes dielectric surface changes “does not flow to the virtual photon gas.”²⁰⁰ Altering physical parameters of the device therefore, can change the total work done by the Casimir force, in contrast to gravitational or hydroelectric systems. **Unique to the quantum world, the type of surface and its variation with optical irradiation is a key to the transducer operation.** Normally, changing the reflectivity of a surface will affect the radiation pressure on the surface but not the energy density of the real photons. However, in the Casimir force case, Pinto explains, “...the normalized energy density of the radiation field of virtual photons is drastically affected by the dielectric properties of all media involved via the source-free Maxwell equations.”²⁰¹

Specifically, Pinto discovered that the absolute value of the vacuum energy can change “just by causing energy to flow from a location to another inside the volume V.”²⁰² This finding predicts a major breakthrough in utilization of a quantum principle to create a *transducer of vacuum energy*. Some concerns are usually raised, as mentioned previously, with whether the vacuum energy is conserved. In quantum systems, **if the parameters (boundary conditions) are held constant, the Casimir force is strictly conservative in the classical sense, according to Pinto.** “When they are changed, however, it is possible to identify closed paths along which the total work done by this force does not vanish.”²⁰³

To conclude the energy production analysis, it is noted by Pinto that 10,000 cycles per second are taken as a performance limit. Taking the lower estimate of 100 erg/cm² per cycle, power or “wattage” is calculated to be about 1 kW/m² which is on par with photovoltaic energy production. However, on the scale of interest, where s in Figure 31 is always less than 1 μm , the single cantilever transducer is expected to produce about 0.5 nW and establish a millivolt across a kilohm load, which is still fairly robust for such a tiny machine.²⁰⁴

The basis of the dielectric formula starts with Pinto’s analysis that the Drude model of electrical conductivity is dependent on the mean electron energy $\langle E \rangle$ (less than hf) and estimated to be in the range of submillimeter wavelengths. The Drude model, though classical in nature, is often used for comparison purposes in Casimir calculations.²⁰⁵ The detailed analysis by Pinto shows that carrier concentrations and resistivity contribute to the estimate of the total dielectric permittivity function value, which is frequency dependent. The frequency dependence is of increasing concern for investigations into the Casimir effects on dielectrics.²⁰⁶

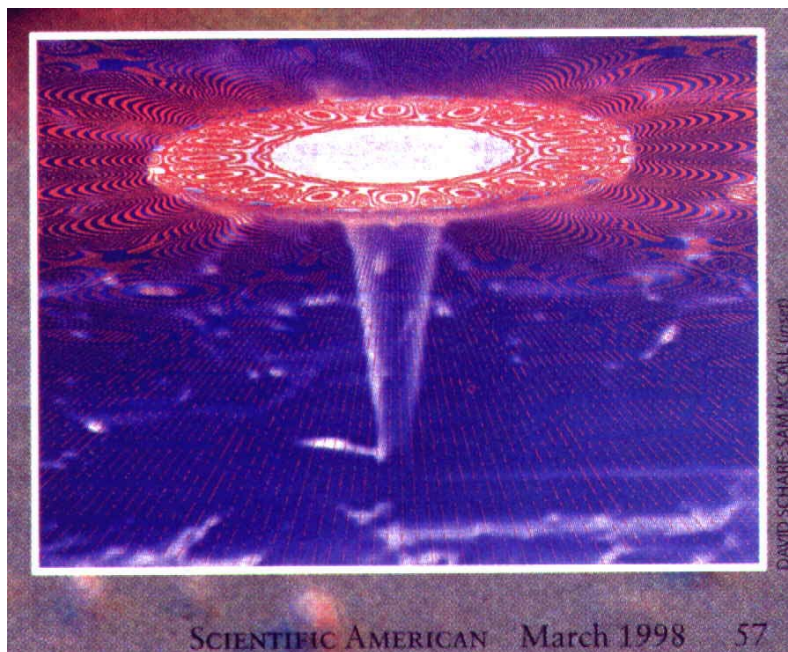


Figure 32 – Microlaser on a pedestal (computer simulation)

Analyzing the invention for engineering considerations, it is clear that some of the nanotechnology necessary for fabrication of the invention have only become available very recently. The one-atom microlaser, invented in 1994, should be a key component for this invention since about ten photons are emitted per atom.²⁰⁷ However, it has been found that new phenomena, (1) the virtual-photon tunnel effect and (2) the virtual-photon quantum noise, both have an adverse effect on the preparation of a pure photon-number state inside a cavity, which may impede the performance of the microlaser if placed inside a cavity.²⁰⁸ Pinto concurs that such a low emission rate is necessary since the lasing must take place “as a

succession of very small changes”²⁰⁹

Another suggested improvement to the original invention could involve a femtosecond or attosecond pulse from a disk-shaped semiconductor microlaser (such as those developed by Bell Laboratories). The microlaser could be used in close proximity to the cantilever assembly. Such microlaser structures, called “microdisk lasers” measuring 2 microns across and 100 nm thick, have been shown to produce coherent light radially (see Figure 32). A proper choice of laser frequency would be to tune it to the impurity ionization energy of the semiconductor cantilever. In this example, the size would be approximately correct for the micron-sized Casimir cavity.

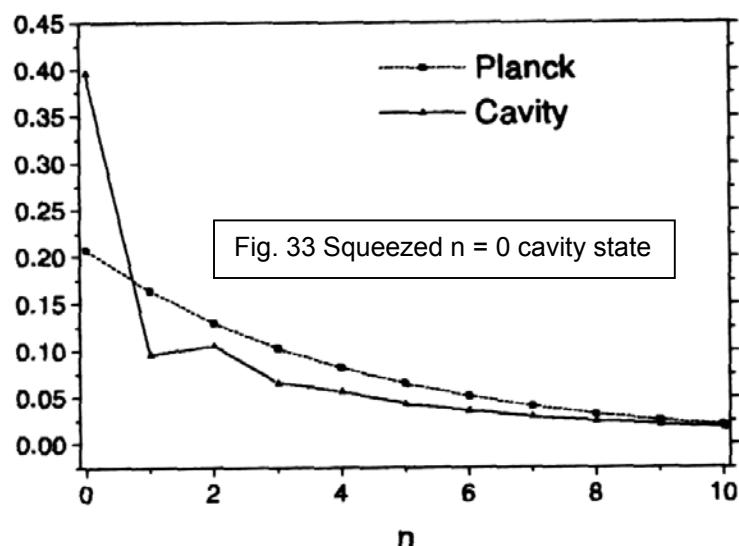
Pinto chooses to neglect any temperature effects on the dielectric permittivity.²¹⁰ However, since then, the effect of finite temperature has been found to be intimately related to the cavity edge choices that can cause the Casimir energy to be positive or negative.²¹¹ Therefore, the contribution of temperature variance and optimization of the operating temperature seems to have become a parameter that should not be ignored. Also supporting this view is the evidence that the dielectric permittivity has been found to depend on the derivative of the dielectric permittivity with respect to temperature.²¹²

Cavity QED Controls Vacuum Fluctuations

It is known from the basic physics of “cavity QED” that just the presence of the walls of a cavity will cause any atoms within it to react differently. For example, “the spontaneous emission rate at wavelength should be completely suppressed if the transition dipole moment is parallel to the mirror plates” where the walls of the cavity are reflecting conductors.²¹³ In other words, “a confined antenna cannot broadcast at long wavelengths. An excited atom in a small cavity is precisely such an antenna, albeit a microscopic one. If the cavity is small enough, the atom will be unable to radiate because the wavelength of the oscillating field it would ‘like’ to produce cannot fit within the boundaries. As long as the atom cannot emit a photon, it must remain in the same energy level; the excited state acquires an infinite lifetime...[because] there are no vacuum fluctuations to stimulate its emission by oscillating in phase with it.”²¹⁴ Such effects are noticed for cavities on the order of hundreds of microns and smaller, precisely the range of Pinto’s cavity. Therefore, it can be expected that **carefully choosing the fundamental resonant frequency of the cavity will provoke the emission of photons so that the dielectric effect on the walls may be enhanced with less input of energy.**

Furthermore, the most important Casimir force research relating to Pinto’s invention may be the analysis of a vibrating cavity. If the *membrane oscillation frequency* is chosen, for example, to be close to a multiple frequency (harmonic) of the fundamental unperturbed field mode of the cavity, resonant photon generation will also provoked. Such resonant photon generation in a vibrating cavity like Pinto’s has been studied in the literature.^{215, 216}

Another aspect of the Pinto experiment apparently not discussed in his article is the relative concentration of gas molecules in the vacuum energy transducer of Figure 30. Though a complete evacuation of air would be preferable, especially when compression of the membrane could be impeded by increasing gas pressures, it is naturally expected that too many gas molecules will still remain airborne even with a high vacuum, such as 10^{-10} to 10^{-12} Torr. Therefore, using another characteristic of cavity QED may be recommended. First of all, the selection of the gas is important, so that the atomic transition frequency matches the cavity resonant frequency very closely. Once this is achieved, it would be recommended, from an engineering point of view, to optimize the design of the size of the cavity transducer so that the atomic transition has a slightly higher frequency than the resonant frequency of the cavity. This could easily occur with the resonant wavelength slightly longer than the resonant transition wavelength of the gas in question. **In that way, the gas molecules will be repulsed from entering the cavity, thus creating a lower gas pressure inside.** Logically, this would be accomplished with the cavity transducer in the maximum S_A position in Figure 30. It would thereby add to the compression force of the movable membrane. As the membrane reaches its lowest position in the engine cycle with minimum S_A position, cavity QED dictates that since the atomic transition frequency will then be lower than the resonant frequency of the cavity, the force will be attractive,



pulling gas molecules toward the cavity and increasing the pressure. This condition may be accomplished as well, since the shorter wavelength of the smaller cavity size will now be less than the longer wavelength of the atomic transition wavelength of the gas. Such a condition, with extra gas molecules in the cavity, will assist in pushing the membrane upwards again.²¹⁷ Such detailed planning with gases and cavity dimensions should create a situation where the ZPF is supplying a larger percentage of the energy output, with a minimum of nanolaser input energy. If so, the Pinto vacuum energy generator would offer an unparalleled miniature electricity

source that could fill a wide range of nanotechnology needs and microelectronic needs.

Spatial Squeezing of the Vacuum

The analysis of Pinto's invention is analogous to spatial squeezing of the initial states to decrease the energy density on one side of a surface, below its vacuum value, in order to increase the Casimir force. For an oscillating boundary like Pinto's, this can also create a correlated excitation of frequency modes into squeezed states and "sub-Casimir regions" where the vacuum develops structure. **"Pressing zero-point energy out of a spatial region can be used to temporarily increase the Casimir force."**²¹⁸ This spatial squeezing technique is gaining increasing acceptance in the physics literature as a method for bending quantum rules while gaining a short-term benefit, such as modulating the quantum fluctuations of atomic displacements below the zero-point quantum noise level of coherent phonon (vibrational) states, based on phonon-phonon interactions.²¹⁹

The squeezing technique involves minimizing the expectation value of the energy in a prescribed region, such as a cavity. "In general, a squeezed state is obtained from an eigenstate of the annihilation operator...by applying to it the unitary squeezing (or dilation) operator."²²⁰ Ideally, **"it seems promising to generate squeezed modes inside a cavity by an instant change of length of the cavity."**²²¹ The implied infinite speed or frequency for a movable membrane would not be achievable however. If it were approachable, the squeezing would cause a modification of the Casimir force so that it could become a time dependent oscillation from a maximum to minimum force. Pursuing resonance measurements may turn out to be the most realistic experimental approach in order to exploit the periodic variation in the Casimir force by squeezing.

In Figure 33, the effect of squeezing can be seen in the fundamental cavity mode $n = 0$ where the emission of photons is almost double that allowed by the Planck radiation law Equation (9), where there are quantized field modes. Hu found that the

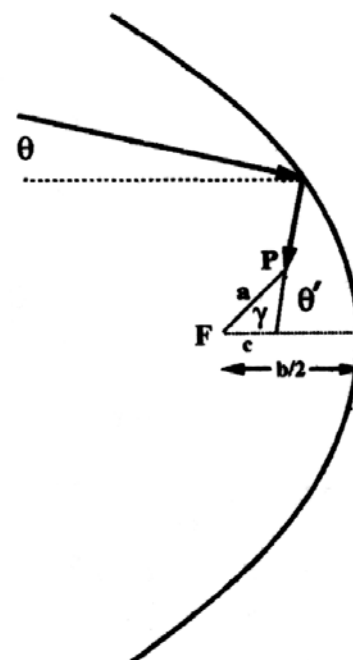


Fig. 34 Vacuum fluctuations focus

other field modes go to a mixed quantum state due to the intermode interaction caused by the classical Doppler effect from the moving mirrors. The theory also predicts that the significant features of the nonstationary Casimir effect are not sensitive to temperature.²²²

Focusing Vacuum Fluctuations

Another development that may directly affect transduction possibilities of ZPE is the theoretical prediction of focusing vacuum fluctuations. Utilizing a parabolic mirror designed to be about 1 micron in size (labeled 'a' in Figure 33), with a plasma frequency in the range of 0.1 micron for most metals, Ford predicts that it may be possible to deflect atoms with room temperatures of 300K, levitate them in a gravitational field, and trap them within a few microns of the focus F.²²³ **A positive energy density results in an attractive force.** Depending upon the parameters, it may alternatively result in a repulsive Van der Waals force at the focus with a region of negative energy density. This type of trapping would require no externally applied electromagnetic fields or photons. The enhanced vacuum fluctuations responsible for these effects are found to arise from an interference term between different reflected rays. The interesting conundrum is the suggestion that parabolic mirrors can focus something even in the absence of incoming light, but vacuum fluctuations are often treated as evanescent electromagnetic fields. The manifestation of the focusing phenomenon is the growth in the energy density and the mean squared electric field near the focus.²²⁴

Focusing vacuum fluctuations in many ways resembles “amplified spontaneous emission” (ASE) which occurs in a gain medium, where the buildup of intensity depends upon the quantum noise associated with the vacuum field.²²⁵

Stress Enhances Casimir Deflection

An interesting Casimir force effect, seen more and more frequently in nano-electromechanical

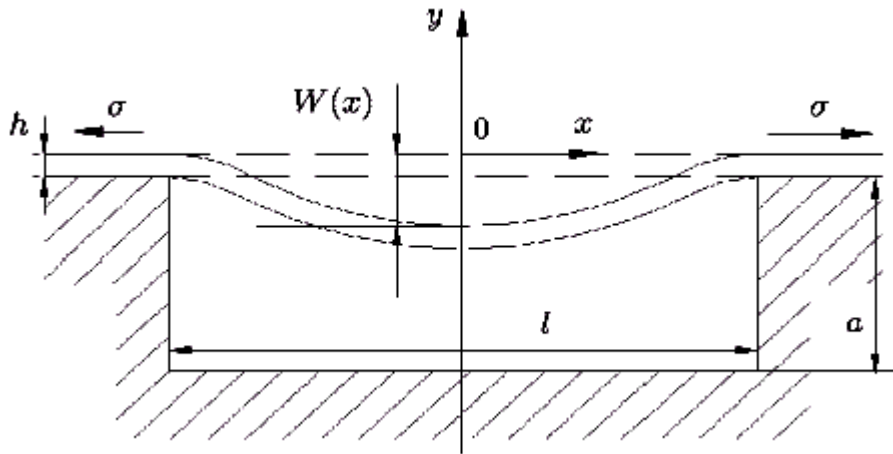


Figure 35 - NEMS
cantilever bridge
deflection caused by
the Casimir force

system (NEMS), is illustrated in Figure 35. Shown is a membrane or cantilever of thickness h that covers a well of width l and height a , which is deflected in the y direction, by an amount of distance $W(x)$ depending upon the position with respect to x .²²⁶ The equation describing the deflection of any point on the membrane is:

$$D \frac{\partial^4 W(x)}{\partial x^4} = F \quad (31)$$

$D = Eh^3/(12-12p^2)$ where E is the elastic modulus, h is the thickness (see Figure 35) of the membrane, and p is the Poisson ratio. The Poisson ratio is the ratio of the transverse contracting strain to the elongation strain.²²⁷ The Casimir force F in Equation (31), due to the proximity to the bottom plate, is an inhomogeneous force in this situation, varying from point to point along x as²²⁸

$$F = - \frac{\pi^2 hc}{210 (a - W(x))^4}$$

(32)

where h , $W(x)$ and a are defined above.

Equations (31) and (32) are then equated to produce a quartic equation dependent on $W(x)$ where the residual applied stress/strain σ can be added as a modifier. Solving for $W(x)$ under conditions of strain (stretching) yields a tendency toward a stationary wave pattern characteristic of buckling, without any appreciable change in the center deflection. Solving for $W(x)$ under conditions of stress (compression) reveals that “compressive residual stress enhances the deflection of the bridge and reduces its [buckling] behaviour.”²²⁹ The amount of enhancement at the center is $W(0) = 0.0074a$ or almost 1%. However, since the Casimir force in Equation (32) increases by the fourth power of the distance ($a - W(x)$), it is also regarded as a positive feedback system, with a tendency of increasing any deflection in a direction toward structural failure.

Casimir Force Geometry Design

Since the Casimir force is such an integral part of the experimental energy manifestations of the ZPF as well as the Chapter 4 analysis, it is worthwhile to review some of its important characteristics. First of all, the attractive Casimir force between two uniform, flat metal plates which are perfectly conducting (and therefore, a reflective surface) is²³⁰

$$F = - \pi^2 \hbar c / 240 d^4 \quad (33)$$

where d is the spacing between the plates. Milonni points out that besides the usual vacuum fluctuations approach, one can also treat the virtual photons of the vacuum as “carriers of linear momentum.” This perspective yields a mathematical proof that the Casimir force can also be classically analyzed as a physical difference of radiation pressure on the two sides of each plate.²³¹ In Equation (33), if $d = 1$ micron, F will turn out to equal about 10^{-3} N/m².

In comparison, the Coulomb force for charged plates, such as with Forward’s charge foliated conductors of Figure 8, is found to be

$$F_{\text{Coul}} = V^2 / 8\pi d^2 \quad (34)$$

Thus, with a potential difference of only $V = 17$ mV at $d = 1$ μm , the Casimir force equals the Coulomb force.²³² This is also the operating principle behind Pinto’s cavity transducer of Figure 30, as the

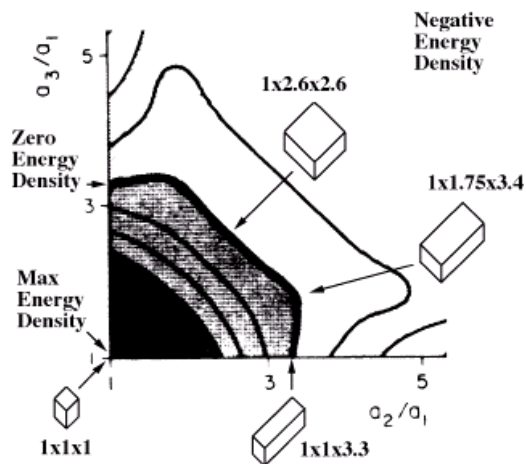


Figure 36
Constant + / 0 / –
Casimir energy
curves for various
rectangular metal
microboxes

Casimir force is varied cyclically.

In Figure 36, a comprehensive “designer’s toolkit approach” by Maclay is made for an arbitrarily-sized box made of perfectly conducting surfaces. As the dimensions of the box deviate from a cubic design (1 x 1 x 1) the Casimir forces change as well.

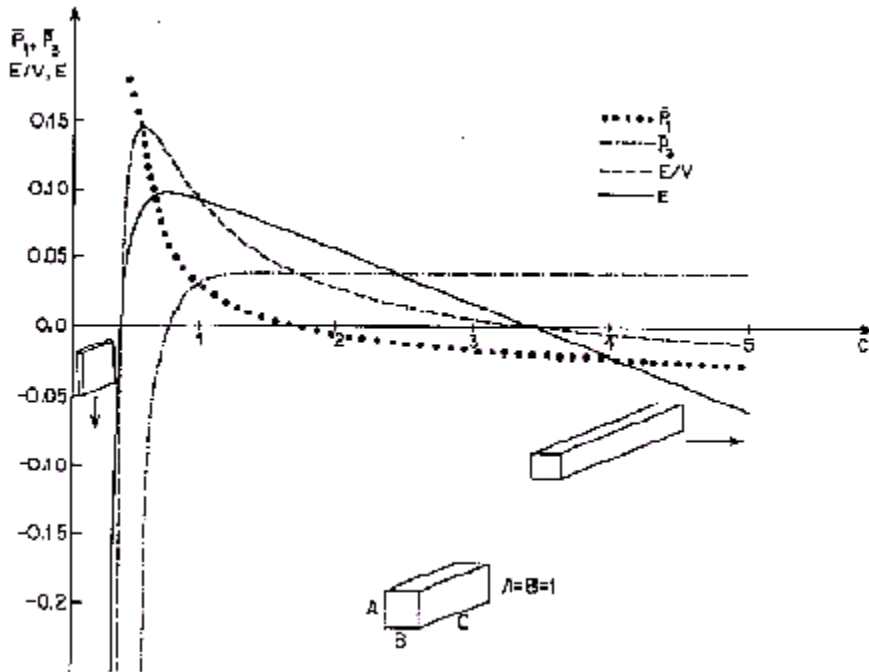


Figure 37
Dotted P_1 is the pressure on the $1 \times C$ face, which varies between + and - pressure; P_3 is the pressure on 1×1 face (small dots); E/V is the energy density (dashed line); E is Casimir energy for the metal box (solid line)

A maximum positive energy density (dark area near the origin) signifies a positive Casimir force or outward pressure. Effectively, positive energy density produces a repulsive Casimir force. The dimensions of $1 \times 1 \times 1.7$ signify the transition zone known as “zero energy density.” Any further increase in size results in a negative or attractive Casimir force. It is readily apparent from these calculations that a similar system, with a movable membrane like Pinto’s Figure 30, offers a restoring force for either deviation from zero, as if the cavity held a compressible fluid.²³³

In Figure 37 is another vacuum engineering toolkit graph, the Casimir forces for a perfectly conducting $1 \times 1 \times C$ rectangular box, expanding from $C = 1$ to an elongated size. Again, as in Figure 36, it can be seen that as $C = 1.7$ the Casimir pressure P_1 crosses the zero energy line. To help distinguish the Casimir energy density E/V and Casimir energy E lines from the rest, it is noted that these two lines cross zero at the same point $C = 3.5$, while the Casimir pressure P_3 line stays constant past $C = 1$. The E/V , E , and P_3 lines are all negative when $C < 1$ showing the dominance of d^4 in the denominator of Equation (33), when two surfaces approach 1 micron or less.

The discovery by Maclay of a particular box dimension ($1 \times 1 \times 1.7$), that sits in the middle of attractive and repulsive Casimir forces, presents a possible scenario for vacuum energy extraction. “This interesting motion suggests that we may be organizing the random fluctuation of the EM field in such a way that changes in pressure directly result, which could lead to work being done. One interesting question is can we design a cavity that will just oscillate by itself in a vacuum. One approach to this would require a set of cavity dimensions such that the force on a particular side is zero, but if the side is moved inward, a restoring force would be created that would tend to push it outward, and vice versa. Hence a condition for oscillation would be obtained. Ideally, one would try to choose a mechanical resonance condition that would match the vacuum force resonance frequency. More complex patterns of oscillation might be possible. The cavity resonator might be used to convert vacuum fluctuation energy into kinetic energy or thermal energy. More calculations of forces within cavities are needed to determine if this is possible, what would be a suitable geometry and how the energy balance would be obtained.”²³⁴ Maclay concedes however, that upon analyzing Forward’s charged parking ramp of Figure 8, with like charges supplying the restorative force to the Casimir attractive force, that no net work would be done for any given oscillation cycle.

When dielectrics are considered, the analysis becomes more involved. “Calculations of Casimir forces for situations more complicated than two parallel plates are notoriously difficult, and one has little

intuition even as to whether the force should be attractive or repulsive for any given geometry.”²³⁵ With a dielectric set of parallel plates, the characteristics of dispersive (phase velocity is a function of frequency) or non-dispersive (all frequencies equally transmitted or reflected) dielectrics enters into the equation. For example, a classic example is two dispersive dielectric parallel plates that have a Casimir energy which depends only on the distance between the plates and the dispersion of the dielectrics.²³⁶

Various geometries of rectangular cavities can also be studied using the principle of virtual work where $E = - \int F dx$. With the Casimir vacuum energy E for a dielectric ball of radius a , for example, the Casimir force per unit area is,

$$F = - \frac{1}{4\pi a^2} \frac{\partial E}{\partial a} \quad (35)$$

For a dilute, dispersive dielectric ball for example, the Casimir surface force is found to be attractive with inward pressure.²³⁷ A system of two dielectric spheres with general permittivities and some chosen values of the refractive index n has also been evaluated for Casimir forces.²³⁸

One application for this type of Casimir force calculation lies with biological cells which are spheres with a high dielectric constant. **Figure 38 shows a B-lymphocyte which is 1 micron across which therefore must experience and compensate for the inward Casimir pressure.** “Biological structures may also interact with the vacuum field. It seems possible that cells, and components of

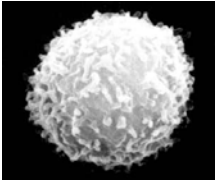


Figure 38
B-lymphocyte

cells, for example, the endoplasmic reticulum may interact with the vacuum field in specific ways. **A cell membrane, with a controllable ionic permeability, might change shape in such a way that vacuum energy is transferred.** Microtubules, in cell cytoskeletons, may have certain specific properties with regard to the vacuum field. Diatoms, with their ornate geometrical structures, must create interesting vacuum field densities; one wonders if there is a function for such fields.”²³⁹ Many of these structures that are less than one micron in size have much higher Casimir pressures to contend with, such as ribosomes which are about 0.02 micron across.²⁴⁰

Other geometrical objects have also been analyzed for the resultant Casimir forces such as hemispheres, pistons, and flat, circular disks.²⁴¹ Instead of solid objects, configurations such as spherically symmetric cavities have also been presented in the literature.²⁴² Rectangular cavities, for example, have also been found to have a temperature dependence and edge design variations which can lead to the Casimir energy being positive or negative.²⁴³

Another interesting area of possible energy extraction from the Casimir effect is in astronomical bodies such as stars. The Casimir effect has been proposed as a source of cosmic energy. In such cosmological objects as white dwarfs, neutron stars, and quasars, the volume effect of the Casimir force is theoretically sufficient to explain the huge output of quasars for example. A calculation of the shift in energy density of the ZPF due to the presence of an ideal conductor in a volume V of space relative to the case with an absence of the volume is the mean value of the stress-energy tensor of QED inside volume V . A conductive material will be conductive for frequencies below the plasma frequency $\omega < \omega_p$ and transparent for frequencies above the plasma frequency $\omega > \omega_p$. The plasma frequency, for nonpropagating oscillations depending only on the total number of electrons per unit volume is, in Gaussian units,²⁴⁴

$$\omega_p^2 = 4\pi n e^2 / m \quad (36)$$

The dielectric constant for high frequencies is also dependent on the plasma frequency (compare with Figure 15),

$$\epsilon(\omega) = 1 - \omega_p^2 / \omega^2 \quad (37)$$

(In dielectric media, Equation (37) applies for $\omega^2 \gg \omega_p^2$.) The shift in the vacuum energy density due to the presence of a volume of ideal conducting material is, expressed in terms of the plasma frequency,

$$\Delta E_{\text{vac}} = - \omega_p^4 \hbar c / 4\pi^2 . \quad (38)$$

With a dramatic increase in the electron density n due to gravitational compression in collapsing stars, an energy creation is predicted that compares with 10^{38} J expected for a nova or 10^{42} J for a supernova if the radius of the star is compressed to approximately $R \approx 10^7$ m.²⁴⁵

Vibrating Cavity Photon Emission

Various cavities have been analyzed so far for the net Casimir effect. However, the case of photon creation from the vacuum due to a non-stationary Casimir effect in a cavity with vibrating wall(s) is unique and has interesting ramifications. Comparing with Pinto's cavity of Figure 30, the cavity chosen by Dodonov to create resonance photon generation also has one moving wall while the rest of the rectangular cavity is stationary. The fundamental electromagnetic mode is $\omega_1 = \pi c / L_0$ where L_0 is the mean distance between the walls of the cavity. The maximum value of the energy is found to be three times the minimum value, depending on the phase. The total energy also oscillates in time and the photon generation rate tends toward a constant value as long as any detuning is less than one.

While changes in the dielectric constant of cavity walls affect the Casimir vacuum force of Pinto's vibrating cavity, there are also effects from a change in the refractive index of a medium. Hizhnyakov presents evidence for the emission of photons from such a distortion of the spectrum of zero point quantum fluctuations. If the medium experiences a time-dependent refractive index, it has been demonstrated that part of the energy will be emitted as real photons. An example is a dielectric medium excited by a rectangular light pulse for about a femtosecond (10^{-15} seconds). The spectral density of the photon energy is shown to depend only upon the rate of change of the refractive index over time, which is unusual. While Hawking and Unruh radiation effects are mixed thermal states, this refractive index derivative effect is said by **Hizhnyakov** to be a pure state equally related to the ZPF as a non-linear quantum optical effect. In terms of energy flow, a picojoule (10^{-9} J) laser pulse lasting for a femtosecond produces about ten megawatts (10 MW/cm^2) of power input and the input pulse has about 10^{-5} cm^2 cross sectional area which gives about a 100 W power input. The output intensity, estimated to be about a picowatt, is calculated to be the sum of two pulses created from the leading and trailing edges of the input refractive index change.²⁴⁶

The Unruh radiation referred to above is actually called the **Unruh-Davies Effect** which refers to a phenomenon related to uniform acceleration. In a scalar field such as the ZPE vacuum, **“the effect of acceleration is to ‘promote’ zero-point quantum field fluctuations to the level of thermal fluctuations.”**²⁴⁷ Milonni points out that it took a half a century after the birth of quantum theory for the thermal effect of uniform acceleration to be discovered. The effective temperature that would be measured by an accelerated detector in a vacuum is

$$T_U = \frac{\hbar a}{2\pi k c} \quad (38)$$

which leads to the interpretation that thermal radiation is very similar to vacuum fluctuation radiation. In Equation (38), k is the wave number (ω/c) and a is the acceleration. Both vacuum probability distribution functions and thermal distributions exhibit a Gaussian probability distribution since the vacuum distribution is the $T \rightarrow 0$ limit of the thermal distribution.²⁴⁸

Looking at Hawking radiation, which is emitted from a black hole, it is based on the premise that pair production from the vacuum can occur anywhere, even at the event horizon of a black hole. The treatment is related to a mathematical manipulation called Wick rotation, where the metric is rotated into the complex plane with time $t \rightarrow -i t$, so that the temperature is inversely equal to the period.

Solving for the region just outside the event horizon $r \geq 2GM$, where G is the gravitational constant, the Hawking temperature is found to be

$$T_H = \frac{\hbar c^3}{8\pi GM} \quad (39)$$

where M is the mass of the black hole.²⁴⁹ Since Planck's constant is included in Equation (39), Zee notes that Hawking radiation is indeed a quantum effect. The similarities between Equations (38) and (39) are referred to by Hizhnyakov (endnote 245).

Fluid Dynamics of the Quantum Vacuum

In the analysis of Figure 37, it was mentioned that the Casimir force within cavities of Pinto and Maclay, possessing one movable wall, behave like a compressible fluid since a restoring force is present for any deviation from the zero-force position. It turns out that more exact analogies to fluids are possible for the quantum vacuum. A hydrodynamic model of a fluid with irregular fluctuations has been proposed by Bohm and Vigier for the vacuum, which also satisfies Einstein's desire for a causal interpretation of quantum mechanics.²⁵⁰ Their work also includes a proof that the wave function probability density $P = |\psi|^2$ used in quantum theory approaches the standard formula for fluid density with random fluctuations. There is also a suggestion of further work regarding how a fluid vortex

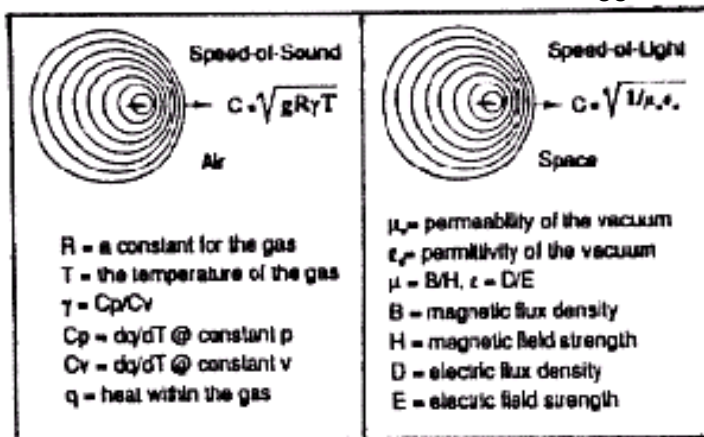


Figure 39
Flight
resistance
vs. speed
utilize the
same form
equation in
air or in
space

provides a very natural model of the non-relativistic wave equation of a particle with spin.

A computational fluid dynamics approach to the ZPF, with the ambitious aim of reducing flight resistance at superluminal speeds has been proposed

by Froning and Roach.²⁵¹ The negative energy density region seen in Figure 37 between Casimir plates is also implicated in resistance to increased speed, which is perceived as inertia. Drawing upon the separate works by **Puthoff and Haisch** (cited in Chapter 2), this approach takes their ZPE-related gravity and inertia theory to the engineering level of experimental simulation. In Figure 40, the analogy is drawn between the well-known equation for the speed of light $c = (\mu_0\epsilon_0)^{-1/2}$ and the aerodynamic gas equation for the speed of sound $c = (gR\gamma T)^{-1/2}$ with compressible fluid graphics for each. The aerodynamic resistance of viscous

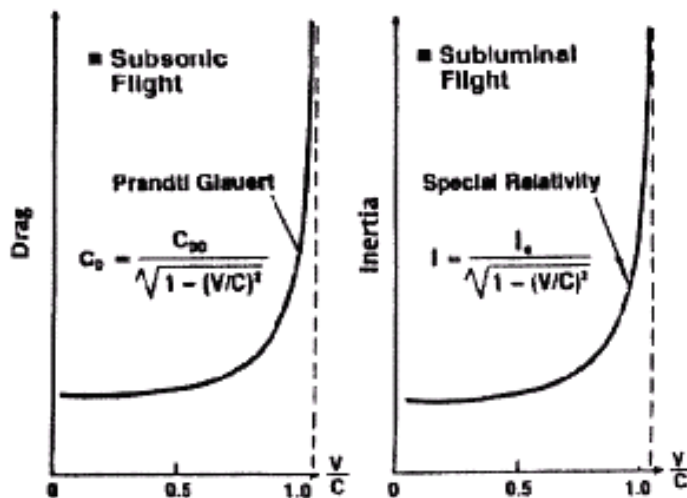


Figure 40
Acoustic
and electro-
magnetic
wave
drag or
inertial
actually
do use
the same
equation!

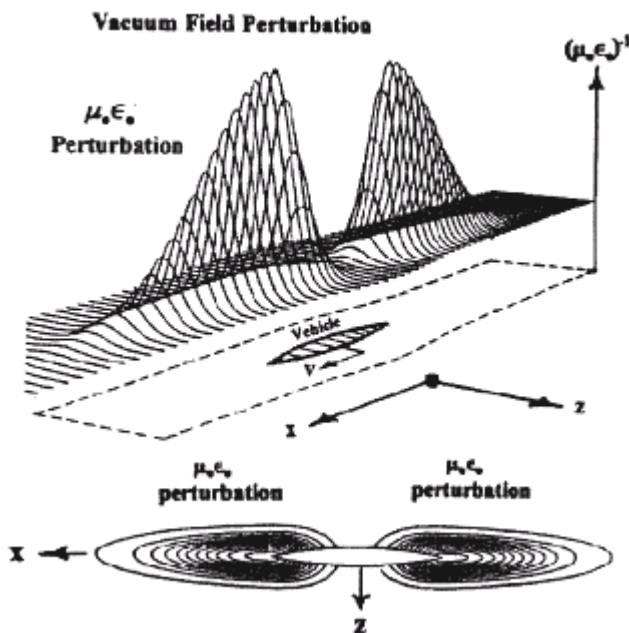
resistance to increased speed, which is perceived as inertia. Drawing upon the separate works by **Puthoff and Haisch** (cited in Chapter 2), this approach takes their ZPE-related gravity and inertia theory to the engineering level of experimental simulation. In Figure 40, the analogy is drawn between the well-known equation for the speed of light $c = (\mu_0\epsilon_0)^{-1/2}$ and the aerodynamic gas equation for the speed of sound $c = (gR\gamma T)^{-1/2}$ with compressible fluid graphics for each. The aerodynamic resistance of viscous

sound $c = (gR\gamma T)^{-1/2}$ with compressible fluid graphics for each. The aerodynamic resistance of viscous

drag exerted on the substructure of a vehicle is compared to the Lorentz force exerted on the substructure of the vehicle by the ZPF, which is also proposed to be a Casimir-like force exerted on the exterior by unbalanced ZPE radiation pressures. **The conclusion drawn from this first-order analysis is that μ_0 and ϵ_0 can be perturbed by propagation speed and possibly vehicle inertia, accompanied by a distortion of the zero-point vacuum.**

A fundamental part of the Froning and Roach approach to the fluid dynamic simulation of superluminal speeds is the proposal that μ_0 and ϵ_0 can be reduced significantly by nonabelian electromagnetic fields of SU(2) symmetry. It is proposed that EM fields of nonabelian form have the same symmetry that underlies gravity and inertia. Their approach is particularly to use alternating current toroids with resonant frequencies. That nonabelian gauge symmetry offers a higher order of symmetry has been seen elsewhere in the literature. Zee, for example, notes that the square of the vector potential A^2 would normally be equal to zero in the abelian gauge, which all standard ("trivial") electromagnetic theory texts use. Instead, he notes that a field strength such as $F = dA + A^2$ can be formulated easily in the nonabelian gauge and shown to be nonzero and gauge covariant (though not invariant). Furthermore, the nonabelian analog of the Maxwell Lagrangian, called the Yang-Mills Lagrangian, includes cubic and quartic terms that describe self-interaction of nonabelian bosons (photons), as well as a nonabelian Berry's phase that is intimately related to the Aharonov-Bohm phase. (The Aharonov-Bohm phase depends exclusively on the vector potential.) Even the strong nuclear interaction is accurately described by a nonabelian gauge theory. "Pure Maxwell theory is free and so essentially trivial. It contains a noninteracting photon. In contrast, pure Yang-Mills theory contains self-interaction and is highly nontrivial...Fields listen to the Yang-Mills gauge bosons according to the representation R that they belong to, and those that belong to the trivial identity representation do not hear the call of the gauge boson."²⁵²

According to **Froning and Roach**, the representation R can be changed by surrounding a saucer-shaped spaceship with a toroidal EM field that distorts and perturbs the vacuum sufficiently to affect its permeability and permittivity. The vacuum field perturbations are simulated by fluid field



Equilibrium is established when the increase in kinetic energy due to recoil balances the decrease in kinetic energy due to the drag.²⁵³

Figure 41 Topology of vacuum field disturbance

perturbations that resulted in the same percentage change in disturbance propagation speed within the region of perturbation. The computational effort was simplified by solving only the Euler equations of fluid dynamics for wave drag. The resulting μ_0 and ϵ_0 perturbation solutions are shown in Figure 41.

In his discussion of the 1910 **Einstein-Hopf** model, Milonni describes their derivation of a retarding force or drag on a moving dipole as a result of its interaction with the vacuum zero-point field, which acts to decrease its kinetic energy. Assuming $v \ll c$, the retarding force due to motion through the ZPF thermal field is described with a fluid dynamics equation, $F = -R v$, where v is the velocity of the dipole and R is a formula depending upon dipole mass and ZPF spectral energy density. **Milonni also notes that due to recoil associated with photon emission and absorption, which are both in the same direction, the ZPF also acts to increase the kinetic energy of a dipole.**

It has been proposed by Rueda and Haisch, with a contract from NASA, that **the ZPF can lose its Einstein-Hopf drag as the absolute**

temperature approaches zero, which would leave only the accelerating recoil force left. (The temperature of outer space is about 3K, or 3 degrees above absolute zero.) Furthermore, they propose that the ZPF can provide a directional acceleration to monopolar particles more effectively than to polarizable particles. They also suggest that “if valid, the mechanism should eventually provide a means to transfer energy, back and forth, but most importantly forth, from the vacuum electromagnetic ZPF into a suitable experimental apparatus.”²⁵⁴

Quantum Coherence Accesses Single Heat Bath

One of the main criticisms of energy extraction from the ZPF is that it represents a single low-temperature bath and the second law of thermodynamics prohibits such an energy conversion. It is well-known that Carnot showed that every heat engine has the same maximum efficiency, determined only by the high-temperature energy source and the low-temperature entropy sink. Specifically, it follows that no work can be extracted from a single heat bath when the high and low temperature baths are the same.

However, a new kind of quantum heat engine (QHE) powered by a special “quantum heat bath” has been proposed by Scully et al. which allows the extraction of work from a single thermal reservoir. In this heat engine, radiation pressure drives the piston and is also called a “Photo-Carnot engine.” Thus, the radiation is the working fluid, which is heated by a beam of hot atoms. The atoms in the quantum heat bath are given a small bit of quantum coherence (phase adjustment) which becomes vanishingly small in the high-temperature limit that is essentially thermal. However, the phase associated with the atomic coherence, provides a new control parameter that can be varied to increase

the temperature of the radiation field and to extract work from a single heat bath. The second law of thermodynamics is not violated, according to Scully et al., because the quantum Carnot engine takes more energy, with microwave input, to create the quantum coherence than is generated.²⁵⁵

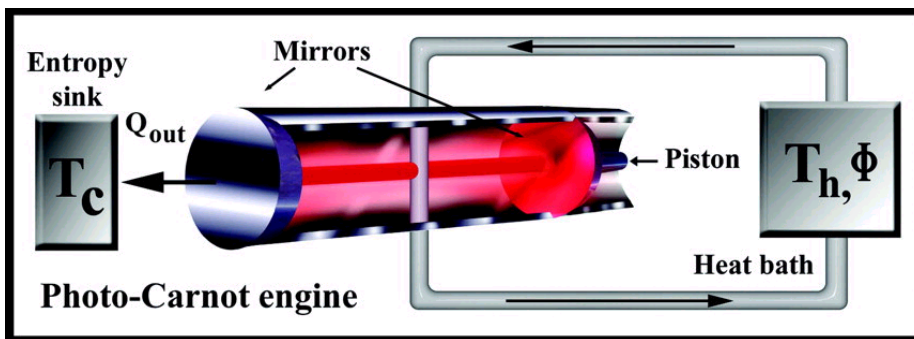


Figure 42 Photo-Carnot heat cycle diagram. Q_{in} is provided by hot atoms

The Photo-Carnot engine, shown in Figure 42, creates radiation pressure from a thermally excited single-mode field that can drive a piston. Atoms flow through the engine from the T_h heat bath and keep the field at a constant temperature for the isothermal $1 \rightarrow 2$ portion of the Carnot cycle (Figure 43). Upon exiting the engine, the bath atoms are cooler than when they entered and are reheated by interactions with the blackbody at T_h and "stored" in preparation for the next cycle.

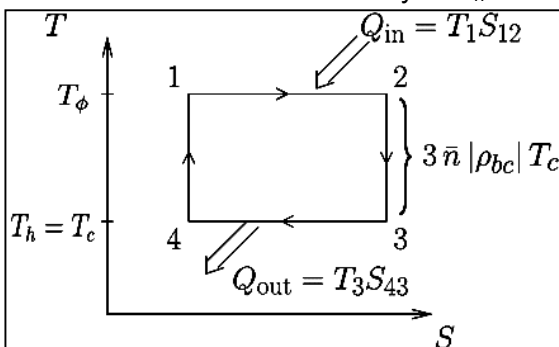


Figure 43 Temperature – entropy diagram for Photo-Carnot engine where input T_h equals the output T_c

The stimulus for the work came from two innovations in quantum optics: the micromaser and microlaser (Figure 32) and lasing without inversion (LWI). In micromasers and microlasers, the radiation cavity lifetime is so long that a modest beam of excited atoms can sustain laser oscillation. In LWI, the atoms have a nearly degenerate pair of levels

making up the ground state. When the lower level pair is coherently prepared, a small excited state population can yield lasing (without inversion). In the QHE, the "engine" is a microlaser cavity in which one mirror is a piston driven by the radiation pressure given by

$$P V = n \hbar \pi c / L \quad (40)$$

where P is the radiation pressure, V is the cavity volume, n is the average number of thermal photons in the right mode (about 10^3), and L is the length of the cavity.²⁵⁶ In Figure 43, an engine cycle diagram is shown which is a temperature versus entropy graph for the Photo-Carnot engine, where $|p_{bc}| \approx 3 \times 10^{-6}$ is an off-diagonal density matrix element in the extension of the quantum theory of a laser without inversion. Figure 43 contains a closed cycle of two isothermal and two adiabatic processes (compare with Pinto's Figure 31). Q_{in} is the energy absorbed during the isothermal expansion and Q_{out} is the energy given to the heat sink during the isothermal compression. However, instead of two states which would render this a classical engine, the QHE has three states, which can result in quantum coherence. "If there is a non-vanishing phase difference between the two lowest atomic states, then the atoms are said to have quantum coherence. This can be induced by a microwave field with a frequency that corresponds to the transition between the two lowest atomic states. **Quantum coherence changes the way the atoms interact with the cavity radiation by changing the relative strengths of emission and absorption.**"²⁵⁷ In Figure 42, as the atoms leave the blackbody at temperature T_h they pass through a microwave cavity that causes them to become coherent with phase Φ before they enter the optical cavity. The temperature that characterizes the radiation is T_Φ which is

$$T_\Phi = T_h (1 - n \varepsilon \cos \Phi) \quad (41)$$

where ε is the magnitude of quantum coherence, $\varepsilon = 3|p_{bc}|$. The second term in Equation (41) is also used in the QHE efficiency equation,

$$\eta_\Phi = \eta - (T_c/T_h) n \varepsilon \cos \Phi \quad (42)$$

"Thus, depending on the value of Φ , the efficiency of the quantum Carnot engine can exceed that of the classical engine – even when $T_c = T_h$. It can therefore extract work from a single heat bath."²⁵⁸

Inexplicably, Scully et al. fail to cite a **previous work by Allahverdyan and Nieuwenhuizen** that utilizes more rigorous physics for same purpose of extraction of work from a single thermal bath in the quantum regime with quantum coherence. The authors, perhaps, have more controversial statements in the article regarding *free energy extraction*. Using the quantum Langevin equation for quantum Brownian motion, they note that it has a Gibbs distribution only in the limit of weak damping, thus preventing the applicability of equilibrium thermodynamics. The reason is related to quantum entanglement and the necessary mixed state. **"Our main results are rather dramatic, apparently contradicting the second law: We show that the Clausius inequality $dQ \leq TdS$ can be violated, and that it is even possible to extract work from the bath by cyclic variations of a parameter ("perpetuum mobile").** The physical cause for this appalling behavior will be traced back to quantum coherence in the presence of the near-equilibrium bath."²⁵⁹ It is also emphasized that the quantum coherence is reflected in the quantum noise correlation time which exceeds the damping time $1/\Gamma$.

Regarding the ZPF, it is interesting that ***the quantum Langevin equation is a consequence of the fluctuation-dissipation theorem of Equation (11)***. The authors note that part of the equation includes the fluctuating quantum noise, which has a maximum correlation time and therefore has a long memory (quantum coherence) at low temperature. The Brownian particle of interest also has semi-classical behavior due to its interaction with the bath, where notably, "there is a transfer of heat, even for $T = 0$."²⁶⁰

The possibility of extracting energy from the bath is due to the nonequilibrium state, which is ensured by the switching energy $\frac{1}{2} \gamma \Gamma \langle x^2 \rangle_0$ that is also a purely classical effect. The switching energy depends upon γ which is the damping constant and Γ which is the cutoff frequency. Both harmonic and anharmonic oscillation potentials are considered. The Brownian quantum particle strongly interacts with the quantum thermal bath, described by the Fokker-Planck equations.

"Two formulations of the second law, namely, the Clausius inequality and the impossibility to extract work during cyclical variations, can be apparently violated at low temperatures. One could thus speak of a '**perpetuum mobile of the second kind.**' We should mention, however, that the number of cycles can be large, but not arbitrarily large. As a result, the total amount of extractable work is modest. In any case, the system energy can never be less than its ground state energy...We call them apparent violations, since, the standard requirements for a thermal bath not being fulfilled, **thermodynamics just does not apply.** Let us stress that also in the classical regime the harmonic oscillator bath is not in full equilibrium, but there noise and damping have the same time scale $1/\Gamma$, allowing the Gibbs distribution to save the day and thermodynamics to apply. Our results make it clear that the characterization of the heat bath should be given with care. If it thermalizes on the observation time, standard thermodynamics always applies. Otherwise, thermodynamics need not have a say...The finding that work can be extracted from quantum baths may have a wide scope of applications such as cooling."²⁶¹

In a physics commentary, Linke defends the second law by insisting that the work done by the Scully et al. piston (in Figure 42) is less than the work required to establish quantum coherence. Linke clarifies the Photo-Carnot process by stating, "When the phase difference is adjusted to the value π ,

destructive interference reduces the likelihood of photon absorption, whereas emission from the upper level is not affected. This deviation from detailed balance between photon absorption and emission increases the photon temperature. The resulting temperature difference between photon gas and heat bath allows the photon Carnot engine to produce work in the absence of a hot bath."²⁶²

Thermodynamic Brownian Motors

There is still another aspect of the ZPF that presents the possibility of energy extraction, which are nonequilibrium fluctuations — a different representation of the single heat bath. Biasing the Brownian motion of a particle in an anisotropic medium without thermal gradients, the force of gravity, or a macroscopic electric field is a way that usable work is theoretically generated from nonequilibrium fluctuations, such as those generated externally or by a chemical reaction far from equilibrium. Fluctuation-driven transport is one mechanism by which chemical energy can directly drive the motion of particles and macromolecules and may find application in a wide variety of fields, including the design of molecular motors called "Brownian motors" and pumps.²⁶³

Brownian motion, the random collisions with solvent molecules by a particle in a liquid, has been studied historically by Einstein as well as by Langevin. **Langevin's equation**, as noted in the previous section, suggested that the forces on the particle due to the solvent can be split into two components: (1) a fluctuating force that changes direction and magnitude frequently compared to any other time scale of the system and averages to zero over time, and (2) a viscous drag force that always slows the motions induced by the fluctuation term. Related to the fluctuation-dissipation theorem of Equation (11), the amplitude of the fluctuating force is governed by the viscosity of the solution and by temperature, so **the fluctuation is often termed thermal noise**. Even in an

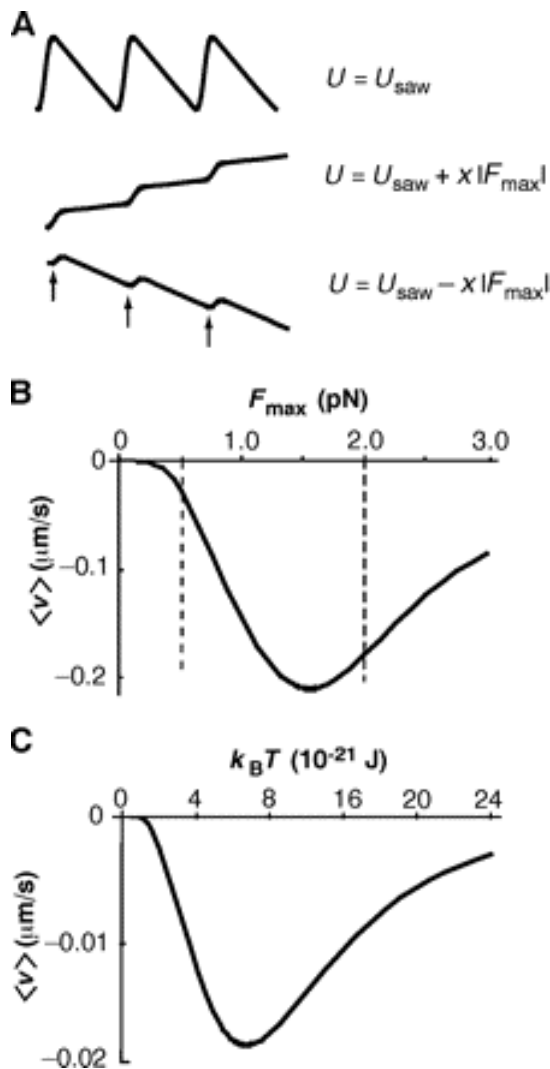


Figure 44 - Fluctuation-driven transport
(B) velocity vs. maximum force;
(C) velocity vs. thermal noise

anisotropic medium, the fluctuations are symmetric as required by the second law of thermodynamics, as are the dissipative drag force. Therefore, when all components of fluctuation-driven system are treated consistently, net motion is not achieved if it is an isothermal system, despite the anisotropy of a ratchet's teeth. However, a thermal gradient in synergy with Brownian motion can cause directed motion of a ratchet and can be used to do work but these are hard to maintain in microscopic and molecular systems. Recent work has focused, instead, on the possibility of an energy source other than a thermal gradient to power a microscopic motor.²⁶⁴

Astumian proposes a fluctuating electrical potential that causes the uphill transport of a particle. A fluctuating potential energy profile is provided with an **anisotropic sawtooth function** U_{saw} and periodically spaced wells with no net macroscopic force. When the potential is off, the energy profile is flat with a uniform force everywhere. When the potential is turned on again, the particle is trapped in one of the wells. The result is resolved into two components: the downhill drift and the diffusive spreading of the probability distribution. For intermediate times, it is more likely for a particle to be trapped in one of the uphill wells if the potential were turned back on, than between the first and second well. Thus, turning the potential on and off cyclically can cause motion to the right and uphill against gravity despite the net force to the left. The theory has been successfully tested with colloidal particles with anisotropic electrodes turned on and off, as well as with an optical trap modulated to create a sawtooth potential.

Figure 44 shows the basic mechanism by which a fluctuating or oscillating force can cause directed motion along a ratchet potential U_{saw} and also some statistics of an example. The presence of thermal noise allows a subthreshold fluctuating force to cause flow. The force is modulated between $\pm F_{\text{max}}$ where the average velocity $\langle v \rangle$ is calculated as a function of F_{max} where the dashed lines (B) indicate the threshold forces. Another example is shown (C) where average velocity is plotted as a function of the thermal noise strength $k_B T$, where k_B is Boltzmann's constant and T is the absolute temperature and $F_{\text{max}} = 0.4$ pN. The (C) graph shows that, up to a point, increasing the noise can actually increase the flow induced by a fluctuating force. However, the (B) graph shows that for forces near the optimum (about 1.5 pN in this example), the velocity decreases with increasing noise.²⁶⁵

A more general approach is suggested for analyzing fluctuation-driven transport using the diffusion equation with a probability density given by the Boltzmann distribution $P(x) \approx \exp(-U/k_B T)$.

Since modulating the potential certainly requires work, Astumian believes there is no question of these devices being perpetual motion machines. The surprising aspect is that flow is induced without a

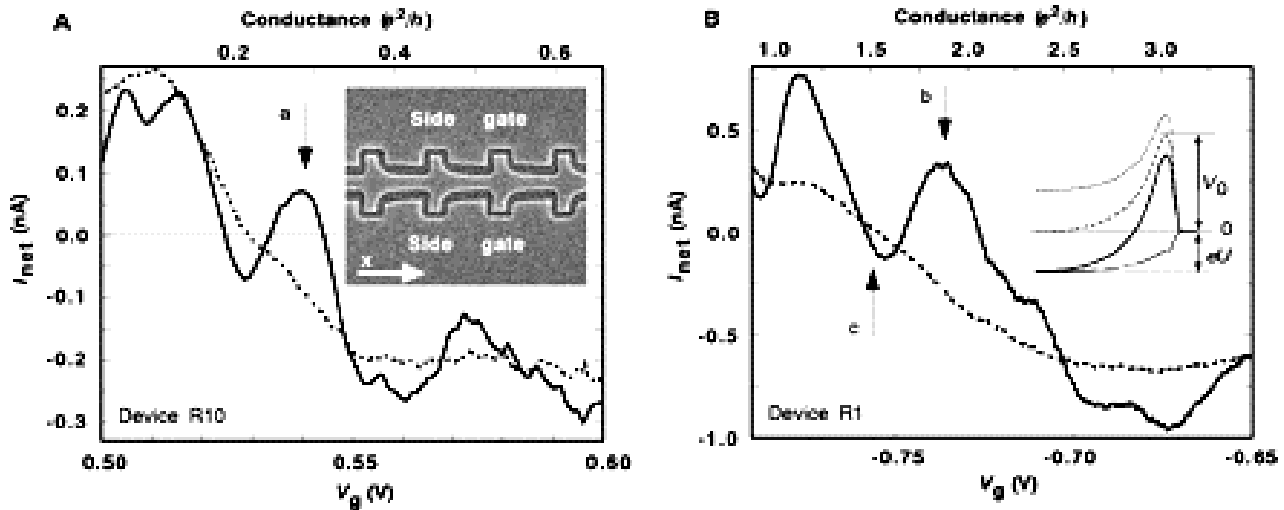


Figure 45 Net current for quantum ratchet. Solid lines, $T = 0.4\text{K}$. Dotted lines, $T = 4\text{K}$. Inset SEM shows four repeating ratchet cells. Temperature-dependent current reversal at a, b, c.

macroscopic force. All of the forces involved are local and act on a length scale of the order of a single period of the potential. Yet the motion persists indefinitely, for many periods. However, the direction of the flow depends upon how the modulation is applied. Such devices are indicated to be consistent with the behavior of molecules.

In a dramatic confirmation of the Astumian theory, two subsequent experiments were performed by Linke et al. which applied an electron ratchet in a tunneling regime with a “rocking-induced current (tunneling through and excitation over the ratchet’s energy barrier) flow in opposite directions. Thus the net current direction depends on the electron energy distribution at a given temperature.”²⁶⁶ The practical aspect of this experimental approach is that a square wave source-drain voltage is applied with the time-averaged electric field being zero, similar to AC electricity, and yet the output net current is DC, similar to a rectifier.

Figure 45A shows in the inset the asymmetrical darker regions which are etched trenches that laterally confine a two-dimensional sheet of electrons located parallel to the surface of a GaAs/AlGaAs heterostructure. Figure 45B inset compares the barrier height V_0 with the electron energy $|eU| \leq 1$ meV. The trench’s periodic variation in width induces a corresponding variation in electron confinement energy that creates asymmetric energy barriers at each constriction. When the square wave source-drain bias voltage is applied, the resulting current I is plotted for two devices R10 and R1. Because of the geometric asymmetry, the electric field along the channel produced by the voltage deforms the barriers in a way that depends on the polarity of the voltage, trapping the electrons in one of the side gates along the x direction. The quantum ratchet is thus established by confining electrons to an asymmetric conducting channel of a **width comparable to the electron wavelength**. The experiment demonstrates importance of resonant design and fulfills the theoretical prediction that a fluctuating voltage is sufficient to cause a unidirectional current.

The detailed theoretical model of the tunneling ratchet is shown in Figure 46. The difference Δt

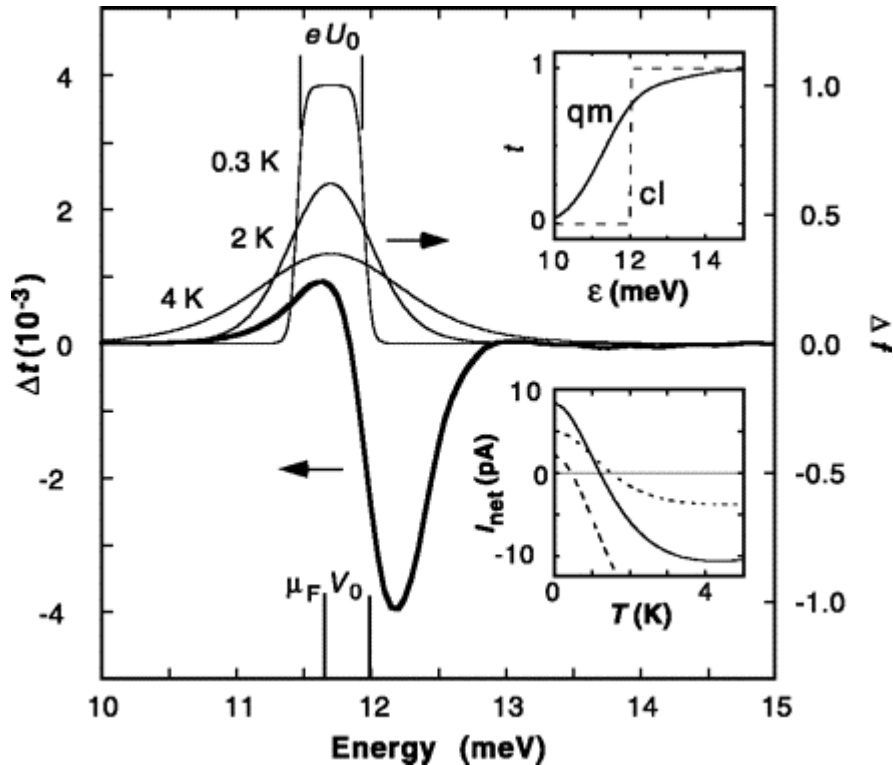


Figure 46 Theoretical model of the quantum electron ratchet

between the transmission functions for the barrier potential V_0 in Figure 45B inset is graphed (solid curve) for a rocking voltage $U_0 = 0.5$ mV. The bottom of Figure 46 shows visually the approximate equality of the barrier height V_0 and the Fermi energy μ_F of 12 meV. The “thin” curves are identified by temperature and are graphed against the energy range Δf of the right hand ordinate axis. The Figure 46 top inset shows the dramatic difference between the solid curve quantum mechanical behavior (qm) and the classical (cl) transmission function versus electron energy ε for $U_0 = 0$. The classical step function occurs at $\varepsilon = V_0$ which is the Fermi energy μ_F . Note the Figure 46 lower inset which summarizes the net current I in picoamperes versus temperature, for rocking voltages $U_0 = 0.7$ mV (dashed curve), 0.5 mV (solid curve), and

0.3 mV (dotted curve). All temperatures in this experiment were within a few degrees of absolute zero.

Transient Fluctuation Theorem

Another development in the thermodynamics of microscopic systems has recently redefined the concept of work. In a system connected to a single heat bath, uncertainties on the order of $k_B T$ will arise from the Boltzmann distribution of energies in the initial and final states, as well as from energy exchange with the heat bath as the system goes from initial to final energy states. Because of the thermal fluctuations or energy uncertainties, it has now been proven by theory and experiment, that the work cannot be uniquely specified, even if the path is known. When the system is microscopic, the fluctuations are significant and a transient fluctuation theorem has evolved to account for the behavior which takes the form,

$$P(W) / P(-W) = e^W \quad (43)$$

where W is the work divided by $k_B T$ and $P(W)$ is the probability of performing positive work over an interval of time, while $P(-W)$ is the probability of performing negative work over the same period of time

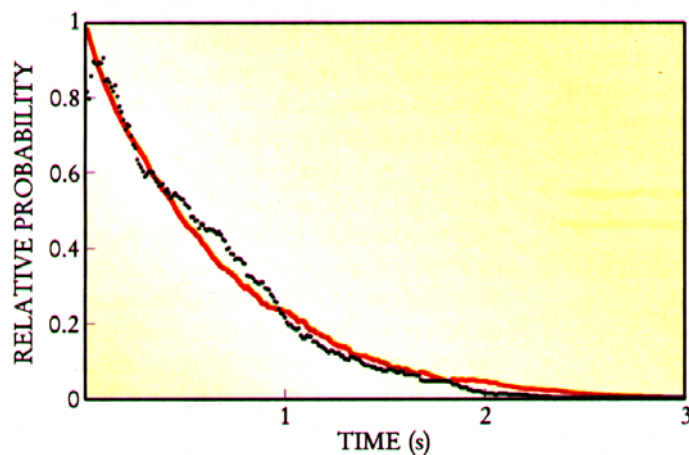


Figure 47 Positive (solid), negative (dots) work over time

It needs to be clarified that in these microscopic systems, work is measured as it is delivered to a vessel but half the time the system goes in reverse, apparently violating the law of entropy. In Figure 47, a Poisson distribution is shown of an optical trap interacting with an experimental vessel having micron-sized beads. Though the trap exerted a restoring force, as for the spring in Figure 2, the experimentally-determined values measured for the bead position in the **integrated fluctuation theorem showed a nonzero probability for negative work, for up to two seconds.**

“Imagine, as is often the case, that after a certain time, the bead has a higher energy than it had initially. Then, if the work done by the trap on the vessel (bead plus bath) is negative, energy has been delivered to both the bead and the optical trap interacting with the vessel. That energy came from the water bath—**just the sort of energy transfer prohibited by the second law in the thermodynamic limit of infinitely large systems: Heat has been converted to work with 100% efficiency.**”²⁶⁸

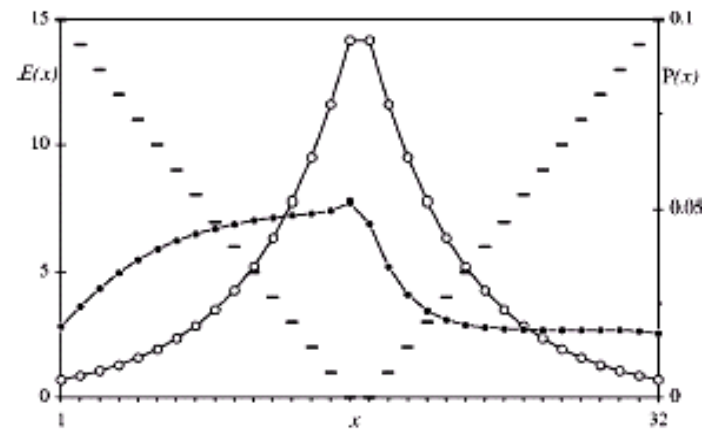


Figure 48 Nonequilibrium Metropolis Monte Carlo simulation

The generalized transient fluctuation theorem has various forms depending upon the application. For example, the probability ratio in Equation (43) can instead relate to entropy production w for forward and reverse time, where microscopic reversibility is an essential requirement. The theorem finds its greatest utility in the application to single heat baths and systems driven by a stochastic (random), microscopically-reversible (time-symmetric), periodic process. Then, the only Gaussian distribution that satisfies the fluctuation theorem has a variance that is twice the mean $2\langle w \rangle = \langle (w - \langle w \rangle)^2 \rangle$, which is a version of the standard fluctuation-dissipation relation of Equation (11).²⁶⁹ It is

noted that entropy production, which is irreversible dissipation, is directly related to the fluctuations.

An example of a systematic application of the fluctuation theorem, reminiscent of the quantum ratchet concept seen previously, is a **Metropolis Monte Carlo** simulation by **Crooks**, illustrated in Figure 48. A single particle occupies a finite number of positions in a one-dimensional box with periodic boundaries and coupled to a heat bath of $T = 5$. The energy surface $E(x)$ is outlined by a series of dashed (–) lines. The equilibrium distribution to be expected from such a potential well is shown as a symmetric hill with open circles O since the particle is free to move with equal probability to the right, left, or to stay put. However, every eight time intervals, the energy surface moves to the right by one position.

In this way, the system is driven away from equilibrium and settles into a time-symmetric, nonequilibrium steady state distribution shown by black dots ●, skewed to the left. The master equation for this system can be solved exactly to compare with the theory.²⁷⁰

Power Conversion of Thermal Fluctuations

While many recent scientific advances in the treatment of nonequilibrium energy fluctuations have been reviewed so far, there are also developments in the area of nonlinear equilibrium thermal fluctuations. Based on the Nyquist theorem (another name for the fluctuation-dissipation theorem) and van Kampen's work on nonlinear thermal fluctuations in diodes, **Yater's** pioneering work involves the use of microscopic diodes in a simple circuit, whose "results gave higher conversion efficiencies than the Carnot cycle for certain limiting cases as these model sizes decreased."²⁷¹ While the use of two heat baths suggests a thermionic energy source, his detailed analysis makes it clear that the energy fluctuation conversion is added to a heat pump thermal conversion cycle, for example, yielding a factor of 10 improvement.²⁷²

Yater offers a simplified master equation for the output rectified current from an independent particle model,

$$I(N) \approx \exp[(\beta - \alpha)(N - \frac{1}{2}) - (\beta m + \alpha n)] - 1 \quad (44)$$

where $\beta = q^2 / k_B T_c C$, N = the number of excess electrons in the total circuit capacitance C , and $\alpha = q^2 / k_B T_r C$. The designation of n and m are related: $n = C_c V / q$ and $m = C_r V / q$ where $C = C_c + C_r$.²⁷³ The forward and reverse diode currents in Figure 49 also combine in textbook fashion to produce the total current of Equation (44):

$$I(N) \approx I_{1a} I_{2b} - I_{2a} I_{1b} \quad (45)$$

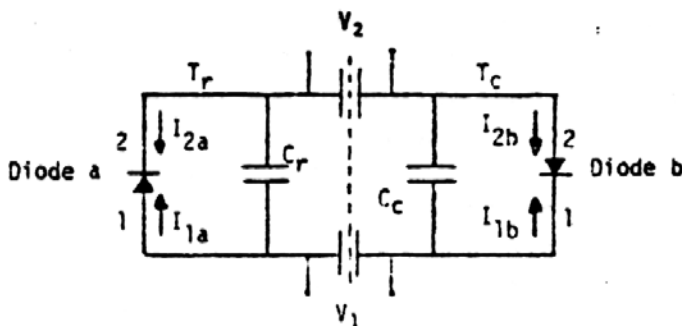


Figure 49 Energy fluctuation conversion circuit

A Schottky barrier diode, for example, at the liquid Helium temperature of $T_c = 1\text{K}$ can be used for the cold bath T_r in Figure 49. For such a diode the nonlinearity factor is $\beta = 1.16 \times 10^4 \text{ e/C}$ where C is the capacitance of the diode ($C \sim 10^{-16}\text{F}$) and e is the charge on the electron. A Schottky diode is also known to be formed between a semiconductor and a metal, with nonlinear rectifying characteristics and fast switching speeds.²⁷⁴

Yater notes that "for the long range design goals, **sub-micron circuit sizes are required** if all the high power goals of megawatts per square meter are to be achieved...The results of an analysis of the independent particle model for both classical and quantum effect, show that the reversible thermoelectric converter with power conversion of energy fluctuations has the potential of achieving the maximum efficiency of the Carnot cycle. The potential applications of this device can be seen to be universal."²⁷⁵ His patent

#4,004,210 clarifies that the electric energy fluctuations are transmitted from the higher temperature diode to the lower temperature diode while the heat transfer is in reverse, which is unusual.

Upon reviewing the literature, Yater summarizes his findings: "The relation of the second law of thermodynamics to the power conversion of fluctuation energy has been of recurring interest and study. The results of these studies have ranged from the conclusion that conversion of fluctuation energy is prohibited by the second law to the conclusion that **the conversion of fluctuation energy is not limited by the second law of thermodynamics.**"²⁷⁶

Rectifying Thermal Noise with Ratchets

Particles that move aperiodically due to thermal or external noise, in the presence of asymmetric periodic potentials, have also been called "**stochastic ratchets.**" These systems have the intriguing ability to rectify symmetric correlated noise and thus have the ability to produce a net electrical current. As a consequence of the fluctuation-dissipation theorem, the ratchet does not drift (as in the Metropolis Monte Carlo simulation of Figure 48) if it is in interaction only with a thermal bath. An external forcing must be used to produce the drift, according to the researchers, **Ibarra-Bracamontes et al.**²⁷⁷

By describing the ratchet system in the Brownian particle regime with the Langevin equation (like Allahverdyan and Nieuwenhuizen), thermal noise is considered to have finite correlation times. This treatment yields a prediction of current production due to a time-dependent external force. In this case, the external force is either sinusoidal or stochastic. The generalized Langevin equation is an embellishment of Newton's equation, $F = ma$, describing a particle of mass m moving in an asymmetric periodic potential $V(x)$ that forms the ratchet,

$$m \, d^2x/dt^2 = - \int d(t') \, \Gamma(t - t') \, dx(t')/dt' - dV(x)/dx + f(t) + F_{\text{ext}}(t) \quad (46)$$

$\Gamma(t)$ is the dissipation kernel, which in this case has memory and correlated with friction. The term, $f(t)$, is the **stochastic fluctuating thermal force** exerted by the bath which has a usual stochastic property

of being Gaussian with zero mean. By a numerical solution, Equation (49) does not show a net current in the absence of external forces (if $F_{\text{ext}}(t) = 0$). However, adding a time-symmetric external force in general is a necessary and sufficient condition for the Langevin equation to yield a current flow in one direction.

Rather than argue in favor of nonequilibrium fluctuations being present with a symmetric correlated force, the emphasis is made in this case in favor of an external origin for the force. In

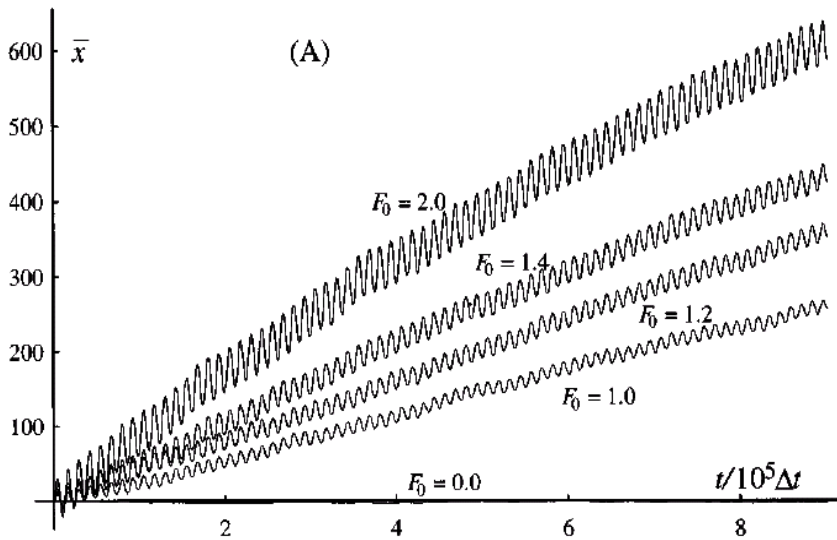


Figure 50 Net current as particle position x versus time t for five different ratcheting external force F_0 values - Ibarra-Bracamontes.

accordance with the second law of thermodynamics, the assertion is also made here that "one cannot extract a current from a thermal bath, whether white or colored."²⁷⁸ Colored noise is where some frequencies dominate the noise spectrum and is also referred to as "pink" noise. The average

position of the electron $\langle x \rangle$ is shown in Figure 50 for five different external force amplitudes versus time. The solution demonstrates the Metropolis Monte Carlo simulation, with a different ratchet design than Figure 48. However, it is not clear that Ibarra-Bracamontes et al. have succeeded in proving their controversial claim that “any external forcing may be used to produce the drift” but **the rectification of thermal noise due to an asymmetric external potential has been demonstrated.**

Ferrofluid Thermal Rectifier Torque Engine

An experimental demonstration of rectifying random thermal fluctuations involves **ferrofluids**, which are colloidal suspensions of nanoparticle ferromagnetic grains (~ 10 nm). In this case, the external potential is an **anharmonic oscillating magnetic field** $\{ f(t) = \cos(\omega t) + A \sin(2\omega t + \beta) \}$ created by Helmholtz coils H_y at a distance from the ferrofluid. It is regarded as a rotating magnetic field since there is a static magnetic field H_x at right angles to the oscillating field which sums to create rotation and angular momentum (Figure 51). The angular momentum of electromagnetic fields is a principle of classical physics. Without thermal fluctuations, relaxation dynamics tend to cause the particles to align with the field in the x-y plane and no average rotation nor torque is created. **In the presence of thermal fluctuations however, stochastic transitions occur due to the magnetic field asymmetry,** yielding slightly different probabilities for the magnetic orientational motion of the ferromagnetic grains, as discovered by Engel et al.²⁷⁹

As with the Photo-Carnot engine, the **Fokker-Planck equation is also used** in this case for a quantitative solution of the induced torque effect in the ferrofluid. Solving the equation by expansion in

spherical harmonics, the transitions between deterministic solutions become possible. “The spatial asymmetry and temporal anharmonicity of the potential results in slightly different rates for noise-induced increments and decrements of [phase] ϕ , respectively. As a result, a noise-driven rotation of the particles arises.”²⁸⁰ There is viscous coupling between the ferromagnetic grains and the carrier liquid so that the individual torques add to create a macroscopic torque per fluid volume, $N = \mu_0 M \times H$. However, Engel et al. admit that the time-averaged N_z is much smaller than the typical values of the time-independent N_z calculated from the Fokker-Planck equation by adopting the effective field method.²⁸¹

With an exploration of nonlinear perturbation techniques, **Engel et al.** admit that only a particularly chosen Langevin function yields the correct time-averaged z-component of the torque N_z , with static and dynamic

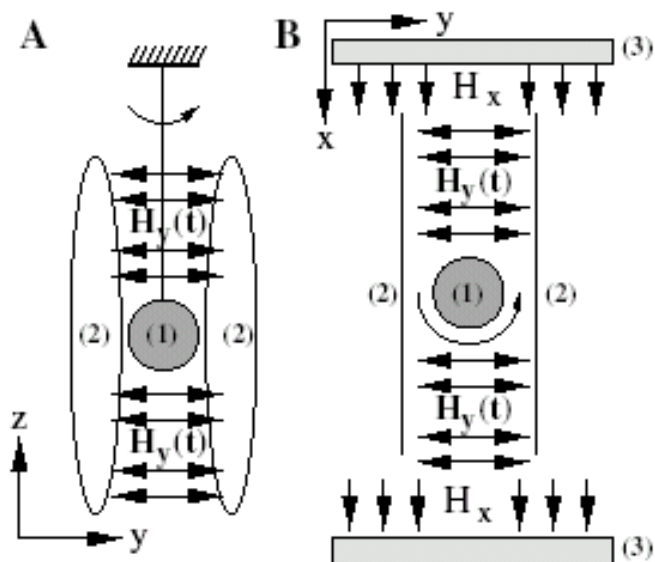


Figure 51 Ferrofluid rotation (A) induced at a distance from a static H_x field added to an oscillating H_y field (B)

magnetic field terms included. The expression for N_z shows that both the static magnetic field and the anharmonic part of the oscillatory component are essential for the directed rotation to occur.

Interestingly, the Brownian relaxation time is another parameter which had to be heuristically determined to achieve agreement between theory and experiment. It corresponded to a particle size of approximately 35 nm which is about three times the average particle size. Engel et al. conclude that the Brownian relaxation time must therefore correspond to the largest grains in the population rather than the average.

Engel et al. succeeded in rectifying rotational Brownian motion angular momentum. It is an experimental realization of “the combined action of many individual nanoscale ratchets to yield a macroscopic thermal noise transport effect.”²⁸²

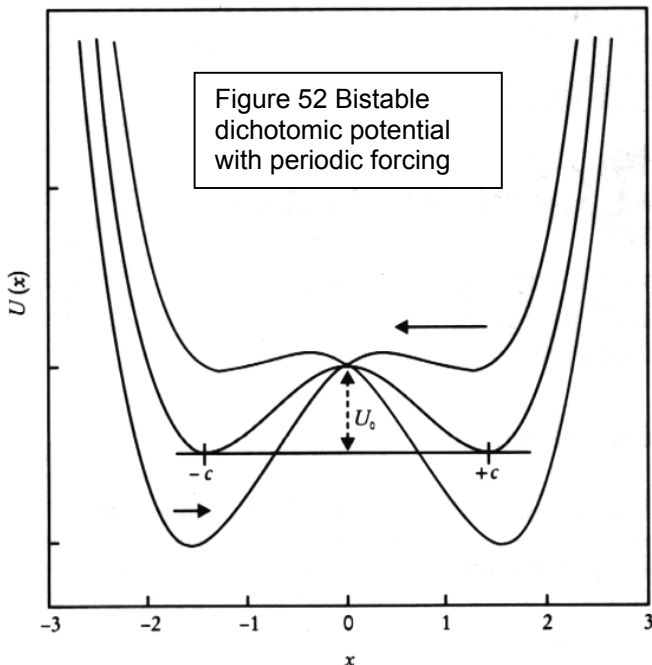
Rectifying Thermal Electric Noise

In regards to rectifying thermal electrical noise, it is worth mentioning the U.S. Patent #3,890,161 by Charles M. Brown that utilizes an array of nanometer-sized metal-metal diodes, capable of rectifying frequencies up to a terahertz (10^{12} Hz). Brown notes that thermal agitation electrical noise (Johnson noise) behaves like an external signal and can be sorted or preferentially conducted in one direction by a diode. The Johnson noise in the diode is also generated at the junction itself and therefore, requires no minimum signal to initiate the conduction in one direction. The thermal noise voltage is normally given by $V^2 = 4k_B TRB$ where R is the device resistance and B is the bandwidth in Hertz.²⁸³ Brown's diodes also require no external power to operate, in contrast to the Yater diode invention. Brown also indicates that heat is absorbed in the system, so that a cooling effect is noticed, because heat (thermal noise) energy energizes the carriers in the first place and some of it is converted into DC electricity. In contrast, the well-known Peltier effect is the closest electrothermal phenomenon similar to this but requires a significant current flow into a junction of dissimilar metals in order to create a cooling effect (or heating). Brown suggests that a million nickel-copper diodes formed in micropore membranes, with sufficient numbers in series and parallel, can generate 10 microwatts. The large scale yield is estimated to be several watts per square meter.

Quantum Brownian Nonthermal Recifiers without Ratchets

While many researchers believe that the asymmetrical ratchet of one form or another is essential in the conversion of stochastic fluctuations, there are others who also find that stochastic resonance (SR) in threshold systems is a sufficient substitute. "The 'cooperation' between the signal and noise introduces coherence into the system...This coherence is conveniently quantified as the power spectral density...of the system response...The earliest definition of SR was the maximum of the output signal strength as a function of noise..."²⁸⁴ An introduction to SR is shown in Figure 52 with a potential barrier U_0 separating two wells at $\pm c$. If the energy is subthreshold, the system will be monotonic but adding an amount of noise on the order of U_0 allows the dichotomic system to oscillate. With a supra-threshold periodic forcing, the two wells may have different net occupation levels (as arrows indicate), with the output signal-to-noise ratio (SNR) following the input SNR closely.

Anomalous transport properties, using SR, which do not exploit the ratchet mechanism have been investigated in **driven periodic tight-binding (TB) lattices near zero DC bias** with the combined



effects of DC and AC fields, or DC field and external noise. In particular, **Goychuk et al.** have found that periodic TB lattices can be **driven by unbiased nonthermal noise generated from the vacuum ZPF**, generating an electrical current as a result of a "ratchetlike mechanism," as long as there is quantum dissipation in the system.²⁸⁵

Theoretically introducing quantum dissipation with an ensemble multi-state model of harmonic oscillators coupled to the driven system, along with an unbiased, time-dependent random force (characterized by an external, time-dependent random electric field, $\eta(t) = e a E_\eta(t)/\hbar$), yields the noise-averaged stationary quantum DC electrical current $J_{st} = e(\lim_{t \rightarrow \infty} d\langle q(t) \rangle / dt)$ and quantum diffusion coefficient D . The nonthermal fluctuations are given discrete, quantum values with probabilities as QED dictates. It is assumed that neither the temperature nor the nonthermal

fluctuations can cause any essential occupation of higher energy levels for the dissipation model.

Goychuk et al. succeed in demonstrating that without dissipation, for any field, the stationary DC current is always zero. An initially localized particle, as in a crystal, does not produce a current in the absence of dissipation. However, considering the effect of adding unbiased fluctuations $\eta(t)$ on Bloch oscillations, Goychuk develops a master equation which includes a real-time quantum Monte Carlo calculation yielding a good approximation for a TB particle at environmental temperatures and/or strong

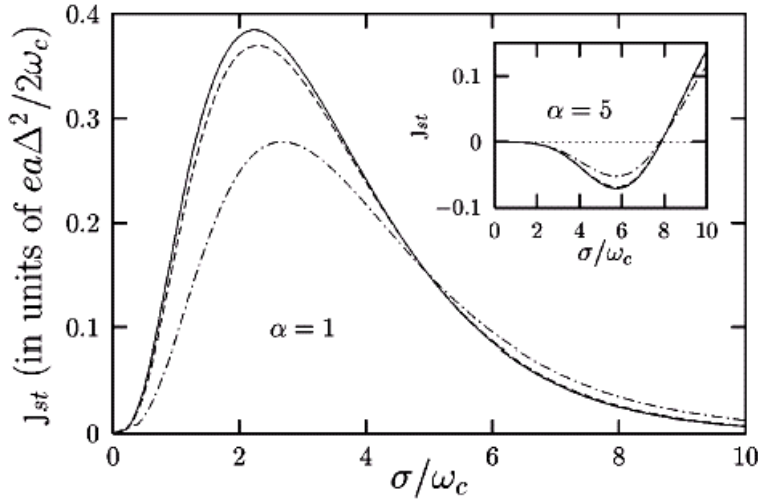


Figure 53 Stationary current versus noise strength for a random process. Solid line is adiabatic approximation. Inset is current reversal with friction.

dissipation when transport includes sequential tunneling. Bloch functions describe an electron in a periodic lattice with a sinusoidal wave function conditioned by a lattice periodicity function.²⁸⁶ Driven tunneling dynamics in Bloch oscillation system is the subject of another paper Goychuk has coauthored with efficient determination of the optimal control of quantum coherence.²⁸⁷

In Figure 53, the production of rectified electrical current J_{st} is shown with an ohmic friction factor $\alpha = 1$ graphed against changes in fluctuation noise strength σ for a dichotomic (two-choced) random process with zero mean and asymmetry parameter of $\xi = 1/2$. While the solid line is adiabatic, the dashed lines depict non-adiabatic autocorrelation times of $0.1\omega_c$ and ω_c respectively from top down, where ω_c is the cutoff frequency. The inset graph is an interesting current reversal that occurs under a case of strong friction $\alpha = 5$ which is related to SR. "Because the current appears as the nonlinear response to the aperiodic external signal, the existence of this maximum [in Figure 53] can be interpreted as a signature of aperiodic quantum stochastic resonance."²⁸⁸

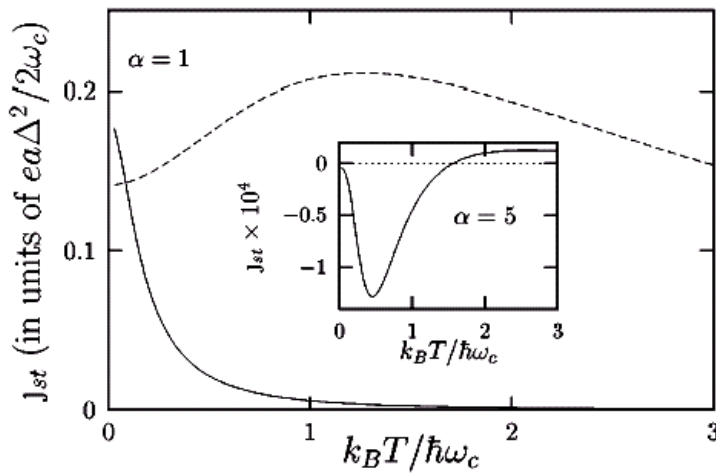


Figure 54 Aperiodic quantum stochastic resonance shown (dashed line with noise $\sigma = 7\omega_c$) with an insert of current reversal under strong friction.

fluctuations are effectively rectified, creating a measurable current. Goychuk believes that the effect should be already observable in superlattices and/or optical lattices.²⁸⁹

dissipation when transport includes sequential tunneling. Bloch functions describe an electron in a periodic lattice with a sinusoidal wave function conditioned by a lattice periodicity function.²⁸⁶ Driven tunneling dynamics in Bloch oscillation system is the subject of another paper Goychuk has coauthored with efficient determination of the optimal control of quantum coherence.²⁸⁷

In Figure 53, the production of rectified electrical current J_{st} is shown with an ohmic friction factor $\alpha = 1$ graphed against changes in fluctuation noise strength σ for a dichotomic (two-choced) random process with zero mean and asymmetry parameter of $\xi = 1/2$. While the solid line is adiabatic, the dashed lines depict non-adiabatic autocorrelation times of $0.1\omega_c$ and ω_c respectively from top down, where ω_c is the cutoff frequency. The inset graph is an interesting current reversal that occurs under a case of strong friction $\alpha = 5$ which is related to SR. "Because the current appears as the nonlinear response to the aperiodic external signal, the existence of this maximum [in Figure 53] can be interpreted as a signature of aperiodic quantum stochastic resonance."²⁸⁸

The stationary current is also found to depend on temperature, which is the **signature of aperiodic quantum stochastic resonance (AQSR)**. In Figure 54, the rectified current is shown versus temperature for a fluctuation noise strength $\sigma = 0.5\omega_c$ (solid line) and $\sigma = 7\omega_c$ (dashed line) while friction $\alpha = 1$ and asymmetry $\xi = 1$.

In the presence of unbiased, asymmetric forcing, a noise-directed current always occurs in a dissipative TB lattice, because of the ratchet-like effect of the asymmetric forcing, like the stochastic

ratchets that rectify thermal noise. **With stochastic resonance, nonthermal**

For reference, it is worth mentioning that with crystal lattices, thermal fluctuations appear at environmental temperatures, with $\frac{1}{2} m \omega_o^2 \langle u^2 \rangle = 3(\frac{1}{2} k_B T)$ energy level where m and ω_o are the mass and frequency of the harmonic oscillations and u is the displacement from a fixed lattice site. The nonthermal oscillations associated with ZPE are $m \omega_o^2 \langle u^2 \rangle = 3(\frac{1}{2} \hbar \omega_o)$ in terms of energy, adding to the lattice thermal fluctuations.²⁹⁰

Zero Point Energy Corresponds to Dark Energy

While some may still question the availability of nonthermal fluctuations from the ZPF in a solid state device, Beck and Mackey experimentally measured the spectral density of current noise in Josephson junctions in 2004. They assert that it provides direct evidence for the existence of zero-point fluctuations. *Assuming that the total vacuum energy associated with these fluctuations cannot exceed the presently measured dark energy of the universe*, they predict an upper cutoff frequency of $\eta_c = (1.69 \pm 0.05) \times 10^{12}$ Hz for the measured frequency spectrum of zero-point fluctuations in the Josephson junction. This provides a reasonable resolution to one of the most hotly contested issues of ZPE: its cutoff frequency. Note that it is significantly less than the Planck cutoff frequency of $\omega_c \approx 10^{43}$ Hz based on the Planck length discussed in Chapter 1. Furthermore, Beck and Mackey help explain astronomy's self-created dilemma of dark energy which has remained unresolved because of misunderstandings of the properties of ZPE.²⁹¹ The largest frequencies that have been reached in the experiments are of the same order of magnitude as η_c and provide a lower bound on the dark energy density of the universe. They show that suppressed zero-point fluctuations above a given cutoff frequency can lead to $1/f$ noise. Therefore, it is quite conceivable that their experiment can measure some of the properties of dark energy in the lab.²⁹²

Vacuum Field Amplification

With the introduction to AQSR along with the rectification of nonthermal noise, it makes sense to investigate the amplification of quantum noise. Milonni points out that "the vacuum field may be amplified...if the spontaneously emitted radiation inside the cavity is amplified by the gain medium, then so to must the vacuum field entering the cavity. Another way to say this is that 'quantum noise' may be amplified."²⁹³ Since the SR TB lattice current output depends on the noise level, as in the Goychuk simulation, the optimum level of energy extraction depends on parameter control, as in quantum optics, which utilizes quantum noise amplification. This is similar to ASE which also uses a gain medium.

The actual content of quantum noise and vacuum polarization may still remain a mystery after all of the Chapter 4 analysis. Milonni notes that even though heavier virtual particle pairs like muons, pions, etc. may take part in virtual polarization, **the majority of the manifested particles will always be electron-positron pairs** because of the $1/m^2$ mass dependence of the nonexchange term between the two current densities for the electron and the negative-energy states of the ZPF.²⁹⁴ Jackson notes that the **Weissaker-Williams "method of virtual quanta"** treats every scattering impact or close encounter between charged particles as a Fourier collection of virtual particles which are equal to the electric field pulse radiated to the target. This method, in consonance with QED, gives the frequency spectrum, cutoff, and number of virtual particles per unit energy interval.²⁹⁵

CHAPTER 5 - Summary, Conclusions and Recommendations

Summary

This study was predicated on the existing volume of data already in the scientific literature regarding the nonthermal vacuum fluctuations that comprise ZPE. The assessment of the feasibility of zero-point energy extraction by humans from the quantum vacuum for the performance of useful work in the electrical, fluidic, thermodynamic, and mechanical conversion modalities is determined in this chapter.

Analyzing the specific experiments, theories, simulations, measurements and predictions in this study offers a wealth of details concerning the energetic operation of ZPE throughout the universe. As a result, it can possibly be argued from an historical perspective that, because nature already extracts ZPE for the performance of useful work, humans eventually will be able to do so as well. Acknowledging the need for robust, concentrated energy sources in the world, any study of the concept of energy extraction and production should address the corresponding utility and energy quality. Therefore, this summary addresses the electrical power output and the practicality of the conversion mode and method.

This study finds that at the present time, the categories of the present major inventive ZPE conversion modes includes 1) electromagnetic conversion, 2) Casimir cavity mechanical engine, 3) fluid dynamics techniques, and 4) quantum thermodynamic rectifiers. Under these major headings are individual methods such as 1a) focusing vacuum fluctuations, 2a) cavity QED, 2b) spatial squeezing, 2c) Casimir cavity geometry design, 2d) Casimir stress enhancement, and 2e) vibrating cavity photon emission, 3a) inertial effects, 3b) hydrodynamic model, 3c) Casimir cavity, 4a) quantum coherence, 4b) Brownian motors, 4c) transient fluctuations, 4d) thermal fluctuation rectifiers, and 4e) nonthermal Brownian rectifiers, as shown in Table 1 with relevant author names.

Table 1 - ZPE Conversion Modes & Methods

Electromagnetic	Mechanical	Fluid Dynamic	Thermodynamic
Dual sphere - Mead	Casimir engine - Pinto	Inertia Effects - Froning	Quantum coherence - Allahverdyan, Scully
Focusing ZPE - Ford	Cavity QED - Haroche	Hydrodynamic model – Bohm	Brownian motors - Astumian
	Spatial squeezing- Hu	Casimir cavity - Maclay	Transient fluctuation theorem - Crooks
	Casimir cavity optimized design - Maclay		Thermal fluctuation rectifiers – Brown, Ibarra-Bracamontes, Engel
	Vibrating cavity photon emission - Hizhnyakov		Quantum Brownian nonthermal rectifiers - Goychuk

Electromagnetic Conversion

In the electromagnetic energy conversion process, the proposed Mead configuration of two spheres in close proximity was analyzed for four different size categories, each of which are a thousand times smaller than the previous one. The microsphere category seemed to match the Mead design closely but was found to be lacking in sufficient scattering intensity, even when substituting conducting

spheres which have the highest scattering cross section. The decrease of dielectric constant with frequency also was a problem for most materials. The ZPF energy density and resonant photon energy for the microsphere were only moderate and are summarized in Table 2, along with the other three spheres.

The nanosphere, as shown in Figures 16 and 17, demonstrates the present state of the art in nanotechnology assembly. The spectral energy density of Equation (16) for the nanosphere increases by a billion times over the microsphere even though the sphere size is reduced by a billion times. Upon integrating over a decade of frequencies with Equation (21) (see Table 2), a thousand times *increase in ZPE density is calculated with each successively smaller sphere*. However, no significant vacuum polarization is available for nano-sized particles, which is an energetic, physical manifestation of ZPE.

The picosphere is interesting in that Mead's beat frequency concept can theoretically be realized with pairs of atoms very close in atomic weight such as platinum and gold or hydrogen and deuterium. However, the engineering challenges of such an assembly would be prohibitive, even if one could foresee a significant overunity energy production per pair. Furthermore, even with the advanced techniques such as Ford's focusing of vacuum fluctuations, textbook upscattering or resonant fluorescence, etc., paired atoms of choice still have a technological barrier, lacking compatibility with any existing amplification or conversion transducer, such as those seen in Figure 21.

With the femtosphere, QED principles inherent to ZPE, start to emerge. In one sense, the femtosphere has become almost too small to manage individual particles, if they are in contact. In another sense, the size presents other opportunities such as with the ion trap, where electron femtospheres can be collected, for example. However, even as the advantage of working with electrons as ZPE receivers becomes more apparent, it is obvious much more research is needed.

Overall, the Mead patented method for utilizing ZPE collectors and resonators certainly presents a design or a collector that amplifies scattering, though Mead only analyzes a single sphere. The ZPF energy density of Equation (21) is the most relevant, showing the quartic increase of energy with frequency even though there is a cubic decrease of volume with each successive sphere. In the final assessment, given the extent of the experimentation that is required for success with this concept for extraction of useful energy, all four spheres of interest still do not receive a feasibility rating of overall confidence that would qualify it for endorsement from scientists, engineers, or investors. Using the realistic power production level or anticipated work output as a measure of energy quality, this invention receives a poor energy quality rating.

Table 2 – Energy and Cross Section of the Spheres

	Microsphere	Nanosphere	Picosphere	Femtosphere
Photon energy & frequency	1 eV 10^{14} Hz	1keV 10^{17} Hz	1 MeV 10^{17} Hz	1 GeV 10^{20} Hz
E = mc² comparison	Si: 10^{44} eV	Ag: 10^{17} eV	Pt: 10^{11} eV	p: 940 MeV
ZPE energy density	390 meV/ μm^3	390 eV/nm ³	390 keV/pm ³	390 MeV/fm ³
Physical cross section area	3×10^{-12} m ²	3×10^{-18} m ²	3×10^{-24} m ²	3×10^{-30} m ²
Scattering cross section	10^{-8} m ²	10^{-15} m ²	10^{-21} m ²	10^{-30} m ²

Table 2 presents more energy data for each sphere, with photon energy for the corresponding wavelength and the Einstein energy content added for comparison. The main observation with this tabular summary is that the ZPE energy for a given spherical volume finally equals (same order of magnitude) the Einstein energy content of matter as well as the photon energy of the corresponding wavelength. While the scattering cross section may seem to offer some advantages at larger sphere

diameters, the equal weighting of light, matter, and vacuum for a femtosphere has to be extraordinarily inviting for the vacuum engineer and an area worthy of further research.

Mechanical Casimir Force Conversion

The Casimir force presents a fascinating exhibition of the power of the ZPF offering about one atmosphere of pressure when plates are less than one micron apart. As is the case with magnetism today, it has not been immediately obvious, until recently, how a directed Casimir force might be cyclically controlled to do work. The optically-controlled vacuum energy transducer however, proposed by Pinto, presents a powerful theoretical case for rapidly changing the Casimir force by a quantum surface effect, excited by photons, to complete an engine cycle and transfer a few electrons. The exciting part of Pinto's invention is the QED rigor that he brings to the analysis, offering a convincing argument for free energy production. The nano-fabrication task that is presented, however, is overwhelming. Besides mounting nanolasers inside the Casimir cavity, the process suggests that a 10 Khz repetition rate is possible with a moving cantilever, without addressing the expected lifespan. The energy production rate is predicted to be robust (0.5 nW per cell or 1 kW/m^2), which could motivate a dedicated research and development project in the future. However, the Casimir engine project of Pinto's appears to be a long-term, multi-million dollar investment at best.

Utilizing some of the latest cavity QED techniques, such as mirrors, resonant frequencies of the cavity vs. the gas molecules, quantum coherence, vibrating cavity photon emission, rapid change of refractive index, spatial squeezing, cantilever deflection enhancement by stress, and optimized Casimir cavity geometry design, the Pinto invention may be improved substantially. The process of laser irradiation of the cavity for example, needs to be replaced with one of the above-mentioned quantum techniques for achieving the same variable Casimir force effect, with less hardware involved. At the present stage of theoretical development, the Pinto device receives only a moderate rating of feasibility. Its energy quality rating, however, is very high.

Fluid Dynamics

In the fluid dynamics analysis of the vacuum presented by Froning, it was convincingly argued that the permittivity and permeability of the vacuum can be reduced effectively by nonabelian electromagnetic fields, specifically by utilizing alternating current toroids at resonant frequencies.

While this research does not directly produce electricity, the energy extraction indirectly achieved by the use of the Froning prototype is in the form of energy conservation. By reducing the drag and inertia normally experienced by a spaceship in space, it will save a significant amount of energy, which is equivalent to generating it. The referenced information from Rueda and Haisch as well as from Maclay supports the validity of Froning's fluid dynamic approach. At its present stage of development, the feasibility rating is low, with an energy quality rating of high.

Thermodynamic Conversion

The Photo-Carnot engine is an interesting theoretical device that relies upon quantum coherence to yield a cyclical radiation pressure for the piston-driven engine. The phase induced with the quantum coherence, provides a new control parameter that can be varied to increase the temperature of the radiation field and to extract work from a single heat bath. The claim is made that the second law of thermodynamics is not violated, according to Scully et al., because the quantum Carnot engine takes more energy, with microwave input, to create the quantum coherence than is generated. However, it is possible that as efficiency improvements are made, the output will exceed the input as is the trend with the other thermodynamic engines analyzed in this study. After all, depending on the value of the phase Φ , the efficiency of the quantum Carnot engine can already exceed that of the classical engine – even when $T_c = T_h$. The capability of extracting heat from a single reservoir should be regarded as a requirement for a ZPE thermodynamic transducer. With the added endorsement of Allahverdyan and Nieuwenhuizen, the Photo-Carnot engine is raised to a 'perpetuum mobile of the second kind.' The number of cycles cannot be arbitrarily large apparently, and the total amount of extractable work is modest. However, the standard requirements for a thermal bath are not

fulfilled, according to Allahverdyan and Nieuwenhuizen, so thermodynamics just does not apply. For these reasons, the Photo-Carnot invention has great potential for becoming a ZPE energy producer and receives a high feasibility rating, with moderate energy quality rating.

The Brownian motors proposed by Astumian (Figures 44) utilize Langevin's equation, also mentioned in connection with the quantum coherence of Scully et al. Astumian emphasizes the fluctuating energy source (thermal noise) and the dissipation (viscous drag) that is essential to the fluctuation-dissipation theorem, fundamentally important to the ZPF. With Astumian's Brownian motors, the oscillating potential also needs an asymmetrical ratchet to ensure one-way transport. The ratchet concept, while very feasible and proven by two experiments, offers only a limited production of current with underunity efficiency. Astumian notes that with the viscous drag of the solvent, all of the energy gained by the ratchet steps is dissipated with an overall thermodynamic efficiency of less than 5%.²⁹⁶

The tunneling electron ratchet experiment performed by Linke et al., seen in Figures 45-46, is an encouraging demonstration of the Brownian motor. Linke generates a maximum of 0.2 nA with about a millivolt of source-drain rocking voltage, at the picowatt or picojoule level, which is encouraging. However, with only between 1% and 5% rectification of the total current, the efficiency is also quite as low as Astumian.

With the analysis of the transient fluctuation theorem, it becomes apparent that with microscopic systems, the performance of negative work has a high probability, apparently violating the law of entropy. The Metropolis Monte Carlo simulation of Crooks in Figure 48 is similar to the quantum ratchet concept however, and doesn't offer an advantage over the other techniques.

The Yater method for power conversion of energy fluctuations is in the same category as rectifying thermal noise. While the Yater invention has an impressive assembly of patents and journal articles, the process requires two heat sources separated by a large spread in temperature. This makes the overall analysis of the device difficult to analyze except by conventional means with underunity energy output projections. His claims for a 10 times improvement over heat pumps is intriguing and the detailed plans in his patent encourage further research, with a reasonable feasibility projected and high energy quality.

The work by Ibarra-Bracamontes et al. is another confirmation of rectifying thermal fluctuation noise. It is interesting for theoretical analysis but the type of signals that are possible for external forcing is not made clear. Rectifying random thermal fluctuations with ferrofluids adds a new twist that is unique, especially when rotational energy is not available directly from the ZPF. Engel et al. offer a fascinating experiment for consideration, consistent with the rectification of thermal fluctuations for linear motion. However, the driving potential is a complex oscillating magnetic field with a field intensity as high as the static field which is also required (several kA/m). Both are generated by a commercial electromagnet. The work output that should be calculated in time-averaged torque multiplied by rotational distance will predictably be only a few percent of the input, at best. It is a good demonstration but does not seem to represent a practical concept for motoring or rotational work. Therefore, it receives a high feasibility rating but low energy quality.

The Brown patent rectifying thermal electrical noise with nano-sized metal-metal diodes is probably the most exciting invention analyzed in Chapter 4. Though the inventor does not acknowledge a ZPE contribution to Johnson noise, it is reasonable to project that the Brown diode arrays will rectify nonthermal fluctuations as well as thermal noise. With *no external input needed* for conduction, nor a minimum voltage to overcome the usual diode barrier, the potential for free energy production seems quite high. The attractiveness and projected consumer interest for such a solid state, zero-maintenance device is also very high. Not only is the fabrication understandable and straightforward but the description of a cooling effect (negative kinetic energy) from the conversion of thermal noise (positive kinetic energy) is also scientifically and thermodynamically acceptable. The energy density of several watts per square meter is reasonable and robust. However, this quantity should be calculated in watts per cubic meter, since the filled Millipore sheets can easily be stacked vertically as well. Another important calculated parameter for space power is the amount of *watts per kilogram*, which is probably

moderate to high in this case. It is possible with modern nanotechnology that this invention could compete with the battery market. Not only is the feasibility given the highest rating for this invention, but the energy quality rating is also given the highest rating as well.

Stochastic resonance is an emerging energy field that now is being used to substitute for ratcheting in the Brownian rectifiers. The work by Goychuk demonstrates the aperiodic quantum stochastic resonance (AQSR) that is essential for these rectifiers to work in a solid state environment of a tight-binding crystal lattice. With near zero DC bias, the invention is very attractive for many reasons. The “ratchetlike mechanism” of Goychuk is a valuable substitute for the Astumian style of Brownian motor requiring physically fabricated ratchets. It does not require a static bias, which is a distinct improvement over previously analyzed Brownian motor requirements. The stationary current is also found to be nonzero for unbiased noise, *demonstrating a DC rectification*, as long as there is some degree of asymmetry in the noise. As a result, the invention combines the noise and the asymmetric driving force into one signal, which is also an advantage over lesser ZPE models. The AQSR design has the ability to rectify asymmetric, unbiased, nonthermal noise, including quantum fluctuations as well, producing a measurable electrical current in a solid state crystal lattice. The only remaining variables are the amount of quantum dissipation required for the effect, the optimum operating temperature, the anticipated energy efficiency and the projected difficulty inherent in creating asymmetry with nonthermal noise that naturally tends to be symmetric in time and space. These variables may be of a sufficiently minor concern for the Goychuk invention to actually offer a gateway to the future of ZPE electricity generation. Many parts of the invention fit the ideal “impedance” matching of energy source behavior with energy transducer behavior. For example, quantum fluctuations are shown by Goychuk to simply require quantum dissipation and a slight asymmetry, which is less energy intensive overall than creating a quantum coherence. This invention is given the highest rating for feasibility and the highest rating for energy quality.

Conclusions

The risk analysis that is often integrated into a feasibility study that is dedicated to a single development plan is really a process to assign a degree of likelihood to stages of a project.²⁹⁷ The feasibility rating standard adopted in Chapter 5 is equivalent to such an analysis.

The results of this study finds varying feasibility ratings and energy quality ratings for the four modes of energy conversion from the ZPF. For the Electromagnetic modality, in the present stage of development, the overall method is rated unfeasible with poor energy quality, given the limitations of today’s technology capabilities. The Mechanical modality fares better with a moderate feasibility rating, at the overall present stage of development, with a very high energy quality rating. The Fluid Dynamic modality drops back with a low feasibility rating but high energy quality rating. **The Thermodynamic modality shines with the highest feasibility rating and the highest energy quality rating.**

The overall conclusions drawn from this study support the introductory physical description of the quantum vacuum. Furthermore, the hypothesis of a ZPF vibrating with measurable mechanical pressure, electromagnetic activity, and nonthermal energy is also supported by the scientific evidence uncovered by this study. The fluid dynamics information about ZPE was a reassuring fulfillment of the fourfold modality expectation. There is also a consistency with previous research going back to the early days of QED, which adds a reliability and confidence level to the normally unsettling nature of ZPE. Further research is needed however, as outlined briefly in the next section, to fully exploit the discoveries of energy extraction from the quantum vacuum.

The implications of this study to the emerging field of discipline called vacuum engineering are enormous and far-reaching: An up-to-date assessment of the state of the art has been accomplished by this comprehensive study. **Based on this engineering physics achievement, with the feasibility and energy quality ratings therein, it can be reasonably expected that at least one business plan will be generated for a ZPE invention, perhaps for the first time in history.** Such a development offers the business world an opportunity to benefit from the most plentiful energy source that also now has been found to have a certain level of practicality and moderate risk assessment, compatible with

competing enterprises. As a result of this study, an opportunity has emerged for the public to benefit from some of the ZPE unusual ubiquitous qualities, such as making many completed ZPE transducers completely portable and possibly installing lifetime ZPE transducers in every appliance. **The implications of this study are that future generations may finally relinquish fossil fuels in favor of ZPE.**

Recommendations

Based on the quality of research uncovered and the level of agreement between theory and experiment demonstrated, specifically by the thermodynamic mode of ZPE conversion, it is recommended that further attention and funding be primarily dedicated to the exploitation of zero-point energy extraction, beginning with the microscopic realm. While the other three modalities offer interesting and promising developments, the feasibility rating and energy quality rating is the highest with the thermodynamic mode. In particular, it is recommended that **1) metal-metal nanodiodes** should be researched, with attention to the Johnson noise voltage and purported lack of diode barrier, along with the possible mass production of high density substrates; **2) more ratchet and ratchetlike asymmetries** should be researched, by government, industry and academia, so that a TB lattice or diode assembly may one day offer a truly solid state transducer for ZPE; **3) research should continue into quantum coherence, refractive index change, and stochastic resonance** with a goal of reducing the present relatively large energy investment, so that more robust avenues of product development in ZPE thermodynamics may be achieved. Brownian motors, thermal fluctuation rectifiers, and quantum Brownian nonthermal rectifiers utilizing AQSR have already achieved a level of theoretical and experimental confidence where further physics research and engineering studies can offer fruitful rewards in the production of rectified DC electricity. This mode of ZPE conversion research and development needs to be continued with earnest in order to expand mankind's woefully limited portfolio of energy choices.

A broad outline of how to undertake the recommended development work would include specific tasks and milestones associated with a) the confirmation of ZPE quantum effects described in this study on a larger scale; b) replication of results but also optimization of results; and c) engineering tasks of conductor and semiconductor design, nanowires and ohmic contacts. All of these, along with other tasks not mentioned, need to be included. The project would also include estimates of output current and energy production with any given geometry. Parallel development paths in research and development will always accelerate the completion of the optimum design. A market study should also accompany the work, so a clear focus on the existing niche to be filled is maintained. A national or international project proposal that estimates the required *project scope, resources, break-even point and identifies major milestones*, has to be formulated, if major progress in ZPE usage is to be achieved. Simply commissioning another study to follow up this study will lead only to institutionalizing the effort without accomplishment of set goals.

This feasibility study of ZPE extraction for useful work has presented a balanced and detailed assessment with scientific integrity, engineering utility and the likelihood of success for further development. **It can be concluded that zero-point energy is deserving of more attention by engineers and entrepreneurs as a serious and practical energy source for the near future.** The proposed project plan for ZPE development, yet to be written, has been reduced to a business endeavor and an exercise in return on investment.

Table 3 - Vacuum Engineer's Toolkit

Tool	Effect	Page
Aperiodic quantum stochastic resonance (AQSR)	Generates electrical current from nonthermal and thermal fluctuations	65-67
Brownian motors	Biases Brownian motion of particles, often in an anisotropic medium	58
Casimir engine	Electrical current generator designed by Pinto using a microcantilever, microlaser and Casimir force	44-47
Casimir force	Attractive (or repulsive) force from two parallel plates about 1 micron apart	6, 18, 50
Cavity QED	Alters atomic transition probability in small cavities	20
Dark energy	ZPE that powers galactic acceleration, also measured in the lab	67
Dielectric constant of surface	Affects Casimir force when illuminated by light	45, 52, 53
Einstein-Hopf drag	Retarding force from vacuum due to motion $F = -Rv$	55
Electromagnetic ZPE Converter	Dual sphere device using beat frequencies to downshift ZPE	27-44
Femtosphere	Particle size where QM and Rutherford scattering applies	40-44
Fluctuation-Dissipation theorem	Source+dissipation=fluctuation; Predicts and explains fundamental nature of ZPF	11, 57
Fluctuation-driven transport	mechanism that can convert chemical energy into motion of particles and macromolecules	58
Focusing vacuum fluctuations	Increases energy density of ZPE and attractive Casimir force	48-49
Fokker-Planck equation	Can apply to ferrofluid system to predict noise-driven motion of particles	64
Langevin's equation	Like F-D theorem, helps design Brownian motors	58, 63
Lasing without inversion (LWI)	Sustained laser output from microlasers which have long radiation cavity lifetime	56
Magnetic field	Inhibits Casimir force	20
Microbox geometry	Varies Casimir force from + attractive to - repulsive	50-51
Microcantilever	Flexible membrane that displays Casimir deflection	44, 49
Microlaser	Solid state laser 2 microns across	46
Nonresonant ion trap	Electrified cavity that concentrates charged particles	44
Photo-Carnot engine	Allows extraction of work from a single thermal reservoir where radiation is the working fluid	56
Quantum coherence	Changes relative strengths of emission and absorption in a cavity	57
Quantum ratchet	Repeating cells that move particles with fluctuation-driven transport	59-60
Recoil	Increases the energy of a dipole, associated with photon absorption and emission, both of which are in the same direction	55
Rectifying thermal noise	Generates electrical current with asymmetric external potential	64
Resonance	Can trap scattering particles into bound state	42
Resonant fluorescence	Dramatically increases absorption when incident energy equals binding energy of target	41
Sonoluminescence	ZPE caused light emission due to extreme temperature and pressure	21
Spatial squeezing of vacuum	Can double photon emission from cavity by changing dimensions abruptly	48
Temperature	Increase will broaden resonance peak	39
Thermal fluctuations/noise	temperature-caused stochastic oscillations and vibrations	62-63
Time-dependent refractive index	Causes part of ZPE to convert to real photons	53
Transient fluctuation theorem	Nonzero probability for negative work for short periods of time	61
Unruh-Davies Effect	Acceleration causes ZPE to create thermal fluctuations	53
Upscattering	Gain of energy to incident particle up to 10 kT energy	39
Vacuum field amplification	Increases quantum nonthermal noise with a gain medium	67
Vacuum field perturbations	Nonabelian EM field may alter speed of light/object	55
Vacuum polarization	Increase in local activity in the quantum vacuum near the edge of a physical charged particle	10

* This page may be freely copied and distributed with acknowledgment of source *
 Practical Conversion of Zero-Point Energy: Feasibility Study, Revised Edition 2005 by
 Thomas Valone PhD, PE

FIGURE CREDITS

1. NASA website: www.grc.nasa.gov
2. Zinkernagel, Henrik. "High Energy Particles and Reality." Ph.D. Thesis, University of Copenhagen, 1999, p. 25
3. Petersen, I. "Peeking inside an electron's screen." Science News. Vol. 151, Feb. 8, 1997, p. 89
4. Deffeyes, Kenneth. Hubbert's Peak: The Impending World Oil Shortage. Princeton University Press, Princeton, 2001, p. 5
5. Isaev, P. S. Quantum Electrodynamics at High Energies. American Institute of Physics, NY, 1989, p.33
6. Yam, Philip. "Exploiting Zero-Point Energy." Scientific American. December, 1997, p. 84
7. Browne, Malcolm. "Physicists confirm power of nothing, measuring force of quantum 'foam.'" The New York Times. January 21, 1997, p. C2
8. Forward, Robert. "Extracting electrical energy from the vacuum by cohesion of charged foliated conductors." Phys. Rev. B. 30, 4, 1984, p.1700
9. Mead, Frank. "System for Converting Electromagnetic Radiation Energy to Electrical Energy" U.S. Patent #5,590,031, Dec. 31, 1996, Figure 1
10. Fink, Donald. Electrical Engineers' Handbook, McGraw-Hill, New York, 1975, p.10-39
11. Mead, Frank., Figure 5
12. Cox, Larry T. "Calculation of Resonant Values of Electromagnetic Energy Incident Upon Dielectric Spheres" Phillips Laboratory, Air Force Material Command, PL-TR-93-3002, February, 1994, p. 17
13. Seto, William W. Schaum's Outline Series: Theory and Problems of Mechanical Vibrations. Schaum Pub. Co., New York, 1964, p.22
14. Mead, Frank., Figure 6
15. Fink, Donald., p. 6-36
16. Morse, Philip M. and Herman Feshbach. Methods of Theoretical Physics, Part II, McGraw-Hill, New York, 1953, p.1485
17. Ibid., p. 1485
18. Jackson, J.D. Classical Electrodynamics. J. Wiley, New York, Second Edition, 1975, p. 452
19. Sun, Yugang, et al. "Shape-Controlled Synthesis of Gold and Silver Nanoparticles" Science, Vol. 298, No. 5601, p. 2176
20. Snow, T. P. and J. M. Shull. Physics, West Pub. Co., St. Paul, 1986, p. 744
21. Fink, p. 10-42
22. "Electromagnetic Spectrum" TRW, Inc., Electronics Systems Group, Redondo Beach, CA, October, 1986
23. Tipler, Paul A. Foundations of Modern Physics. Worth Publishers, NY, 1969, p. 195
24. Duderstadt, James and L.. Hamilton, Nuclear Reactor Analysis, J. Wiley & Sons, New York, 1976, p. 54
25. Ibid., p. 49
26. Jackson, p. 803
27. Baym, Gordon. Lectures on Quantum Mechanics. Benjamin/Cummings, Reading, 1978, p. 211

28. Brink, G. O., "Nonresonant Ion Trap" Review of Scientific Instruments, Vol. 46, No. 6, June, 1975, p. 739
29. Ibid., p. 740
30. Pinto, F. "Engine cycle of an optically controlled vacuum energy transducer" Phys. Rev. B, Vol. 60, No. 21, 1999, p. 14745
31. Ibid., p. 14746
32. Gourley, P. "Nanolasers" Scientific American, March, 1998, p. 57
33. Dodonov, V.V. "Squeezing and photon distribution in a vibrating cavity" " J. Phys. A: Math Gen. V. 32, 1999, p. 6720
34. Ford, L.H. et al. "Focusing Vacuum Fluctuations" Casimir Forces Workshop: Recent Developments in Experiment and Theory, Harvard University, November 14-16, 2002, p. 19
35. Zheng, M-S., et al. "Influence of combination of Casimir force and residual stress on the behaviour of micro- and nano-electromechanical systems" Chinese Physics Letters, V. 19, No. 6, 2002, p. 832
36. Maclay, J. "Unusual properties of conductive rectangular cavities in the zero point electromagnetic field: resolving Forward's Casimir energy extraction cycle paradox" Proceedings of Space Technology and Applications International Forum (STAIF), Albuquerque, NM, January, 1999, Figure 1, p. 3
37. Ibid., Figure 2, p. 4
38. Sagan, Carl. Cosmos, Random House, New York, 1980, p. 37
39. Froning, H.D. and R.L. Roach "Preliminary simulations of vehicle interactions with the quantum vacuum by fluid dynamic approximations" Proceedings of 38th AIAA/ASME/SAE/ASEE Joint Propulsion Conference, July, 2002, AIAA-2002-3925, p. 52236
40. Ibid., p. 52237
41. Ibid., p. 52239
42. Scully, M.O. et al. "Extracting work from a single heat bath via vanishing quantum coherence" Science, Vol. 299, Issue 5608, 2003, Figure 1, p. 862
43. Ibid., Figure 2, p. 865
44. Astumian, R. D. "Thermodynamics and Kinetics of a Brownian Motor" Science, Vol. 276, Issue 5314, Figure 3, p. 919
45. Linke, H. et al. "Experimental Tunneling Ratchets" Science, Vol. 286, Issue 5448, 1999, Figure 1, p. 2314
46. Ibid., Figure 3, p. 2317
47. Blau, S. "The Unusual Thermodynamics of Microscopic Systems" Physics Today, September, 2002, Figure 1, p. 19
48. Crooks, G.E. "Entropy production fluctuation theorem and the nonequilibrium work relation for free energy differences" Physical Review E, Vol. 60, No. 3, September, 1999, p. 2724
49. Yater, J.C. "Relation of the second law of thermodynamics to the power conversion of energy fluctuations" Physical Review A, Vol. 20, No. 4, October, 1979, Figure 1, p. 1614
50. Ibarra-Bracamontes, et al. "Stochastic ratchets with colored thermal noise" Physical Review E, Vol. 56, No. 4, October, 1997, Figure 2A, p. 4050

51. Engel, A., et al. "Ferrofluids as Thermal Ratchets" Physical Review Letters, Vol. 91, No. 6, 2003, Figure 2, p. 060602-3
52. Bulsara, A.R. et al. "Tuning in to Noise" Physics Today, March, 1996, p. 39
53. Goychuk, I. et al. "Nonadiabatic quantum Brownian rectifiers" Physical Review Letters, Vol. 81, No. 3, 1998, Figure 1, p. 651
54. Ibid., Figure 2, p. 651

REFERENCES

- ¹ Barlett, D. and James Steele. "Special Report: The New Energy Crisis." Time, July 21, 2003, p.36
- ² Boyer, Timothy. "The Classical Vacuum." Scientific American, August, 1985, p. 70
- ³ Valone, Thomas. Harnessing the Wheelwork of Nature: Tesla's Science of Energy. Adventures Unlimited Press, Kempton, 2002, p. 9
- ⁴ Obousy, Richard K. "Concepts in Advanced Field Propulsion." University of Leicester, Birmingham, Department of Physics, Lecture 5, Sec. 5.8, 1999, p.14
- ⁵ Baym, Gordon. Lectures on Quantum Mechanics. Benjamin/Cummings, Reading, 1978, p.99
- ⁶ Ibid., p. 126
- ⁷ Boyer, 1985, p. 77
- ⁸ Isaev, P. S. Quantum Electrodynamics at High Energies. American Institute of Physics, NY, 1989, p.86
- ⁹ Milonni, Peter. The Quantum Vacuum. Academic Press, San Diego, 1994, p. 156
- ¹⁰ Rueda, A. and Bernard Haisch. "Electromagnetic Zero Point Field as Active Energy Source in the Intergalactic Medium." 35th AIAA/ASME/SAE/ASEE Joint Propulsion Conference. June 20, 1999, AIAA paper #99-2145, p. 4
- ¹¹ Puthoff, Harold. "Gravity as a zero-point-fluctuation force." Physical Review A. Vol. 39, No. 5, March 1989, p. 2336
- ¹² Isaev, p. 98
- ¹³ Lapedes, Daniel. Dictionary of Physics and Mathematics. McGraw-Hill, NY, 1978, p. 745
- ¹⁴ Puthoff, 1989, p. 2339
- ¹⁵ Ibid., p. 2333
- ¹⁶ Forward, Robert. "An Introductory Tutorial on the Quantum Mechanical Zero Temperature Electromagnetic Fluctuations of the Vacuum." Mass Modification Experiment Definition Study. Phillips Laboratory Report #PL-TR 96-3004, 1996, p. 3
- ¹⁷ Milonni, p. 5
- ¹⁸ Ibid., p. 9
- ¹⁹ Planck, M. "Über die Begründung des Gesetzes der schwarzen Strahlung." Ann. d. Phys. 37, 1912, p. 642
- ²⁰ Milonni, p. 10

-
- ²¹ Baym, p. 126
- ²² Granger, S., and G.W. Ford. "Electron Spin Motion in a Magnetic Mirror Trap," Phys. Rev. Lett., 5, 1972, p. 1479
- ²³ Milonni, p. 416
- ²⁴ Ibid., p.49
- ²⁵ Fulcher, L., and J. Rafelski, A. Klein. "The Decay of the Vacuum." Scientific American, Dec. 1979, p. 153
- ²⁶ Petersen, I. "Peeking inside an electron's screen." Science News. Vol. 151, Feb. 8, 1997, p. 89
- ²⁷ Lamoreaux, S. K. "Demonstration of the Casimir force in the 0.6 to 6 μm range." Phys. Rev. Lett. 78, 5, 1997, p. 1
- ²⁸ Zinkernagel, Henrik. "High Energy Particles and Reality." Ph.D. Thesis, University of Copenhagen, 1999, p. 125
- ²⁹ Dirac, P. A. M. "The Quantum Theory of the Emission and Absorption of Radiation." Proc. Roy. Soc. Lond. A 114, 1927, p.243
- ³⁰ Callen, H. B. and T. A. Welton. "Irreversibility and Generalized Noise." Phys. Rev. 83, 1951, p. 34
- ³¹ Milonni, p. 54
- ³² Nyquist, H. "Thermal Agitation of Electric Charge in Conductors." Phys. Rev. 32, 1928, p. 110
- ³³ Johnson, J. B. "Thermal Agitation of Electricity in Conductors." Phys. Rev. 32, 1928, p. 97
- ³⁴ Callen et al., p. 34
- ³⁵ Ibid., p. 34
- ³⁶ Feynman, Richard. The Feynman Lectures on Physics, Volume II. Addison-Wesley, Reading, 1965, p. 28-8
- ³⁷ Callen et al., p. 38
- ³⁸ Ibid., p. 38
- ³⁹ Yam, Philip. "Exploiting Zero-Point Energy." Scientific American. December, 1997, p. 82
- ⁴⁰ Forward, Robert. "Extracting electrical energy from the vacuum by cohesion of charged foliated conductors." Phys. Rev. B. 30, 4, 1984, p.1700
- ⁴¹ Obousy, Richard K., Appendix
- ⁴² Barrow, John. The Book of Nothing. Pantheon Books, New York, 2000, p. 210

-
- ⁴³ Mann, Charles. "Getting Over Oil." Technology Review. Jan-Feb., 2002, p. 33
- ⁴⁴ Deffeyes, Kenneth. Hubbert's Peak: The Impending World Oil Shortage. Princeton University Press, Princeton, 2001, p. 1
- ⁴⁵ Brown, Lester, and Christopher Flavin, Hilary French. The State of the World, Worldwatch Institute, Washington, 1999, p.26
- ⁴⁶ Roosevelt, Margot. "Not in My Back Bay." Time. September 30, 2002, p. 62
- ⁴⁷ Greer, Steven. "Disclosure: Implications for the Environment, World Peace, World Poverty and the Human Future." Disclosure Project Briefing Document, The Disclosure Project, April, 2001, p. 2
- ⁴⁸ Haisch, Bernard, and Alfonso Rueda, Harold Puthoff. "Inertia as a zero-point-field Lorentz force." Physical Review A. Vol. 49, No. 2, Feb., 1994, p. 678
- ⁴⁹ Clarke, Arthur C. 3001, The Final Odyssey. Ballantine Books, NY, 1997, p. 245
- ⁵⁰ Joos, Georg. Theoretical Physics. Dover, NY, 1986, p. 743
- ⁵¹ Planck, M., p. 642
- ⁵² Milonni, p. 10
- ⁵³ Einstein, A. "Zur gegenwartigen Stand des Strahlungsproblems." Phys. Zs. 10, 1909, p. 185
- ⁵⁴ Ibid., p. 19
- ⁵⁵ Einstein, A. and O. Stern. "Einige Argumente fur die Annahme einer molekularen Agitation beim absoluten Nullpunkt." Ann. d. Phys. 40, 1913, p. 551
- ⁵⁶ Einstein, A. "Zur Quantentheorie der Strahlung." Phys. Zs. 18, 1917, p. 121
- ⁵⁷ Dirac, P. A. M. "The Quantum Theory of the Emission and Absorption of Radiation." Proc. Roy. Soc. Lond. A 114, 1927, p. 243
- ⁵⁸ Dirac, P. A. M. "The Quantum Theory of the Electron." Proc. Roy. Soc. Lond. A 117, 1928, p. 610
- ⁵⁹ Debye, P. "Interferenz von Rontgenstrahlen und Warmebewegung." Ann. d. Phys. 43, 1914, p. 49
- ⁶⁰ Wu, T. Y. The Physical and Philosophical Nature of the Foundation of Modern Physics. Linking Pub. Co., Taiwan, 1975, p. 33
- ⁶¹ Pauling, L. and E. B. Wilson, Introduction to Quantum Mechanics. McGraw-Hill, NY, 1935, p. 74
- ⁶² Pauli, Wolfgang. Selected Topics in Field Quantization. Dover Pub., NY, 1973, p. 3
- ⁶³ Snow, T. P. and J. M. Shull. Physics, West Pub. Co., St. Paul, 1986, p. 817

-
- ⁶⁴ Halliday, D., and R. Resnick, Physics Part II. John Wiley & Sons, NY, 1967, p. 1184
- ⁶⁵ Einstein, A., 1917, p.121
- ⁶⁶ Snow et al., p. 877
- ⁶⁷ Isaev, p. 4
- ⁶⁸ Ibid., p. 33
- ⁶⁹ Casimir, H. B. G. "On the attraction between two perfectly conducting plates." Proc. K. Ned. Akad. Wet. 51, 1948, p. 793
- ⁷⁰ Sparnaay, M.J. "Measurements of Attractive Forces between Flat Plates," Physica (Utrecht). V. 24, 1958, p. 751
- ⁷¹ Lamoreaux, S. K. "Demonstration of the Casimir force in the 0.6 to 6 μm range." Phys. Rev. Lett. 78, 5, 1997, p. 1
- ⁷² Browne, Malcolm. "Physicists confirm power of nothing, measuring force of quantum 'foam.'" The New York Times. January 21, 1997, p. C1
- ⁷³ Milonni, p. 275
- ⁷⁴ Puthoff, Harold. "Ground State of Hydrogen as a Zero-Point Fluctuation-Determined State." Phys. Rev. D 35, 1987, p. 3266
- ⁷⁵ Milonni, p. 81
- ⁷⁶ Isaev, p. 15
- ⁷⁷ Hawton, Margaret. "One-photon operators and the role of vacuum fluctuations in the Casimir force." Phys. Rev. A. 50, 2, 1994, p. 1057
- ⁷⁸ Ibid., p. 1057
- ⁷⁹ Milonni, p. 80
- ⁸⁰ Forward, 1984, p. 1700
- ⁸¹ Iacopini, E. "Casimir effect at macroscopic distances." Phys. Rev. A. 48, 1, 1993, p. 129
- ⁸² Haroche, S. and J. Raimond. "Cavity Quantum Electrodynamics." Scientific American. April, 1993, p. 56
- ⁸³ Weigert, Stefan. "Spatial squeezing of the vacuum and the Casimir effect." Phys. Lett. A. 214, 1996, p. 215
- ⁸⁴ Lambrecht, Astrid, and Marc-Thierry Jaekel, Serge Reynaud. "The Casimir force for passive mirrors." Phys. Lett. A. 225, 1997, p. 193
- ⁸⁵ Cougo-Pinto, M. V. "Bosonic Casimir effect in external magnetic field." J. Phys. A: Math. Gen. V. 32, 1999, p. 4457

-
- ⁸⁶ Pinto, F. "Engine cycle of an optically controlled vacuum energy transducer." Phys. Rev. B. V. 60, No. 21, 1999, p. 14740
- ⁸⁷ Ibid., p. 14740
- ⁸⁸ Liu, Z. and L. Zeng, P. Liu. "Virtual-photon tunnel effect and quantum noise in a one-atom micromaser." Phys. Lett. A. V. 217, 1996, p. 219
- ⁸⁹ Valone, Thomas. "Inside Zero Point Energy." Journal of New Energy. Vol. 5, No. 4, Spring, 2001, p. 141
- ⁹⁰ Yater, Joseph. "Power conversion of energy fluctuations." Phys. Rev. A. Vol. 10, No. 4, 1974, p. 1361
- ⁹¹ Yater, Joseph. "Relation of the second law of thermodynamics to the power conversion of energy fluctuations." Phys. Rev. A. Vol. 20, No. 4, 1979, p. 1614
- ⁹² Yater, Joseph. "Rebuttal to 'Comments on "Power conversion of energy fluctuations."'" Phys. Rev. A. Vol. 20, No. 2, 1979, p. 623
- ⁹³ Astumian, R. D. "Thermodynamics and Kinetics of a Brownian Motor." Science, 276, 1997, p. 5314
- ⁹⁴ Barber, Bradley P., and Robert Hiller, Ritva Lofstedt, Seth Putterman, Keith Weninger, "Defining the Unknowns of Sonoluminescence." Physics Reports. 281 (2), March, 1997, p. 69
- ⁹⁵ Eberlein, Claudia. "Sonoluminescence as Quantum Vacuum Radiation." Phys. Rev. Lett. V. 76, No. 20, 1996, p. 3842
- ⁹⁶ Liberati, S., and M. Visser, F. Belgiorno, D. Sciama. "Sonoluminescence as a QED vacuum effect: probing Schwinger's proposal." J. Phys. A: Math. Gen. 33, 2000, p. 2251
- ⁹⁷ Puthoff, 1989, p. 2336
- ⁹⁸ Haisch, et al., 1994, p. 678
- ⁹⁹ Ibid., p. 690
- ¹⁰⁰ Feigel, A. "Quantum vacuum contribution to the momentum of dielectric media." Physical Review Letters, Vol. **92**, p. 020404, 2004
- ¹⁰¹ Cole, Daniel, and Harold Puthoff. "Extracting energy and heat from the vacuum." Physical Review E. Vol. 48, No. 2, August, 1993, p. 1562
- ¹⁰² Ibid., p. 1563
- ¹⁰³ Puthoff, Harold, and S. R. Little, M. Ibison. "Engineering the zero-point field and polarizable vacuum for interstellar flight." Journal of the British Interplanetary Society. Vol. 55, 2002, p.137
- ¹⁰⁴ Ibid., p. 137
- ¹⁰⁵ Rueda et al., 1999, p. 1
- ¹⁰⁶ Ibid., p. 4
- ¹⁰⁷ Milonni, 1994, p. 111
- ¹⁰⁸ Casimir, 1948, p. 793

-
- ¹⁰⁹ Boyer, 1980, p. 66
- ¹¹⁰ Milonni, 1994, p. 19
- ¹¹¹ Puthoff, 1989, p. 233
- ¹¹² Puthoff, 1987, p. 3266
- ¹¹³ Haisch et al., 1994, p. 678
- ¹¹⁴ Lamb, 1947, p. 241
- ¹¹⁵ Baym, 1978, p. 99
- ¹¹⁶ Planck, p. 642
- ¹¹⁷ Callen et al., p. 34
- ¹¹⁸ Eberlein, p. 842
- ¹¹⁹ Milonni, 1994, p. 111
- ¹²⁰ Baym, p. 126
- ¹²¹ Milonni, 1994, p. 99
- ¹²² Boyer, p. 790
- ¹²³ Lamoreaux, p.2
- ¹²⁴ Forward, 1984, p. 1701
- ¹²⁵ Dierauf and Court. Unified Concepts in Applied Physics. Prentice-Hall, 1979, p. 82
- ¹²⁶ Stevens, R. E., and P. K. Sherwood. How to Prepare a Feasibility Study. Prentice-Hall, 1982
- ¹²⁷ "A feasibility study: Can you manage it?" November 01, 2002 ZDNet Australia. URL: <http://www.zdnet.com.au/newstech/hr/story/0,2000024989,20269565,00.htm>
- ¹²⁸ Ozaki, S., and R. Palmer, M. Zisman, and J. Gallardo. "Feasibility Study-II of a Muon-Based Neutrino Source" 2001, <http://www.cap.bnl.gov.mumu/studyii/FS2-report.html>
- ¹²⁹ "The Feasibility Study / Proposed Plan" December 2000 U.S. Environmental Protection Agency. <http://www.epa.gov/ HUDSON/feasibility.htm>
- ¹³⁰ "The Feasibility Study" November 2002 Nonviolent Peaceforce. <http://www.nonviolentpeaceforce.org/research/summary.htm>
- ¹³¹ Jackson, J.D. Classical Electrodynamics. J. Wiley, New York, Second Edition, 1975, p. 418
- ¹³² Mie, G., Annals of Physics. Vol. 25, No. 377, 1908
- ¹³³ Cox, Larry T. "Calculation of Resonant Values of Electromagnetic Energy Incident Upon Dielectric Spheres" Phillips Laboratory, Air Force Material Command, PL-TR-93-3002, February, 1994, p. 7

- ¹³⁴ Ibid., p. 16
- ¹³⁵ Jackson, p. 775
- ¹³⁶ Stratton, J., Electromagnetic Theory. McGraw-Hill Book Co., New York, 1941
- ¹³⁷ Cox, p, 2
- ¹³⁸ Ibid., p. 8 & 15
- ¹³⁹ Gryna, Frank M. Quality Planning & Analysis. McGraw-Hill Irwin, New York, 2001, p. 54
- ¹⁴⁰ Halliday et al., p. 1204
- ¹⁴¹ Jackson, p. 411-452
- ¹⁴² Milonni, p. 15
- ¹⁴³ Ibid., p. 54
- ¹⁴⁴ Seto, William W. Schaum's Outline Series of Mechanical Vibrations. Schaum Pub. Co., New York, 1964, p.22
- ¹⁴⁵ Fink, Donald G. Electronics Engineers' Handbook. McGraw-Hill Book Co. New York, 1975, p.10-40
- ¹⁴⁶ Jackson, p. 411
- ¹⁴⁷ Ibid., p. 414
- ¹⁴⁸ Morse, Philip M. and Herman Feshbach. Methods of Theoretical Physics, Part II, McGraw-Hill, New York, 1953, p.1066
- ¹⁴⁹ Jackson, p. 16
- ¹⁵⁰ Jackson, p. 417
- ¹⁵¹ Morse, et al. p. 1485
- ¹⁵² Ibid., p. 1488
- ¹⁵³ Jackson, p. 447
- ¹⁵⁴ Ibid., p. 448
- ¹⁵⁵ Ibid., p. 451
- ¹⁵⁶ Schiff, Leonard. Quantum Mechanics, 3rd Edition, McGraw-Hill, New York, 1968, p. 125
- ¹⁵⁷ Milonni, p. 49
- ¹⁵⁸ Ibid., p. 803
- ¹⁵⁹ Sun, Yugang, et al. "Shape-Controlled Synthesis of Gold and Silver Nanoparticles" Science, Vol. 298, No. 5601, December 13, 2002, p. 2176

-
- ¹⁶⁰ Snow et al., p. 744
- ¹⁶¹ Murphy, Catherine. "Nanocubes and Nanoboxes" Science, Vol. 298, No. 5601, December 13, 2002, p. 2139
- ¹⁶² Ibid., p. 2139
- ¹⁶³ Metz, Clyde R. Schaum's Outline Series: Theory and Problems of Physical Chemistry, 2nd edition, McGraw-Hill, New York, 1989, p. 435
- ¹⁶⁴ Milonni, p. 84
- ¹⁶⁵ Fink, p. 10-42
- ¹⁶⁶ "Electromagnetic Spectrum" TRW, Inc., Electronics Systems Group, Redondo Beach, CA, October, 1986
- ¹⁶⁷ Tipler, Paul A. Foundations of Modern Physics. Worth Publishers, NY, 1969, p. 195
- ¹⁶⁸ Dunning, F. Barry. "Ryberg Atoms, Giants of the Atomic World" Science Spectra, Issue 3, 1995, p. 34
- ¹⁶⁹ Jackson, p. 644
- ¹⁷⁰ "Table of Periodic Properties of the Elements" WLS-18806, Sargent-Welch VWR International, Buffalo Grove, IL, 2002, Side 2
- ¹⁷¹ Gautreau, R. and W. Savin. Schaum's Outline Series, Theory and Problems of Modern Physics, McGraw-Hill, New York, 1978, p. 107
- ¹⁷² Duderstadt, James and L.. Hamilton, Nuclear Reactor Analysis, J. Wiley & Sons, New York, 1976, p. 53
- ¹⁷³ Milonni, p. 144
- ¹⁷⁴ Duderstadt, p. 49
- ¹⁷⁵ "Table of Periodic Properties of the Elements," Side 2
- ¹⁷⁶ Jackson, p. 682
- ¹⁷⁷ Ibid., p. 627
- ¹⁷⁸ Ibid., p. 647
- ¹⁷⁹ Gautreau et al., p. 77
- ¹⁸⁰ Jackson, p. 646
- ¹⁸¹ Feynman, Vol. I, p. 1-1
- ¹⁸² Jackson, p. 803
- ¹⁸³ Ibid., p. 681
- ¹⁸⁴ Schiff, p. 457
- ¹⁸⁵ Baym, p. 211

-
- ¹⁸⁶ Schiff, p. 457
- ¹⁸⁷ Tipler, p. 438
- ¹⁸⁸ Schiff, p. 125
- ¹⁸⁹ Ibid., p. 126
- ¹⁹⁰ Mittleman, Dehmelt, and Kim "Cold Kilo-Electron Ball as Probe for Charge-Proportional Cyclotron Frequency Shift in Penning Trap Cavity" Phys. Rev. Letters, V. 75, 1995, p. 2839,
- ¹⁹¹ Weisskopf, Victor "Recent developments in the theory of the electron" Reviews of Modern Physics, Vol. 21, No. 2, April, 1949, p. 309
- ¹⁹² Milonni, p. 85
- ¹⁹³ Ibid., p. 81
- ¹⁹⁴ Brink, G. O., "Nonresonant Ion Trap" Review of Scientific Instruments, Vol. 46, No. 6, June, 1975, p. 739
- ¹⁹⁵ Weisskopf, p. 310
- ¹⁹⁶ Pinto, F. "Engine cycle of an optically controlled vacuum energy transducer" Physical Review B, Vol. 60, No. 21, 1999, p. 14740
- ¹⁹⁷ Milonni, p. 221
- ¹⁹⁸ Haroche, p. 57
- ¹⁹⁹ Pinto, p. 14748
- ²⁰⁰ Ibid., p. 14743
- ²⁰¹ Ibid., p. 14743
- ²⁰² Ibid., p. 14742
- ²⁰³ Ibid., p. 14744
- ²⁰⁴ Ibid., p. 14752
- ²⁰⁵ Falomir, H., et al. Divergencies in the Casimir energy for a medium with realistic ultraviolet behaviour" J. Phys. A Math. Gen. V. 34, August 17, 2001, p. 6291
- ²⁰⁶ Brevik, I. "Casimir Effect in Dielectrics: On the Low-Frequency Contributions" Casimir Forces Workshop: Recent Developments in Experiment and Theory, Harvard University, November 14-16, 2002, p.1
- ²⁰⁷ An, K., et al. "Single-atom laser" Physical Review Letters, Vol. 73, 1994, p. 3375
- ²⁰⁸ Liu, Z. et al. "Virtual-photon tunnel effect and quantum noise in a one-atom micromaser" Physics Letters A, V. 217, 1996, p. 219
- ²⁰⁹ Pinto, p. 14750
- ²¹⁰ Ibid., p. 14746

-
- ²¹¹ Cheng, H. "The Casimir energy for a rectangular cavity at finite temperature" J. Phys. A: Math Gen. Vol. 35, March 8, 2002, p. 2205
- ²¹² Klimchitskaya, G. "Problems with the Thermal Casimir Force between Real Metals" Casimir Forces Workshop: Recent Developments in Experiment and Theory, Harvard University, November 14-16, 2002, p.1
- ²¹³ Milonni, p. 187
- ²¹⁴ Haroche, S. et al., p. 54
- ²¹⁵ Dodonov, V.V. "Resonance photon generation in a vibrating cavity" J. Phys. A Gen. V. 31 Dec. 11, 1998, p. 9835
- ²¹⁶ Andreatta, M.A. "Energy density and packet formation in a vibrating cavity" J. Phys. A: Math. Gen. V. 33, April 28, 2000, p. 3209
- ²¹⁷ Haroche, S., p. 60
- ²¹⁸ Weigert, p. 215
- ²¹⁹ Hu, Z. et al. "Squeezed Phonon States: Modulating Quantum Fluctuations of Atomic Displacements" Phys. Rev. Lett. V. 76, 1996, p. 2294
- ²²⁰ Wiegert, p. 217
- ²²¹ Weigert, p. 219
- ²²² Dodonov, V.V. et al. "Squeezing and photon distribution in a vibrating cavity" J. Phys. A: Math Gen. V. 32, 1999, p. 6721
- ²²³ Ford, L.H. et al. "Focusing Vacuum Fluctuations" Casimir Forces Workshop: Recent Developments in Experiment and Theory, Harvard University, November 14-16, 2002, p. 1
- ²²⁴ Ibid., p. 19
- ²²⁵ Milonni, p. 200
- ²²⁶ Zheng, M-S., et al. "Influence of combination of Casimir force and residual stress on the behaviour of micro- and nano-electromechanical systems" Chinese Physics Letters, V. 19, No. 6, 2002, p. 832
- ²²⁷ Lapedes, p. 754
- ²²⁸ Sperry, M. et al. "The role of the Casimir effect in the static deflection and stiction of membrane strips in microelectromechanical systems (MEMS)" Journal of Applied Physics, V. 84, No. 5, 1998, p. 2501
- ²²⁹ Zheng, et al., p. 834
- ²³⁰ Milonni, p. 58
- ²³¹ Ibid., p. 97
- ²³² Ibid., p. 219

-
- ²³³ Maclay, J. "Unusual properties of conductive rectangular cavities in the zero point electromagnetic field: resolving Forward's Casimir energy extraction cycle paradox" Proceedings of Space Technology and Applications International Forum (STAIF), Albuquerque, NM, January, 1999, p. 3
- ²³⁴ Ibid., p. 5
- ²³⁵ Maclay, J., et al. "Of some theoretical significance: Implications of Casimir effects" European Journal of Physics, Vol. 22, 2001, p. 6
- ²³⁶ Lifshitz, E.M. et al. Statistical Physics, Part 2, Nauka Pub., Moscow, 1978, Chapter 8
- ²³⁷ Marachevsky, V.N. Modern Physics Letters A, V. 16, 2001, p. 1007
- ²³⁸ Brevik, I. et al. "Casimir problem of spherical dielectrics: Numerical evaluation for general permittivities" Phys. Rev. E, Vol. 66, 2002, p. 26119
- ²³⁹ Maclay, 1999, p. 6
- ²⁴⁰ Sagan, C. Cosmos, Random House, New York, 1980, p. 37
- ²⁴¹ Eberlein, C. "Fluctuations of Casimir forces on finite objects. I. Spheres and hemispheres, II. Flat circular disk" J. Phys. A: Math. Gen. Vol. 25, 1992, p. 3015
- ²⁴² Cognola, G. et al. "Casimir energies for spherically symmetric cavities" J. Phys. A: Math. Gen. Vol. 34, 2001, p. 7311
- ²⁴³ Cheng, H. "The Casimir energy for a rectangular cavity at finite temperature" J. Phys. A: Math. Gen. Vol. 35, 2002, p.2205
- ²⁴⁴ Jackson, p. 288
- ²⁴⁵ Sokolov, I. "The Casimir effect as a possible source of cosmic energy" Physics Letters A, Vol. 223, 1996, p. 163
- ²⁴⁶ Hizhnyakov, V.V. "Quantum emission of a medium with a time-dependent refractive index" Quantum Optics, Vol. 4, 1992, p. 277
- ²⁴⁷ Milonni, p. 64
- ²⁴⁸ Ibid., p. 68
- ²⁴⁹ Zee, A. Quantum Field Theory in a Nutshell, Princeton University Press, 2003, p. 265
- ²⁵⁰ Bohm, D. and J.P. Vigier "Model of the Causal Interpretation of Quantum Theory in Terms of a Fluid with Irregular Fluctuations" Phys. Rev. Vol. 96, No. 1, 1954, p. 208
- ²⁵¹ Froning, H.D. and R.L. Roach "Preliminary simulations of vehicle interactions with the quantum vacuum by fluid dynamic approximations" Proceedings of 38th AIAA/ASME/SAE/ASEE Joint Propulsion Conference, July, 2002, AIAA-2002-3925, p. 52236
- ²⁵² Zee, p. 233
- ²⁵³ Milonni, p. 12
- ²⁵⁴ Rueda and Haisch, p. 4

-
- ²⁵⁵ Scully, M.O. et al. "Extracting work from a single heat bath via vanishing quantum coherence" Science, Vol. 299, Issue 5608, 2003, p. 862
- ²⁵⁶ Ibid., p. 866
- ²⁵⁷ Milonni, P.W. "Photon Steam Engines" Physics World, April, 2003, p. 2
- ²⁵⁸ Ibid., p. 3
- ²⁵⁹ Allahverdyan, A.E. and T.M. Nieuwenhuizen "Extraction of work from a single thermal bath in the quantum regime" Physical Review Letters, vol. 85, No. 9, August, 2000, p. 1799
- ²⁶⁰ Ibid., p. 1800
- ²⁶¹ Ibid., p. 1802
- ²⁶² Linke, H. "Coherent Power Booster" Science, Vol. 299, Issue 5608, 2003, p. 841
- ²⁶³ Astumian, R. D., p. 917
- ²⁶⁴ Ibid., p. 918
- ²⁶⁵ Ibid., p. 921
- ²⁶⁶ Linke, H. et al. "Experimental Tunneling Ratchets" Science, Vol. 286, Issue 5448, 1999, p. 2314
- ²⁶⁷ Blau, S. "The Unusual Thermodynamics of Microscopic Systems" Physics Today, September, 2002, p. 19
- ²⁶⁸ Ibid., p. 20
- ²⁶⁹ Crooks, G.E. "Entropy production fluctuation theorem and the nonequilibrium work relation for free energy differences" Physical Review E, Vol. 60, No. 3, September, 1999, p. 2725
- ²⁷⁰ Ibid., p. 2724
- ²⁷¹ Yater, J.C. "Power conversion of energy fluctuations" Physical Review A, Vol. 10, No 4, October, 1974, p. 1361
- ²⁷² Yater, J.C. "Rebuttal to 'comments on "Power conversion of energy fluctuations"' " Physical Review A, Vol. 20, No. 2, August, 1979, p. 623
- ²⁷³ Yater, J.C. "Relation of the second law of thermodynamics to the power conversion of energy fluctuations" Physical Review A, Vol. 20, No. 4, October, 1979, p. 1614
- ²⁷⁴ Lapedes, p. 868
- ²⁷⁵ Yater, J.C. "Reversible Thermoelectric Power Conversion of Energy Fluctuations" Proceedings of the Second International Conference on Thermoelectric Energy Conversion, Arlington, Texas, IEEE No. 78CH1313-6, 1978, p. 107
- ²⁷⁶ Yater, J.C. (October, 1979), p. 1614
- ²⁷⁷ Ibarra-Bracamontes, et al. "Stochastic ratchets with colored thermal noise" Physical Review E, Vol. 56, No. 4, October, 1997, p. 4048

-
- ²⁷⁸ Ibid., p. 4050
- ²⁷⁹ Engel, A., et al. "Ferrofluids as Thermal Ratchets" Physical Review Letters, Vol. 91, No. 6, 2003, p. 060602-1
- ²⁸⁰ Ibid., p. 060602-2
- ²⁸¹ Ibid., p. 060602-2
- ²⁸² Ibid., p. 060602-4
- ²⁸³ Millman, J. and Halkias, C. Electronic Devices and Circuits, McGraw-Hill, New York, 1967, p. 474
- ²⁸⁴ Bulsara, A.R. et al. "Tuning in to Noise" Physics Today, March, 1996, p. 39
- ²⁸⁵ Goychuk, I. et al. "Nonadiabatic quantum Brownian rectifiers" Physical Review Letters, Vol. 81, No. 3, 1998, p. 649
- ²⁸⁶ Lapedes, p. 100
- ²⁸⁷ Hartmann, L. et al. "Driven tunneling dynamics: Bloch-Redfield theory versus path-integral approach" Physical Review E, Vol. 61, No. 5, May, 2000, p. R4687
- ²⁸⁸ Goychuk, et al., p. 651
- ²⁸⁹ Ibid., p. 652
- ²⁹⁰ Milonni, p. 30
- ²⁹¹ See for example Physics World, "Dark Energy," <http://physicsweb.org/article/world/17/5/7>
- ²⁹² Beck, Christian and Michael Mackey, Astrophysics preprint, "Has Dark Energy Been Measured in the Lab?" <http://xxx.arxiv.org/abs/astro-ph/0406504> June 23, 2004
- ²⁹³ Ibid., p. 198
- ²⁹⁴ Ibid., p. 417
- ²⁹⁵ Jackson, p. 724
- ²⁹⁶ Astumian, p. 923
- ²⁹⁷ Stevens et al., p. 37

Proposed Use of Zero Bias Diode Arrays as Thermal Electric Noise Rectifiers and Non-Thermal Energy Harvesters

Thomas F. Valone

*Integrity Research Institute
5020 Sunnyside Avenue, Suite 209
Beltsville MD 20705
301-220-0440; IRI@starpower.net*

Abstract. The well known built-in voltage potential for some select semiconductor p-n junctions and various rectifying devices is proposed to be favorable for generating DC electricity at "zero bias" (with no DC bias voltage applied) in the presence of Johnson noise or 1/f noise which originates from the quantum vacuum (Koch, 1982). The 1982 Koch discovery that certain solid state devices exhibit measurable quantum noise has also recently been labeled a finding of dark energy in the lab (Beck, 2004). Tunnel diodes are a class of rectifiers that are qualified and some have been credited with conducting only because of quantum fluctuations. Microwave diodes are also good choices since many are designed for zero bias operation. A completely passive, unamplified zero bias diode converter/detector for millimeter (GHz) waves was developed by HRL Labs in 2006 under a DARPA contract, utilizing a Sb-based "backward tunnel diode" (BTD). It is reported to be a "true zero-bias diode". It was developed for a "field radiometer" to "collect thermally radiated power" (in other words, 'night vision'). The diode array mounting allows a feed from horn antenna, which functions as a passive concentrating amplifier. An important clue is the "noise equivalent power" of 1.1 pW per root hertz and the "noise equivalent temperature difference" of 10°K, which indicate sensitivity to Johnson noise (Lynch, et al., 2006). There also have been other inventions such as "single electron transistors" that also have "the highest signal to noise ratio" near zero bias. Furthermore, "ultrasensitive" devices that convert radio frequencies have been invented that operate at outer space temperatures (3 degrees above zero point: 3°K). These devices are tiny nanotech devices which are suitable for assembly in parallel circuits (such as a 2-D array) to possibly produce zero point energy direct current electricity with significant power density (Brenning et al., 2006). Photovoltaic p-n junction cells are also considered for possible higher frequency ZPE transduction. Diode arrays of self-assembled molecular rectifiers or preferably, nano-sized cylindrical diodes are shown to reasonably provide for rectification of electron fluctuations from thermal and non-thermal ZPE sources to create an alternative energy DC electrical generator in the picowatt per diode range.

Keywords: Diodes, Rectifiers, Energy Harvesting, Quantum Vacuum, Zero Point Energy, Direct Current, Nonthermal Noise, 1/F Noise, Shot Noise, Johnson Noise

PACS: 07.50.Hp, 05.40.-a, 03.75.Lm, 85.35.Gv, 81.07.N

INTRODUCTION

The US currently spends between 5 and 10 cents per kilowatt-hour (kWh) depending upon whether we are a residential or commercial customer. Furthermore, the US Electric Power Industry generates approximately 4,000 billion kWh on an annual basis (www.eia.doe.gov). These figures indicate that electricity consumption is about a \$300 billion market commanded by the public utilities. It is proposed that distributed single cubic-meter electricity generating units may become a reality in the near future with the emergence of zero point energy (ZPE) rectifiers deployed in the form of three-dimensional arrays. This event is predicted to create a disruptive effect on the public utilities, while it empowers ordinary individuals from all walks of life including third world countries, opening up vast areas of the world that are presently uninhabitable due to the lack of on-site energy generation capability.

The built-in voltage potential across the ends of semiconductor p-n junctions, caused by the charge q difference between the positive p-doped and negative n-doped material, is about 0.6 volts for silicon diodes and normally depends primarily upon kT/q and the ratio of charge carrier concentrations (about 0.026 eV for silicon at room temperature) where k is the Boltzmann constant and T is the absolute temperature. Furthermore, it requires an equivalent voltage bias to overcome the potential barrier and create electronic conduction through the diode rectifier. However, there are other forms of rectifying devices suitable for generating DC electricity with much lower bias voltage requirements. The class of rectifiers that are compatible with ZPE levels of energy are those that operate at “zero bias” (with no bias DC voltage applied whatsoever). Tunnel diodes are one class of rectifiers that are qualified. Microwave rectenna diodes are also good choices since many are designed for zero bias operation. Reference articles are attached showing the use of “broadband spiral antennas” and phase conjugate mirrors for amplifying electromagnetic frequencies that make up quantum noise. The tunneling current in the diodes can also be influenced by the use of magnetic fields as low as 10 gauss as well.

With the numerous discoveries of the various energetic features of the quantum vacuum, as devices get smaller and smaller, it is a predictable certainty that more and more nanotechnology devices will begin exhibiting chaotic zero point energy. It is also noted that developments in molecular nanoelectronics have presented a wide range of molecular and nano-crystal diode options, including Schottky photodiodes based on organic molecules (Reed, 2003). There are many features of Casimir effect and other ZPE-related phenomena which lend themselves to possible generation of electricity (Valone, 2003). One example is the dramatic change of dielectric constant of a cantilever cavity by illumination with a microlaser in order to increase the Casimir force as Pinto proposes and generate 0.5 nW (nW = nanowatt = 10^{-9} W) of electricity with a 100 micron device (Pinto, 1999). Presently, the Casimir force is becoming more commonplace since it is a frequent hazard in the nanotechnology field for the Casimir effect to literally destroy a nano-cantilever when the spacing drops below one micron.

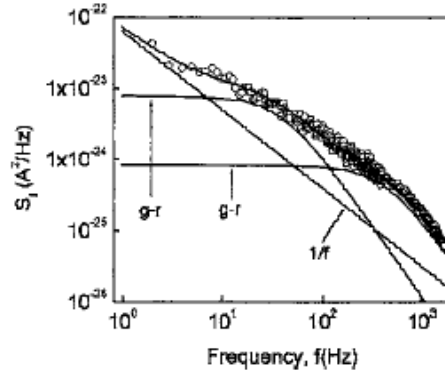


FIGURE 1. Example of $1/f$ noise in the picoampere current range from a diode rectifier, along with contributed noise (g-r lines) from two quantum dot devices (Tsormpatzoglou, 2005).

LABORATORY MEASUREMENT OF NON-THERMAL NOISE CURRENT

Considering electronic circuits, it is important to note that $1/f$ noise (noise that decreases with frequency) in carbon shunt resistors and electronic components is also very commonplace (Figure 1). One textbook estimates a noisy operational transresistor circuit used to condition small currents, using parameters for an AD549 electrometer op amp (Analog Devices, Norwood, MA) to have the dominant term coming from Johnson noise (often regarded only as thermal noise) and a minimum noise current of about 0.12 microamps DC (Northrop, 1997). In tunnel junction diodes, thermal fluctuations will lead to a voltage difference across the junction and stimulate tunneling electrons (Sheng, 1978). Furthermore, the electronic fluctuations of ZPE have been measured in the laboratory as some university researchers have been careful to isolate the thermal component of noise (equation (3)) in order to evaluate the *non-thermal, broad spectrum noise* more closely. In a resistively shunted Josephson junction (RSJ), which normally operates at liquid helium temperatures, the non-thermal portion of noise has been unequivocally been measured. With good agreement with the quantum correction to the Nyquist noise generated in the shunt resistor, the spectral density of noise in the resistor, including zero-point fluctuations is found to be (Koch, 1980):

$$S(f) = (hf / \pi R) \coth(hf / 2kT) \quad (1)$$

Koch (1982) notes that in the extreme quantum limit $eV \gg kT$, the observed noise is generated solely by zero-point fluctuations in the shunt resistor R , which has a current spectral density of $hf/\pi R$ where h is Planck's constant and f is the frequency. However, treating the electron as a quantum mechanical wave packet, which has some probability of penetrating the barrier by macroscopic quantum tunneling (MQT), a need for a quantitative theory that deals with both zero-point fluctuations and MQT is needed. Koch (1982) measured about a 10% contribution of $1/f$ noise to the white noise spectral density and focused on the noise generated solely at the junction, taking into account all extraneous sources of noise.

For frequencies ν up to 500 GHz, Koch (1982) verified that the spectral density of the Josephson junction was in excellent agreement with the prediction of equation (2). Furthermore, the presence of the zero-point energy coefficient term $2hf/R$ was demonstrated at frequencies of $hf > kT$.

$$S_j(f) = (2hf / R) \coth(hf / 2kT) \quad (2)$$

In Figure 2, the spectral density of the measured noise is plotted as compared to the dashed lines, which show what the data would look like *without* a ZPE fluctuation term contribution. The graph also clearly shows the upper frequency limit of ZPE fluctuations that Koch measured for the noise spectrum. This work sets the stage for further investigation of other circuit elements and devices that may also exhibit similar behavior of a broadband white noise spectral density due to ZPE that may be buried in thermal Johnson noise as well.

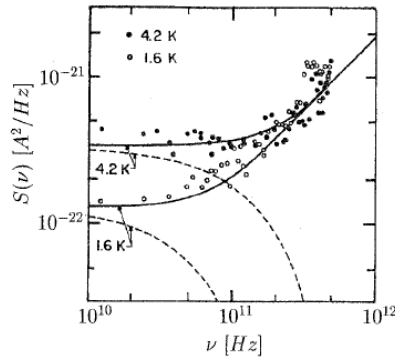


FIGURE 2. Measured spectral density of current noise in the shunt resistor of Josephson junction at 4.2K (solid circles) and 1.6K (open circles) up to 500 GHz. Solid lines are the prediction of Equation 2 while the dashed lines represent the theoretical prediction in the absence of the zero-point energy term and fall far below the data at the higher frequencies (Koch, 1982).

Further considering resistor-based noise from the quantum vacuum, Blanco *et al.* (2001) have proposed a method for enhancing the ZPE-induced voltage fluctuations in circuits. Treating a coil of wire theoretically as an antenna, they argue that the antenna-like radiation resistance of the coil should be included in the total resistance of the circuit, and they suggest that it is this total resistance that should be used in the theoretical computation of the ZPE-induced voltage fluctuations. Because of the strong dependence of the radiation resistance on the number of coil turns (scaling quadratically), coil radius (quartic scaling), and frequency (quartic scaling), these enhanced ZPE-induced voltage fluctuations should be measurable in the laboratory at quite accessible frequencies in the 100 MHz range (Davis, 2006). To clarify, Koch (1982) emphasized the existence of ZPE fluctuation broadband white noise which is found in the semiconductor junction and more prominently in the shunt resistor. However, as equation (1) and equation (2) demonstrate, the resistance R is found in the denominator and so it is unlikely that high resistance is an advantage when attempting to transduce ZPE fluctuation noise in a circuit.

As we look at the dominant contribution to electronic noise, thermal voltage fluctuations are proportional to the resistance as seen in equation (3). Therefore, high resistance may be recommended for rectifying thermal fluctuations.

$$V_N = 4kTRF_{BW} \quad (3)$$

Voltage noise V_N from thermal fluctuations has the form of equation (3) and depends upon the Boltzmann constant k (1.38×10^{-23}), absolute temperature T (Kelvin), the resistance R of the circuit, and the frequency bandwidth F_{BW} in Hertz. It may be emphasized that ZPE fluctuation circuits working at room temperature will automatically include

thermal fluctuations and perhaps should be designed to maximize both contributions. Furthermore, optimizing a resistance circuit for thermal fluctuation rectification should also include zero bias diodes for high efficiency, which will also therefore, absorb heat from the environment. The recent discovery of a Brownian refrigerator also called “the world’s smallest fridge” accentuates the availability of additional spinoffs from the development of a molecular diode rectifier array for noise transduction (Van den Broeck, 2006).

ARGUMENT FOR THE USE OF CERTAIN DEVICES FOR ZPE CONVERSION

Regarding the existence of substantive experiments showing extraction of energy from the quantum vacuum, a summary of the most robust examples has been published (Valone, 2007). It also includes the discovery that there exists a class of diodes (rectifiers) that operate at “zero-bias” (no voltage applied to make them work) and well into microwave frequency bands, that are suitable for generating trickle currents from the zero point energy quantum vacuum because of natural nonthermal electrical ZPE fluctuations ($1/f$ or Johnson noise), in addition to a serendipitous “piggy back” inclusion of electrical noise from thermal fluctuations, as well as any and all ambient electromagnetic field (EMF) radiation that happens to impinge on the diode generators. In effect, such zero bias diode arrays are predicted to act as broadband *energy harvesters* for a vast range of wasted electromagnetic interference which, especially in urban environments, can have a reasonably valuable power amplitude from radio, cellular, television, radar, satellite, short-wave, ELF, VLF, Schumann and other EMF transmissions.

Furthermore, there are patents and published studies that review tunneling semiconductor devices at zero voltage (zero bias). Several microwave diodes also exhibit this feature. However, it is important to appreciate that looking in the noise level ($1/f$ noise or Johnson noise) is where ZPE manifests (Valone, 2004). Nature has also been helpful since broadband white, $1/f$ and thermal noise in the diode is also generated at the junction itself and therefore, requires no minimum signal to initiate the conduction in one direction.

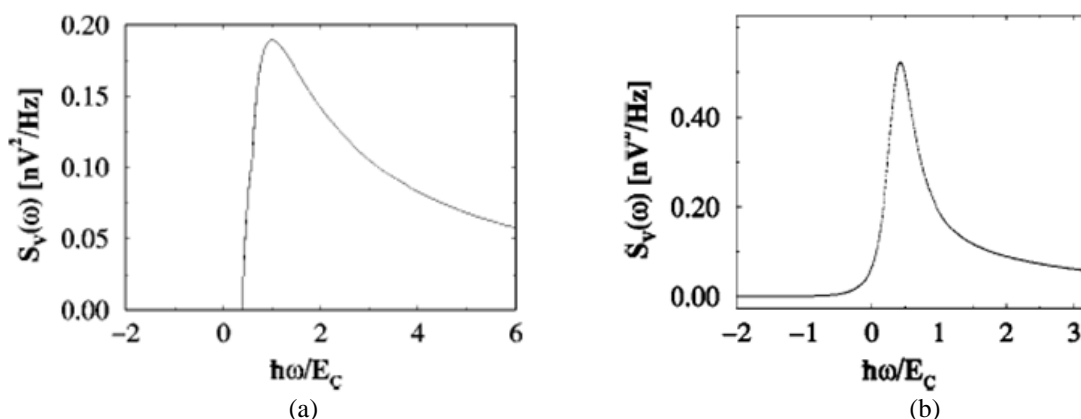


FIGURE 3. Spectral density of voltage noise in a single-electron transistor (a) in the off-state as compared to the (b) normal run mode at 1.5 nA and $E_C = 2.5$ K (Kach, 2003)

It should also be noted that the work of Yasutomi (2004) with peptide molecular photodiodes just 1 nm across is advantageous for possible 2-D parallel arrays of diodes. Many of these molecular diode rectifiers are also self-assembling, which facilitates fabrication techniques (Dhirani, 1997). However, most organic molecular diodes exhibit high resistance and fairly large junction bias voltage. Even single-electron transistors (SET), which can be viewed as back-to-back diodes (p-n-p or n-p-n) display a spectral noise density similar to a black body radiation curve (Figure 3). SET's sometimes have "the highest signal to noise ratio" near zero bias. Furthermore, these "ultrasensitive" devices that convert radio frequencies have been invented that operate at outer space temperatures (3 degrees above zero point: 3°K). These devices are tiny nanotech devices so it is possible that lots of them could be assembled in parallel (such as an array) to produce ZPE electricity with significant power density (Brenning *et al.*, 2006).

Beginning with the patent literature, the following US patents are perhaps the most significant for indicating ZPE research in this area. "Diode Array" by Charles Brown #3,890,161 and "Type II Heterostructure Device" by Capasso

#4,704,622 actually acknowledge ZPE for their functional nature (Note: www.google.com/patents is a good source of printable, pdf-format patents). Capasso, an IBM engineer, indicates that his tunneling device only works if ZPE is present, analogous to what Planck discovered a century ago with his well-known second radiation law that matched the black body curve for the first time. Brown suggests that metal-metal diodes probably will be a popular brand for ZPE usage with millipore sheet assembly. While Brown patented his invention back in 1975, his idea has been revived and rejuvenated by Kuriyama's "Method for Manufacturing a Semiconductor Device" US Patent #7,183,127 which cites Brown's patent and others with similar cylindrically shaped pores for p-n junction design. It is encouraging to note that Kuriyama's preferred range of diameter for each cylindrical diode is not smaller than 1 nanometer (nm) and not larger than 10 nm. In addition, several references are cited for nano-hole and nano-wire construction techniques, especially with regard to p-n or p-i-n junctions. A typical example of aluminum-silicon nano-structures has achieved an average diameter of 3 nm per cylinder with a 7 nm spacing between them, with a length of 200 nm per cylinder. Kuriyama also notes that these dimensions also hold if germanium is substituted for silicon. He also includes the important option of an electrode plate on the top and bottom of the diode array, or an electro-conductive substrate for the bottom common conductor. The smallest diameter that Kuriyama cites as a practical example has a 1 nm cylinder width with a 3 nm spacing between the diodes in 1000 nm square semiconductor dies, as seen in Fig. 4. This creates a diode density of approximately 10^{12} diodes per cm^2 which is on the order of self-assembled quantum dot GaAs Schottky diodes grown by atomic layer molecular beam epitaxy (ALMBE) with InAs dots which have a diode density of 10^{11} per cm^2 (Hastas, 2003).

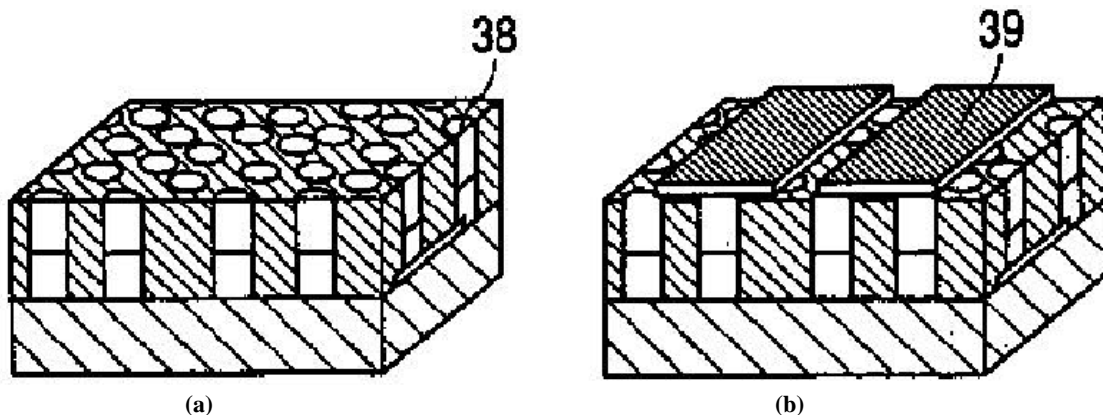


FIGURE 4. Updated version of a Brown's p-n junction (a) diode array (38) and (b) with parallel conductors (39) added (Kuriyama, A., Miyata, H., Otto, A., Ogawa, M., Okura, H., Fukutani, K., and Den, T., "Method for Manufacturing a Semiconductor Device", U.S. Patent 7,183,127, Feb. 27, 2007, Fig. 4D and 4E).

To summarize this section, the diodes reviewed provide the ability for greater than uncertainty generation of energy from ZPE and can be enhanced with resistance in the circuit for thermal noise rectification as well (Davis, 2006). Davis cites the multiple papers that Koch published decades ago. Davis presented this interest at the 2006 STAIF conference and has approached Lockheed Martin to fund a replication of Koch's work. Dr. Christian Beck, who also cites Koch's paper, uses the Koch experiment to argue that dark energy is measurable in the laboratory (Beck, 2005). The next section contains specific detail that further helps to explain zero bias diodes (Valone, 2007).

EXAMPLES OF ZERO BIAS DIODES USEFUL FOR ENERGY GENERATION

An invention developed in 2005 by the University of California Santa Barbara is the "semimetal-semiconductor rectifier" for similar applications, to rival the metal-semiconductor (Schottky) diodes that are more commonly known for microwave detection. Figure 5 shows the zero-bias rectifier that is capable of high "RF-to-DC current responsivity" 20 A/W which operates at room temperature with a noise equivalent power (NEP) of 8.9×10^{-13} W/Hz^{1/2}. Most importantly, the inventors claim that the new diodes are about 20 dB more sensitive than the best available zero-bias diodes from Hewlett-Packard (Young *et al.*, 2005).

Solid-state diodes which exhibit the ability to rectify EMF energy include the class of "backward diodes" which operate with zero bias (no external power supply input). This includes US patent #6,635,907 "Type II Interband Heterostructure Backward Diodes" and also US patent 6,870,417 "Circuit for Loss-Less Diode Equivalent". These

devices have been used in microwave detection for decades but have apparently never been tested for nonthermal zero point energy fluctuation conversion. There is every reason to presume they include such ZPE radiation conversion in their everyday operation but it is unnoticed with other EMF energy being so much larger in amplitude. US Patent #6,635,907 from HRL Laboratories describes a diode with a very desirable, "highly nonlinear portion of the I-V curve near zero bias."

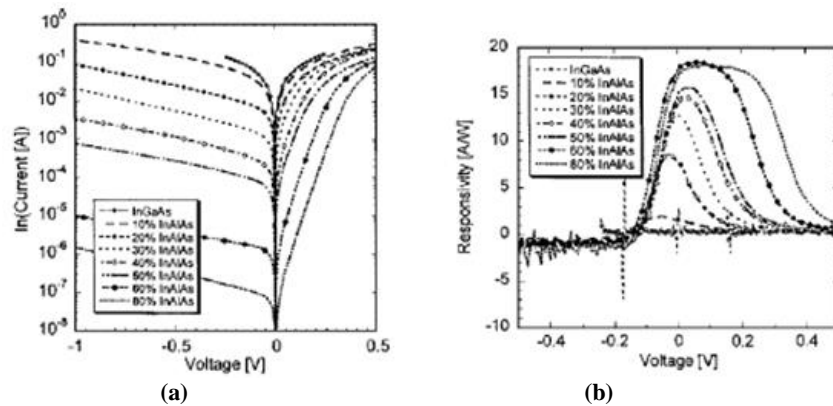


FIGURE 5. Example of a modified Schottky diode (semimetal-semiconductor) InGaAs rectifier for sensitive room-temperature microwave detection that operates well at zero bias voltage, where (a) shows increasing current levels in amperes with lower InAlAs percentage and (b) shows increased responsivity in A/W at zero bias voltage and higher InAlAs levels (Young, 2005).

These diodes produce a significant current of electrons when microwaves in the gigahertz range are present. Another example (Figure 6) is Morizuka's Patent #5,930,133 from Toshiba entitled, "Rectifying device for achieving a high power efficiency." They use a tunnel diode in the backward mode so that "the turn-on voltage is zero." Could there be a better device for small voltage ZPE fluctuations that don't like to jump big barriers?

In 1994, Smoliner reported, for the first time, resonant tunneling while applying no voltage at all to the one-dimensional quantum wells that his team had created. They used "anharmonic oscillation" to substitute for zero point energy, which they ignored "for simplicity" though it was powering the tunneling of their electrons in each well, where the electrons prefer a zero voltage bias for the best results (Smoliner, 1994). In Figure 7, Smoliner reports wave function calculations for quantum dot tunneling diodes that show a maximum at zero bias voltage (Smoliner, 1996). Such work with quantum dots also cite the "zero-bias voltage anomaly" which displays a Kondo resonance and coherent coupling that enhances transport at zero bias and low temperatures (Schmid, 1997).

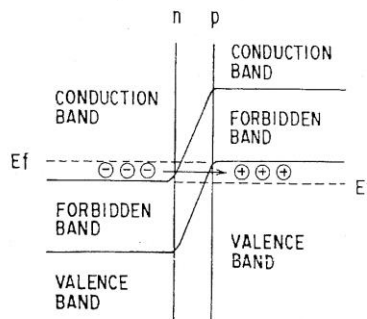


FIGURE 6. Tunneling current in a reverse-bias, backward tunnel diode used as a rectifying device at zero bias (Morizuka, K., "Rectifying device for achieving high power efficiency," U.S. Patent 5,930,122, July 27, 1999, Figure 5)

A completely passive, unamplified zero bias diode converter/detector for millimeter (GHz) waves was developed by HRL Labs in 2006 under a DARPA contract, utilizing a Sb-based "backward tunnel diode" (BTD). It is reported to be a "true zero-bias diode" that does not have significant 1/f noise when it is unamplified. It was developed for a "field radiometer" to "collect thermally radiated power" (in other words, 'night vision'). The diode array mounting allows a feed from horn antenna, which functions as a passive concentrating amplifier. The important clue is the "noise equivalent power" of 1.1 pW per root hertz (picowatts or a trillionth of a watt) and the "noise equivalent temperature difference" of 10K, which indicate sensitivity to Johnson noise which includes ZPE. Perhaps HRL Labs has one of the recommended devices for passive thermal and non-thermal electric energy generation (Lynch, *et al.*, 2006).

Dr. Peter Hagelstein from Eneco, Inc. was thinking along the same lines when in 2002 he patented his "Thermal Diode for Energy Conversion" (US Patent #6,396,191) which uses a thermopile bank of thermionic diodes. These are slightly different, more like thermocouples, than the diodes that are advocated in this article. However, Hagelstein's diodes are so efficient that he predicts that, with only a 10°C temperature difference, a water pool of six meters on a side could supply the electricity for a house. He also suggests their use as "efficiency boosters" for augmenting the performance of electric or hybrid cars.

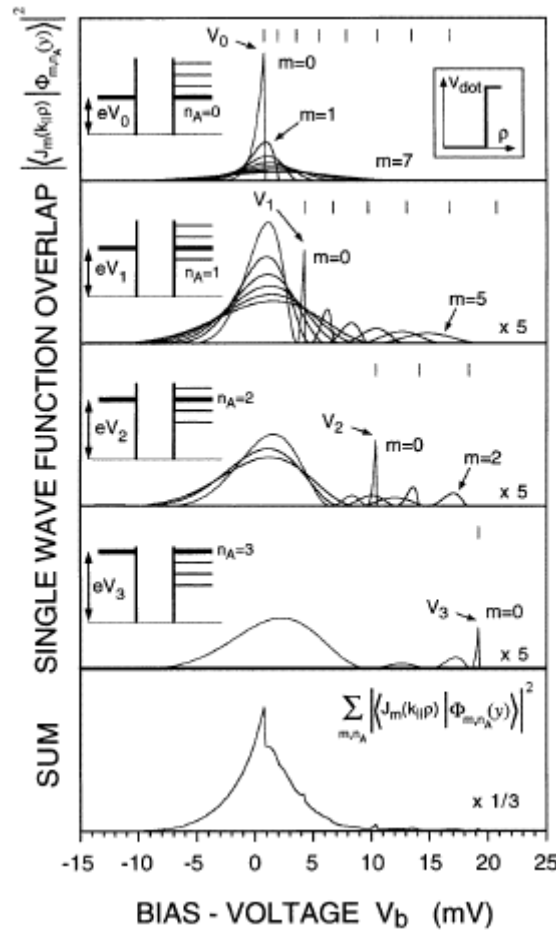


FIGURE 7. Calculated wave function overlap between the 2D state and the lowest three 0D states for a quantum dot with a rectangular potential of finite height (for example, an ultra-small, pillar-shaped double-barrier resonant tunneling diode), including the sum over all 0D subbands showing a maximum at zero bias voltage (Smoliner, 1996).

Other devices which also will provide the fuelless electrical energy cars, planes and homes need simply use zinc oxide or titanium oxide films that can convert ambient heat into electricity, as used in photovoltaic panels. A few

reports indicate that these work reliably for years. Such solid-state diode converters will also grab the nonthermal ZPE in the process and therefore can work in outer space, even without solar exposure.

THEORETICAL ENERGY DENSITY CONSIDERATIONS

Since the ZPE spectral density depends upon the third power of the frequency, which is inversely proportional to the wavelength, an interesting exercise is to see how much energy is available from the quantum vacuum or the DEAC is to calculate the ZPE spectral density for various frequency ranges. This can also be regarded, using $c = \lambda f$, to correspond to certain minimum volumes based on an assumption of a resonant cavity, such as with the physics approach to scattering problems or electromagnetic radiation. Both models apply to treatments of virtual particle radiation. A more in depth treatment of this topic is found in my book on the subject (Valone, 2004). Integrating over the frequency range of interest produces a higher, fourth power dependence of the ZPE spectral density on frequency f , where the angular frequency $\omega = 2\pi f$ (Milonni, 1994).

$$\int_{\omega_1}^{\omega_2} \rho(\omega) d\omega = \frac{\hbar}{8\pi^2 c^3} (\omega_2^4 - \omega_1^4) \quad \text{eV/m}^3 \quad (4)$$

Initially we assume that a resonant frequency of 10^{17} Hz will correspond to a wavelength on the order of the junction size. Roughly estimating a typical nano-sized diode junction to be on the order of a cubic nanometer (1 nm^3) for the Kuriyama nano-size cylinder-shaped diode, the spectral energy density of the zero point field in that volume would possibly suggest what the maximum energy is theoretically available in that small volume from the quantum vacuum. A preliminary estimate of the photon energy at the frequency of interest using the Einstein equation $E = hf$ yields a keV range of energy or by conversion, radiation energy in the femtojoule (10^{-15} J) range. Therefore, it is expected that the ZPE spectral density will also be of the same order of magnitude. Substituting a resonant frequency of 10^{17} Hz into equation (4) yields about 390 eV/nm^3 which when converted tells us that an energy density of about a terajoule per cubic meter (10^{12} J/m^3) is available from the quantum vacuum up to that frequency but only about a femtojoule of energy in a cubic nanometer (10^{-15} J/nm^3) which is about the same as the simple photon energy calculation.

However, in order to justify a power level of a picowatt per diode, it would be advantageous to show that at least a picojoule per diode is available theoretically from the zero point field, since watts equal joules per second. Therefore, two considerations usually are introduced at this point. One is that the maximum accessible frequency must be higher than 10^{17} Hz and secondly, perhaps the resonant cavity or scattering volume size needs to be correspondingly reduced. The second consideration, to quantum vacuum engineers and physicists, is easy to justify since the Zitterbewegung or quantum fluctuations affects individual atoms and electrons directly, more than atomic clusters of crystal lattices in a semiconductor junction. The volume of an atom (picosphere = $10^{-12} \text{ m}^3 = 1 \text{ pm}^3$) or electron (femtosphere = $10^{-15} \text{ m}^3 = 1 \text{ fm}^3$) would then be more appropriate for resonant frequency considerations of the influence of ZPE-induced noise. (The classical electron radius e^2/mc^2 is about 2.8 fm .) Respectively, equation (4) yields about 390 keV/pm^3 and about 390 MeV/fm^3 due to the X-ray (10^{20} Hz) and gamma ray (10^{23} Hz) ranges of the corresponding resonant frequencies. Using a gamma ray frequency as the upper limit in equation (4) and converting, *the latter ZPE spectral energy density is therefore at least 62 pJ per electron*. Thus exceeding the desired order of one picojoule, it would then be multiplied by the number of electrons expected to be present in the 1) *the Hastas self-assembled GaAs Schottky diodes* or 2) *the Kuriyama high density nano-size cylinder-shaped diodes*, since the non-thermal random activity of electron noise is the essence of Johnson noise and the focus of attention for a ZPE converter.

POWER ESTIMATES FOR DIODE ARRAY ENERGY CONVERTER

Energy generation solutions for deep space travel where solar energy is minimal and the temperature hovers near absolute zero may not emerge for several years besides nuclear power which has a limited life span. However, power estimates for the diode array energy converter (DAEC) at room temperature on earth will normally be swamped by thermal noise. Therefore, designing the ideal ZPE diode power capability specifications to encompass both environments seems to be an expedient answer, with a bandwidth range of frequencies to include at least 1 to 10^{12} Hz as suggested from Figure 2 and Figure 8.

To initiate power estimates for the DEAC, it is helpful to compare with the textbook order of magnitude estimates for broadband noise in solid state circuit components, whose range from the previous discussion also apply to the DEAC. Figure 8 displays the $1/f$ noise region for an FET input amp in the 1 to 10 Hz range, with white noise extending from 10 to 10^5 Hz, above which the estimated noise becomes proportional to f (Northrop, 1997). The important observation for this section is that thermal and nonthermal sources produce voltage fluctuation noise in the nanovolt (nV) range per root hertz and current fluctuation noise in the femtoampere (fA) range per root hertz. Therefore, a rough power estimate over our ideal bandwidth would be to multiply them both for a power calculation with $P = IV$, using the lowest common amplitude of $(10 \text{ nV/Hz}^{1/2})(10 \text{ fA/Hz}^{1/2})(10^{12} \text{ Hz}) = 0.1 \text{ nW}$ per device. This estimate is also of the same order of magnitude as the Pinto Casimir electrical generator mentioned earlier. Pinto among others like the Brown patent, make reasonable calculations of the energy density of arrays of vacuum engines similar to ZPE diodes, which conservatively reach estimates of hundreds of kilowatts/cubic meter (kW/m^3) according to Pinto (1999). Converting 0.1 nW to the equivalent $100 \text{ pW} = 100 \times 10^{-12} \text{ Watt}$ and conservatively taking into account unseen conversion losses, frequency limits, etc., it can be further trimmed by estimating this calculation as a *range* of 1 pW at the lowest (assuming 1% efficiency) to 10 pW (at 10% efficiency) as a maximum power per diode, thus factoring in a 1/100 loss factor as a buffer against overestimates.

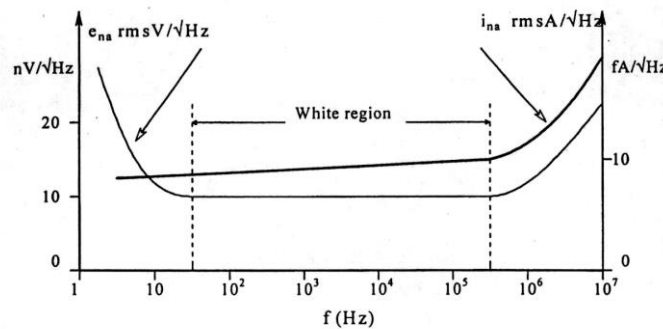


FIGURE 8. Plots of typical input noise root power spectrums for an FET input amplifier (Northrop, 1997)

The most interesting arrangement of diodes and resistors may be a convenient 10 cm^3 (10 cc) box but could be larger if the diode packing density requires it. The proposed DEAC box will perhaps involve a choice of 1) *the Hastas self-assembled GaAs Schottky diodes* or 2) *the Kuriyama high density nano-size cylinder-shaped diodes*, both estimated to be in the range of 10^{11} per cm^2 diode density. Using a conservative packing density of 2 mm per layer (with 1.1 mm substrates), we can pack 5 diode array layers in 1 cc and therefore, 50 diode layers in 10 cc. This raises the diode density to 5×10^{12} diodes (5 trillion diodes) in a 10 cc box. This is a favorable quantity for the estimated picowatt (1 to 10 pW) power level per diode, which yields a minimum of a 50 Watt DC generator from thermal and non-thermal noise combined, for the lowest estimate of 1 pW per diode. It is worthwhile noting that an array of a trillion molecular switches has been proposed using less than 100 zJ (100×10^{-21} joules) per switch based on direct experimental measurement of a single molecule (Loppacher, 2003). Loppacher et al. also note that it requires “less than a femtojoule of energy” to switch a solid state transistor, which may be useful in an advanced design of a switching DEAC for AC output.

Surprisingly, the DEAC may reach into the optimal region of 50 W if 10 pW per diode is possible, though this may only be possible with the additional input of thermal and ambient EMF *energy harvesting*. Note that the increase above 10 nV and 10 fA in voltage and current noise levels clearly produced at the low frequencies and most importantly, at the higher frequencies, in Figure 8, as well as any ambient electromagnetic smog, have been ignored for convenience. Of course, this estimate translates to hundreds of kilowatts/cubic meter (kW/m^3) if such arrays were manufactured in larger sizes of a cubic meter.

Looked at another way, Figure 9 shows that Hastas measured a forward current of 10^{-10} A or 100 picoamperes experimentally for a typical self-assembled ALMBE GaAs Schottky diode at zero bias voltage. With 500 trillion diodes in the 10 cc box example, this equates to 50 kA of current at 10 millivolts (10 mV) generated for a 500 W estimated output. In such a case, assembling a certain number of the diodes *in series* to create a convenient voltage for power conversion would be an obvious method for electrical energy utilization and ultracapacitor storage.

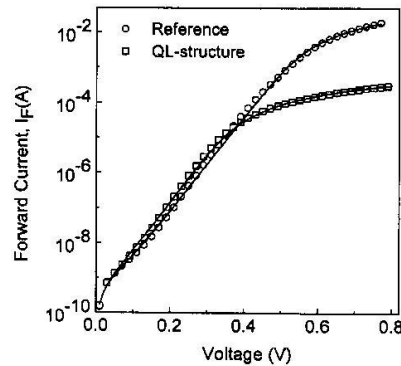


FIGURE 9. Experimental forward current-voltage characteristic of a typical Au/n-GaAs Schottky diode for a reference GaAs sample and the GaAs with InAs QL structure sample showing 10^{-10} A current conduction at zero bias voltage (Hastas, 2003).

A third perspective is offered with the Diode Array US patent #3,890,161 of Charles Brown mentioned previously. Brown suggested arrays of diode cylinders 25 nm in diameter for thermal and non-thermal electric noise conversion. With an estimated frequency bandwidth of 10^{10} Hz and a 50% loss factor, his power estimate is 10^{-5} Watts for a million diodes or equivalently, 5000 W for 500 trillion diodes, which is in the middle of the range estimated by two other approaches. It is also noted that the 25 nm diameter of the Brown diode can be reduced to a limit of 1 nm that is achievable today, as suggested above in Kuriyama's manufacturing patent, with Hastas' Schottky diodes or other molecular diodes.

It is also worth noting that the perspective offered above is consonant with the present industrial effort to accomplish *energy harvesting* and electromagnetic reception on a small scale today. A tunneling nanotube radio, using a single tunable nanotube for example, has been proposed and simulated (Dragoman, 2008). Therefore, it is important to emphasize that on the ground, especially near urban environments, a large amount of broadband EMF noise is available for energy harvesting with DEACs, that will conceivably overwhelm the small amount of energy available from thermal and non-thermal noise sources by several orders of magnitude. As such, the proposed DEAC operating as a broadband radiation scavenger would be more suitably labeled an "electromagnetic field energy harvesting urban generator of electricity" (EMFEHUGE) for commercial marketing purposes. An example of such a concept is the integrated environmental energy extractor that has been developed by General Electric, with supporting electronics such as diodes, to rectify and extract energy from movement of a capacitor or of a dielectric material (Ghezzi, Mario et al., "Integrated Environmental Energy Extractor", U.S. Patent 6,127,812, Oct. 3, 2000). A microscopic antenna system for focusing ZPE and amplifying its resonant frequencies for electricity generation has been patented by the U.S. Air Force (Mead, Franklin B. and Nachamkin, Jack, "System for Converting Electromagnetic Radiation Energy to Electrical Energy", U.S. Patent 5,590,031, Dec. 31, 1996). The Air Force approach to including a hemisphere collector or preferably a parabolic collector may also be advantageous with the proposed DEAC as well as other electromagnetic wave amplification techniques. It is also noted that "sub-picowatt signal level" detection has already been accomplished with only a 120-element microbolometer diode array, designed for *low noise* performance by NIST, where random noise is systematically filtered out (Luukanen, 2004).

PRACTICAL CONSIDERATIONS

Diode arrays of self-assembled molecular rectifiers or nano-sized cylindrical diodes have been shown to reasonably provide for rectification of electron fluctuations from thermal and non-thermal ZPE sources to create an alternative energy DC electrical generator. Any additional noise perhaps contributed by a series carbon resistor will also increase these estimates for the thermal noise though at the same time is expected to reduce the power output (Northrop, 1997). Since these calculations have been done at room temperature, it should be noted that if solar heat or any other heat source is added, such estimates will also increase proportionally, such as with the Schottky photodiodes mentioned earlier. However, every DEAC is designed to rectify thermal noise and therefore cause refrigeration instead of the typical semiconductor heat generation, which serendipitously helps in a time of

increasing global warming. In the expected near future scenario of climate change, thousands of people in temperate zones are at risk during the summer for heat stroke (over 2000 people died in France during a heat wave that lasted two weeks). Therefore, having a solid-state, square meter sealed cube that generates electricity and cools the building will serve both vital purposes. Ideally, it will also make rural areas and third world countries habitable while lessening developed countries' dependence on centralized grid power.

A practical consideration is the fact that the thermal conversion to electricity causing refrigeration is expected to occur at the junction of each diode, while possible heat generation could be expected from the rest of the circuitry and wiring leading the electrical current out of the DEAC. Therefore, typical silicon carbide heat conductors, which are also electrical insulators, can be used advantageously in this situation to manage thermal dissipation and heat exchange.

Though today's trend toward energy harvesting is cited as supportive of this article's thesis, it should be noted that the proposed DEAC is novel and untested, apart from the diodes and devices referenced. With the entire electronics industry focused solely on *noise reduction*, it is no surprise that no one has built a practical DEAC prototype so far. Even the U.S. Patent Office simply allows "constructive reduction to practice" instead of actual reduction to practice for patenting inventions and no working model has been requested by the entire Office for decades. Proving that broadband electrical noise exists is easy. Designing the best zero bias diode array for the job of harvesting it is another engineering effort worthy of a future article. Certainly, a new research direction is warranted in order to reverse the present noise reduction trend in zero bias diodes in favor of noise amplification, noise equivalent power increase, and high noise to signal ratios suitable for energy harvesting rectifiers. Such a research effort is found in the literature with the investigation of the necessary conditions for enhancement of shot noise attributed to "electrostatic-potential fluctuations" and that it results in charge accumulation rather than system instability (Song, 2003).

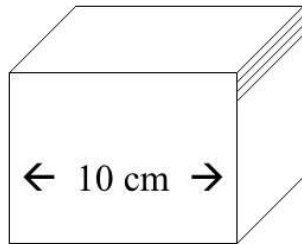
REFERENCES

- Beck, Christian and Mackey, Michael, "Could dark energy be measured in the lab?" *Phys. Letters B*, V. **605**, (2005), p. 295.
- Blanco, R., França, H. M., Santos, E., and Sponchiado, R. C., "Radiative noise in circuits with inductance," *Phys. Lett. A* **282**, (2001), pp. 349-356.
- Brenning, H., Karanov, S., Duty, T., Kubatkin, S., and Delsing, P., "An ultrasensitive radio-frequency single-electron transistor working up to 4.2 K", *J. Appl. Phys.* **100**, (2006), p. 114321.
- Davis, E., Teofilo, V. L., Puthoff, H. E., Nickisch, L. J., Rueda, A., and Cole, D. C., "Review of Experimental Concepts for Studying the Quantum Vacuum Field," in the proceedings of *Space Technology and Applications International Forum (STAIF-06)*, edited by M. S. El-Genk, AIP Conf. Proc. **813**, (2006), p. 1390-1401.
- Dhirani, A., Lin, P. H., Guyot-Sionnest, P., Zehner, R. W., and Site, L. R., "Self-assembled molecular rectifiers" *J. Chem. Phys.*, V. 106 (12), March 22, 1997, p. 5249
- Dragoman, D., and Dragoman, M., "Tunneling nanotube radio", *J. App. Phys.*, V. **104**, (2008), p. 074314.
- Hastas, N. A., and Dimitriadis, C. A., "Low frequency noise of GaAs Schottky diodes with embedded InAs quantum layer and self-assembled quantum dots", *J. App. Phys.*, V. **93**, N. 7, April 1, (2003), p. 3990.
- Kach, A., Wendin, G., Johansson, G., "Full-frequency voltage noise spectral density of a single-electron transistor" *Phys. Rev. B*, V. **67**, (2003), p. 035301.
- Koch, R. H., Van Harlingen, D. J., and Clarke, J., "Quantum-Noise Theory for the Resistively Shunted Josephson Junction" *Phys. Rev. Letters*, Vol. **45**, No. 26, Dec., (1980), p. 2132.
- Koch, R. H., Van Harlingen, D. J., and Clarke, J., "Measurements of Quantum Noise In Resistively Shunted Josephson Junctions", *Physical Review B*, Vol. **26**, No. 1, July, (1982), p. 74.
- Loppacher, C., Guggisberg, M., Pfeiffer, O., Meyer, E., Bammerlin, M., Luthi, R., Schlittler, R., Gimzewski, J., Tang, H., and Joachim, C., "Direct determination of the energy required to operate a single molecular switch", *Phys. Rev. Letters*, V. 90, No. 6, 2003, p. 066107-1
- Luukanen, A., Miller, A. J., Grossman, E. N., "Active millimeter-wave video rate imaging with a staring 120-element microbolometer array", in *Radar Sensor Technology VIII and Passive Millimeter Imaging Technology VII*, edited by Trebits, R., Kurtz, J. L., Appleby, R., Salman, N. A., Wikner, D. A., *Proceedings of SPIE*, Vol. 5410, p. 195
- Lynch, J., Moyer, H., Schulman, J., Lawyer, P., Bowen, R., Schaffner, J., Choudhury, D., Foschaar, J., Chow, D., "Unamplified Direct Detection Sensor for Passive Millimeter Wave Imaging" in the proceedings of *Passive Millimeter-Wave Imaging Technology IX*, edited by Roger Appleby, Proc. of SPIE, V. **6211**, (2006), p. 621101.
- Milonni, Peter, *The Quantum Vacuum*, Academic Press, San Diego CA, 1994, p. 49
- Northrop, Robert, *Introduction to Instrumentation and Measurements*, CRC Press, Boca Raton FL, (1997).
- Oda, Shuri and Ferry, David, *Silicon Nanoelectronics*, Taylor and Francis Group, CRC Press, Boca Raton FL, (2006).

- Pinto, F., "Engine cycle of an optically controlled vacuum energy transducer" *Phys. Rev. B*, Vol. **60**, No. 21, (1999).
- Reed, Mark and Lee, T., *Molecular Nanoelectronics*, American Scientific Publishers, Stevenson Ranch CA, (2003)
- Schmid, J., Konig, J., Schoeller, H., Schon, G., "Resonant tunneling through a single-level quantum dot", *Physica E*, 1997, p. 241
- Sheng, Ping, "Fluctuation-induced tunneling conduction in carbon-polyvinylchloride composites" *Phys. Rev. Letters*, V. **40**, N. 18, (1978), p. 1197
- Smoliner, J., Demmerle, W., Gornik, E., Bohm, G., and Weimann, G., "Tunneling spectroscopy of 0D states" *Semicon. Sci. Tech.*, Vol. 9, 1994, p. 1925
- Smoliner, J., "Tunneling spectroscopy of low-dimensional states," *Semicon. Sci. Tech.* Vol. 11, (1996), Fig. 10, p. 12
- Song, W., Mendez, E., Kuznetsov, V., and Nielsen, B., "Shot noise in negative-differential-conductance devices", *App. Phys. Letters*, Vol. 82, No. 10, 2003, p. 1568
- Tsormpatzoglou, A. "Low-frequency noise spectroscopy in Au/n-GaAs Schottky diodes with InAs quantum dots" *Applied Physics Letters*, V. **87**, (2005), p. 163109.
- Valone, Thomas, *Practical Conversion of Zero Point Energy from the Quantum Vacuum for the Performance of Useful Work*, 2nd Edition, Integrity Research Institute Publishers, Beltsville, MD (2004) www.IntegrityResearchInstitute.org.
- Valone, Thomas, *Zero Point Energy: The Fuel of the Future*, 2nd Edition, Integrity Research Institute Publishers, Beltsville, MD (2007) www.IntegrityResearchInstitute.org.
- Van den Broeck, C. and Kawai, R., "Brownian Refrigerator", *Phys. Rev. Letters*, V. 96, June 2, 2006, p. 210601-1
- Yasutomi, S., Morita, T., Imanishi, Y., Kimura, S., "A Molecular Photodiode System That Can Switch Photocurrent Direction", *Science*, V. **304**, no. 5679 (2004), p.1944.
- Young, A.C., Zimmerman, J. D., Brown, E. R., and Gossard, A. C., "Semimetal-semiconductor rectifiers for sensitive room-temperature microwave detectors", *App. Phys. Letters*, V. **87**, (2005), p.163506

DEAC Power Cell with THz Limit

Assume a **10 cm³ (10 cc) box** and 10% efficiency = 10 pW/diode



Nano-sized diodes = 10^{11} per cm²

assuming 2 mm per layer with 1 mm substrate, yields 50 diode layers =

5 trillion diodes × 10 pW = **50W**

Therefore even a 1 cc cube = 5 W

This conservative estimate, assuming only a 10% efficiency for total energy conversion, still reaches the kW/m³ range of production, 24/7 from ambient thermal and non-thermal energy combined. This calculation also ignores the 1/f and the f range of noise that exceeds 10 nV and 10 fA per root hertz.

Updated for 2013

FIGURE 10. Diode Lecture Slide added to corrected version to summarize proposed DEAC generator